Characterizing vertebrate histone H2A.Z: Acetylation, isoforms and function

by

Deanna Dryhurst
B.Sc, University of Victoria, 2002

A Dissertation Submitted in Partial Fulfillment
of the Requirements for the Degree of

DOCTOR OF PHILOSOPHY

in the Faculty of Science, Department of Biochemistry and Microbiology

Supervisory Committee

Characterizing vertebrate histone H2A.Z: Acetylation, isoforms and function

by

Deanna Dryhurst
B.Sc, University of Victoria, 2002

Supervisory Committee

Dr. Juan Ausio, Department of Biochemistry and Microbiology
Supervisor

Dr. Francis E. Nano, Department of Biochemistry and Microbiology
Departmental Member

Dr. Claire G. Cupples, Department of Biochemistry and Microbiology
Departmental Member

Dr. Francis Choy, Department of Biology
Outside Member

Abstract

Supervisory Committee
Dr. Juan Ausio, Department of Biochemistry and Microbiology
Supervisor
Dr. Francis E. Nano, Department of Biochemistry and Microbiology
Departmental Member
Dr. Claire G. Cupples, Department of Biochemistry and Microbiology
Departmental Member
Dr. Francis Choy, Department of Biology
Outside Member

Histone H2A.Z is a highly conserved replication-independent histone variant that is essential for survival in diverse organisms including *Tetrahymena thermophila*, *Drosophila melanogaster*, *Xenopus laevis*, and *Mus musculus*. H2A.Z has been shown to play a role in many cellular processes including, but not limited to, gene expression, chromosome segregation, cell cycle progression, heterochromatin maintenance and epigenetic transcriptional memory. However, the mechanism by which H2A.Z and its post-translationally modified forms participate in these diverse cellular events and their subsequent effects on chromatin structure and function are not entirely clear. A thorough review of H2A.Z is provided in Chapter 1.

We have isolated native non-acetylated and acetylated forms of H2A.Z and characterized nucleosome core particles (NCPs) reconstituted with these proteins using the analytical ultracentrifuge (Chapter 2). We report that NCPs reconstituted with native non-acetylated H2A.Z exhibit a slightly more compact conformation compared to those reconstituted with H2A. Furthermore, we show that acetylation of H2A.Z in conjunction with acetylation of the histone complement, results in NCPs that are less compact and less stable than H2A.Z-containing NCPs reconstituted with non-acetylated histones.

Acetylated H2A.Z NCPs are nevertheless more compact and stable than acetylated H2A-containing NCPs. We have also identified the presence of two H2A.Z protein isoforms in vertebrates, H2A.Z-1 and H2A.Z-2, and characterized the sites and abundances of their N-terminal peptide acetylation.

Further characterization of the human H2A.Z isoforms is presented in Chapter 3 and indicates that they are expressed across a broad range of human tissues, and that they exhibit a similar but non-identical distribution within chromatin. Our results suggest that H2A.Z-2 preferentially associates with H3 trimethylated at lysine 4 compared to H2A.Z-1, and the phylogenetic analysis of the promoter regions of H2A.Z-1 and H2A.Z-2 indicate that they have evolved separately during vertebrate evolution. Overall, these data suggest that the two isoforms of H2A.Z present in vertebrates may have acquired a degree of functional independence.

In Chapter 4, we show that H2A.Z and an N-terminally acetylated form of H2A.Z associate with the prostate specific antigen (PSA) gene promoter and the levels of these proteins are reduced upon induction of the gene with androgen. Furthermore, H2A.Z protein levels increase in response to treatment with androgen which correlates with an increase in the mRNA expression levels of the H2A.Z-1 gene. Preliminary Western Blot and quantitative PCR analysis of H2A.Z (-1 and -2) levels in a tumor progression model of prostate cancer indicate that increased H2A.Z expression may be involved in the development of androgen independent prostate cancer.

Collectively, our results contribute to our understanding of H2A.Z biology in vertebrates and support a role for this protein and its acetylated forms in poising promoter chromatin for subsequent gene transcription.

Table of Contents

List of Tables

List of Figures

List of Abbreviations

AUT: Acetic Acid Urea Triton

bp: Base pair

ChIP: Chromatin Immunoprecipitation

CTCF: CCCTC-binding factor

Da: Daltons

DMEM: Dulbecco's Modified Eagle Medium

DNA: deoxyribonucleic acid

EDTA: ethylenediaminetetraacetic acid

FBS: Fetal Bovine Serum

HAT: Histone acetyltransferase

HDAC: Histone deacetylase

KAT: Lysine acetyltransferase

MNase: Micrococal nuclease

MS/MS: Tandem mass spectrometry

NCP: nucleosome core particle

PBS: Phosphate Buffered Saline

PTM: post-translational modification

PVDF: Polyvinylidene Fluoride

RD: replication-dependent RI: replication-independent

Acknowledgments

I would like to acknowledge many people who have contributed to this work, directly or indirectly. I have been lucky enough to have truly the best labmates possible without whose help and encouragement I surely would have gone crazy. Andra and Lindsay, thank you for your time and patience, your thought provoking discussions and most of all your friendship. Allison, Alison, Anita, Begonia, Brad, Chema, Ron, Wade, thanks for comic relief and general support. I would also like to sincerely thank my family and friends for putting up with me throughout this whole process. There are many other people who have supported me along the way, thank you to all the lab instructors, Deb, Melinda and Sandra and to Scott and Steve for technical assistance, but mainly for sarcastic wit and general commentary on anything and everything.

I thank my Supervisory Committee, Dr. Francis Nano, Dr. Claire Cupples and Dr. Francis Choy for their encouragement and helpful discussions also, Steve Evans for his kindness when the going got very tough.

Last but never least, I would like to thank my supervisor Juan Ausio, who in response to my thanks would say “No, it’s nothing Deanna you don’t have to thank me”.....it has meant so very much to me to learn from such a great mentor and great person and to have the opportunity to participate in science at this level. Muchisimas gracias.

Dedication

I would like to dedicate this dissertation to Geoff, Leah and Barb. To Geoff for keeping me grounded, for reminding me that this is my life and with him, it is wonderful. To Leah, for amazing advice and understanding……it's that weird sister thing. To Barb, for being the best possible mentor and mother anyone could ever have, your support on all levels and enduring belief in me has made me believe in myself.

Introduction:

Chromatin is the macromolecular assembly of DNA and proteins that constitutes the chromosomes of eukaryotic cells and the template for all nuclear processes that require access to DNA. It is a highly dynamic structure that responds to diverse signalling pathways according to the changing needs of the cell. The major protein component of chromatin is made up of histones whose positive charge partially neutralizes the negative phosphate backbone of DNA and allows it to be efficiently packaged within the nucleus. The basic repeating subunit of chromatin is the nucleosome core particle (NCP) which consists of approximately 146 base pairs of DNA wrapped nearly twice around a histone core octamer. The canonical histone octamer is composed of two copies each of histones H2A, H2B, H3 and H4 arranged as two H2A/H2B dimers and an H3/H4 tetramer (Luger et al., 1997). The association of DNA with the NCP results in the formation of a 10nm fiber with the appearance of 'beads on a string'. The linker DNA that connects adjacent nucleosomes is bound by linker histones, namely histone H1, that bind the DNA as it enters and exits the nucleosome and results in the further compaction of DNA into a 30nm fiber. This fiber can fold upon itself to form the highly condensed metaphase chromosomes; however during interphase the condensation state of different regions of the chromosomes varies greatly. Thus, chromatin can be very broadly classified as either condensed heterochromatin, or open euchromatin based on the level of compaction of the complex.

How are these states of compaction regulated in response to cellular cues? Processes such as replication, repair, recombination and transcription all require access to the DNA

template and therefore all encounter nucleosomes. The structure and composition of these nucleosomes can be altered by three very broad and inter-related processes: Chromatin remodelling occurs via the action of large multi-subunit complexes that remove or slide nucleosomes from one position to another, or alter their composition (Clapier and Cairns, 2009). Post-translational modification (PTM) of histones by diverse enzymes can alter the conformation of the nucleosome directly or serve as a platform for the recruitment of other factors (Kouzarides, 2007). Incorporation of histone variants into the nucleosome may also alter their structure and/or their ability to recruit other proteins (Thambirajah et al., 2009). Theoretically, this allows us to define whether, as a result of histone PTMs and incorporation of histone variants, chromatin is affected in *cis* or in *trans*. *Cis* alterations would occur when the combination of histone variants and/or PTMs would directly affect the structure of the nucleosome or the chromatin fiber. *Trans* alterations would occur when the specific combination of variants and PTMs function to recruit additional factors that then specify a downstream event that may include modulation of chromatin structure. Our understanding of how these three mechanisms interact in different cellular contexts has vastly increased in recent years. Here a brief introduction into general features of histone variants and PTMs is provided, followed by short sections focusing on histone acetylation and methylation.

Histones and histone variants:

Although histones are broadly classified as either linker (H1, H5) or core (H2A, H2B, H3, H4) histones, each individual histone is better thought of as a unique protein family in higher organisms. This is because multiple copies of the canonical histone genes exist,

often in tandemly arranged blocks, throughout the genomes of many organisms. The expression of the canonical histone family genes is tightly regulated occurring during S phase of the cell cycle and resulting in mRNA transcripts containing sequences that create stem-loop structures to signal the end of transcription (Marzluff et al., 2008). S-phase expression allows the newly synthesized DNA to be immediately packaged into nucleosomes, typically in part by the chromatin assembly factor 1 (CAF1) complex whose interaction with the DNA processivity clamp PCNA couples the DNA replication and chromatin assembly machineries (Loyola and Almouzni, 2004). Consequently, these histones are often referred to as 'replication-dependent' (RD). The core histones share several general features, including a globular histone fold domain and intrinsically disordered N- and C-terminal tails, while linker histones contain a globular winged-helix domain.

Another important class of histones, the replication-independent (RI) histone variants, is characterized by polyadenylated transcripts and expression that occurs throughout the cell cycle (Malik and Henikoff, 2003). Curiously, most members of this group are either derived from histone H2A or H3 and they have been shown to participate in diverse cellular processes. Some of these histone variants are present in all organisms studied from yeast to humans, while others exist only in vertebrates or mammals but all exhibit different degrees of homology with the parental RD histone from whose sequence they evolved. For example, the centromeric variant of H3 called CenpA in humans (Cse4 in *S. cerevisiae*), has an identical histone fold domain compared to the RD H3.1 but varies in the N-terminal tail region (Malik and Henikoff, 2003). Conversely, the mammalian-

specific macroH2A variant shows high sequence homology with canonical H2A in the N-terminal and histone fold domains, but contains a large C-terminal non-histone extension (Ausio and Abbott, 2002). The patterns of evolution of RI variants can also differ: Histone variant H2A.Z is derived from an ancient lineage and shows much greater interspecific homology than intraspecific paralogy with RD H2A, while histone H2A.X has emerged independently several times throughout the course of evolution (Eirin-Lopez et al., 2009; Li et al., 2005a).

Emerging evidence indicates that RI histone variants can cooperate with histone PTMs and other factors to specify regions of chromatin for specific functions. The CenpA variant is an essential component of centromeric chromatin, while the H3.3 variant is thought to play a role in transcriptionally active regions of the genome (Malik and Henikoff, 2003). The H2A.X variant becomes specifically phosphorylated at the serine residue of its C-terminal SQE motif in response to double strand DNA breaks and is thought to recruit factors required for DNA repair (Li et al., 2005a). The macroH2A variant becomes localized to the inactive X chromosome of mammals and is thought to help maintain its heterochromatic state (Ausio and Abbott, 2002). Another H2A variant, H2ABbd (for Barr body deficient) is a very rapidly evolving histone that may function in transcriptional activation and also in spermiogenesis (Eirin-Lopez et al., 2008). Finally, the H2A.Z variant has been shown to have several different functions including participating in transcriptional activation, heterochromatin maintenance and epigenetic transcriptional memory (Dryhurst et al., 2004), as will be more thoroughly discussed in chapter 1.

Histone post-translational modification:

The surface of the nucleosome is studded with a multitude of PTMs that are covalently linked to histone proteins at many different amino acid residues. Most, but not all, PTMs occur on the histone tails and they include acetylation, methylation, phosphorylation, ubiquitination, SUMOylation, and poly(ADP-ribosylation). The idea that a specific pattern of histone PTMs forms a code that specifies downstream events is central to the 'histone code hypothesis', which has gained considerable attention in recent years, though it remains very controversial (Jenuwein and Allis, 2001; Strahl and Allis, 2000). However, the function of certain histone PTMs may also be to modify chromatin structure. A complete review of all histone PTMs is beyond the scope of this introduction therefore, highlighted here are certain histone PTMs that have relevance to this dissertation, particularly acetylation and methylation of defined residues.

Histone Acetylation:

Acetylation of histones occurs at the ε-amino group of lysine residues mainly within the N-terminal tails of all four core histones. The notion that histone acetylation is associated with transcriptional activity was first proposed over 40 years ago in 1964 (Allfrey et al., 1964). The enzymes responsible for this modification are called either histone acetyltransferases (HATs) or more broadly lysine acetyltransferases (KATs) owing to the fact they often have multiple non-histone substrates (Choudhary et al., 2009). The action of HATs is opposed by histone deacetylases (HDACs) that remove acetyl groups and the dynamic balance of the actions of these two classes of enzymes allows for levels of acetylation to respond to the changing needs of the cell. A recent genome-wide

localization study highlights this by showing that active genes are associated with both HATs and HDACs while silent genes associate with neither class of enzyme (Wang et al., 2009b). The link between histone acetylation and transcriptional activity is well-established, but what is the purpose of acetylating histones? Does acetylation alter the structure of chromatin in *cis*, or in *trans* or both and if so, does this specify downstream events as part of a code? Clearly this is a complex question for which there is no one definitive answer, but a summary of what is known is presented here.

Unlike the case for other histone PTMs, many studies have now shown that acetylation does have a structural effect on NCPs and chromatin fibers. Early studies indicated that native acetylated mononucleosomes remained folded and intact, but they exhibited increased sensitivity to nuclease and thermal denaturation (Ausio and van Holde, 1986). The structural effects of acetylation on the NCP can be seen as two related processes, a change in the conformation of the nucleosome resulting in a more open structure, and a decrease in the overall stability of the particle (Ishibashi et al., 2009b). The conformational change is due to increased transient unwrapping of the DNA from the edge of the nucleosome, which also likely has an effect on stability (Anderson et al., 2001). The most open conformation, as measured by analytical ultracentrifuge analysis, exhibited by acetylated NCPs occurs when all the histones in the particle are acetylated to some degree because replacement of acetylated H2A with non-acetylated H2A in the context of an acetylated histone complement results in particles that have an intermediate conformation between the fully non-acetylated and fully acetylated particles (Ishibashi et al., 2009b). This indicates either that the N-terminal tail of H2A plays a particularly

important role in mediating the conformational change of the NCP (the effects of the tails of the other histones were not examined in the same way in this study), or that there is a synergistic effect exerted by histone tail acetylation on the conformation of the NCP. By applying increasing amounts of force using atomic force microscopy to preparations of nucleosomes, it was shown that acetylated nucleosomes fall apart under significantly lower forces than non-acetylated particles (Dunker et al., 2001). This same conclusion has been drawn using a variety of other techniques (Ishibashi et al., 2009b; Oliva et al., 1990; Siino et al., 2003). Collectively, these studies indicate that the acetylated mononucleosome adopts a more open conformation and is less stable than non-acetylated particles and that the acetylation of individual histones acts synergistically and most likely in an additive manner to mediate these effects.

Studies concerning the structural effects of histone acetylation on the chromatin fiber have shown that it results in fiber decondensation and unfolding (Annunziato and Hansen, 2000; Garcia-Ramirez et al., 1995; Gorisch et al., 2005). However, this effect is relatively small in the presence of linker histones (Wang et al., 2001). The observed effects in the absence of histone H1 could nonetheless be biologically relevant because acetylated chromatin has been shown to be refractory to H1 binding (Perry and Annunziato, 1991; Ridsdale et al., 1990), and regions of transcriptionally active chromatin are depleted of linker histones (Kamakaka and Thomas, 1990). The contribution of individual acetylated residues to fiber structure is a complex issue whose actual biological relevance is questionable given that patterns of acetylation vary across the genome (Wang et al., 2008). However, special attention has been paid to K16 of H4

because although most of the histone tails were not resolved in the crystal structure of the nucleosome, a portion of the H4 tail that included K16 was observed to contact an adjacent nucleosome in the region of the H2A/H2B dimer (Luger et al., 1997). Thus, it was proposed that acetylation of H4 K16 could regulate the contacts made between nucleosomes in the 30nm fiber. Support for this hypothesis comes from biophysical studies of reconstituted chromatin fibers containing acetylated H4 K16 that indicate these fibers are indeed less condensed (Shogren-Knaak et al., 2006). Therefore, acetylation can also affect the folding of the chromatin fiber.

What is not fully understood is the mechanism of how acetylation mediates its structural effects. The histone N-terminal tails are lysine-rich, lack virtually any secondary structure and interact with the negatively charged DNA that wraps the nucleosome. Lysine acetylation effectively removes one positive charge therefore it was proposed that acetylation would abolish the interaction of the histone tails with the DNA resulting in a more open structure that could increase the access of transcription factors to the DNA (Calestagne-Morelli and Ausio, 2006; Turner, 2005). Histone N-terminal tail acetylation does promote a weakening of their interaction with DNA, but it does not completely abolish them (Mutskov et al., 1998). Another explanation is offered by evidence indicating that acetylation increases the alpha-helical content of the histone tails (Wang et al., 2000) suggesting that perhaps it is this change in secondary structure that affects the interactions with DNA. Most likely it is the combined contribution of electrostatic effects and secondary structure that combine to decondense chromatin fibers and open mononucleosomes in *cis*.

Besides exerting a direct structural effect, acetylation likely also facilitates transcription by modifying chromatin in *trans*. Acetylated nucleosomes have been shown to be more easily remodelled by chromatin remodelling complexes probably owing to the structural contribution of acetylation but also because remodelling and coactivator complexes often contain proteins with bromodomains which is the only known protein domain responsible for binding acetylated lysine residues (Ferreira et al., 2007; Mujtaba et al., 2007). It therefore becomes very difficult to assess the relative contributions of these two effects in isolation in promoting transcription, but it may be biologically irrelevant to do so, considering that many coactivator complexes contain HAT and chromatin remodelling activities (Altaf et al., 2009). A recent paper by the Bustamante group could ultimately provide an explanation for the positive correlation between histone acetylation and transcription. Using optical tweezers, the authors show that the presence of a nucleosome increases RNA Pol II pausing on the DNA template and they conclude that it is the fluctuations in the equilibrium governing DNA wrapping and unwrapping around the nucleosome that allow RNA polymerase to advance along the DNA and act like a ratchet (Hodges et al., 2009). This indicates that RNA Pol II cannot simply push its way through nucleosomes, but that nucleosome 'breathing' allows transient access to DNA that can be taken advantage of by the polymerase. Therefore, increasing the unwrapping of DNA from the nucleosome by histone acetylation probably decreases RNA Pol II pause frequency resulting in increased transcription, though this remains to be shown.

Histone Methylation:

Unlike acetylation which is mainly found associated with open and active regions of the genome, histone methylation is found within both euchromatin and heterochromatin, depending on the residue that is methylated. Lysine residues can be mono-, di-, or trimethylated, while arginine residues can be mono- or asymmetrically or symmetrically di-methylated. Thus the repertoire of structural diversity imposed on histones by methylation is far greater than that generated by acetylation. Methylation of either lysine or arginine does not alter the charge of the residue therefore it is not expected to alter the structure of the nucleosome in *cis*, though this remains to be conclusively shown and does not preclude *trans* alterations. For many years histone methylation was thought to be a permanent mark because no demethylase enzymes had been discovered. However, we now know that there is in fact a rather staggering array of both histone methylases and demethylases that are involved in regulating long-term expression patterns of large regions of the genome (Cloos et al., 2008). The association of particular methylated residues within histone tails with active or repressed regions of the genome suggests that these modified tails can act as signalling platforms for the recruitment of specific complexes in order to mediate downstream effects. For example, generally trimethylation at H3K9, di- and trimethylation of H3K27 and monomethylation at H4K20 are present within transcriptionally silent regions while di- and trimethylated H3K4 and H3K36 as well as dimethyl H3K79 are associated with transcriptionally active regions (Martin and Zhang, 2005; Sims and Reinberg, 2006). The cases of H3K4 and H3K27 methylation are discussed briefly here because they provide opposing examples of the effect of histone

methylation on transcriptional regulation and because they become relevant for later chapters.

Methylation of H3K4 can occur via the action of six known human enzymes, hSet1A and B and MLL1-4 (mixed myeloid leukemia) that associate within several complexes (Shilatifard, 2008). The proper assembly of these complexes is itself regulated by another histone PTM, H2B monoubiquitination (Dover et al., 2002; Sun and Allis, 2002). Unlike histone acetylation which is recognized by only one known protein domain (bromodomain), histone methylations are recognized by the chromodomain, the Tudor domain and the PHD finger (plant homeodomain) (Shilatifard, 2008). Di- and trimethyl H3K4 localize primarily to the 5' regions of active genes (Barski et al., 2007). A positive effect of this histone modification on transcription has been established by its recognition by CHD1, a protein that remodels chromatin and is involved in pre-mRNA splicing (Sims et al., 2007). Furthermore, the yeast NURF chromatin remodelling complex which stimulates preinitiation complex formation, binds di- and trimethylated H3K4 through the PHD finger of BPTF (Wysocka et al., 2006). Importantly, the human ING 1-5 tumour suppressor proteins also bind di- and trimethyl H3K4 with dissociation constants in the 1-10 μM range (Champagne and Kutateladze, 2009; Pena et al., 2006; Shi et al., 2006) which links this modification not only to transcription, but also to DNA repair (Pena et al., 2008). Thus it appears that multiple events can be initiated upon methylation of H3K4. However, there is not an absolute correlation between the presence of methylated H3K4 and transcription of a gene since it appears that many developmentally regulated genes have the H3K4 methyl mark in addition to the trimethyl H3K27 mark which results

in transcriptional repression (Hublitz et al., 2009). Understanding the regulation of these 'bivalent' genes is currently a very active area of research.

The mammalian enzyme responsible for methylating H3 K27 is EZH2, a homolog of the *Drosophila* Enhancer of Zeste (EZ) protein (Cao and Zhang, 2004). This protein forms part of the Polycomb Repressor Complex 2 (PRC2) that results in the recruitment of Polycomb Repressor Complex 1 (PRC1) via the protein Polycomb (Pc) that binds methylated H3 K27 (Schuettengruber et al., 2007). The details of the mechanism of targeting PRC2 to specific regions of the mammalian genome are unclear since the existence of DNA sequences that function as Polycomb response elements (PREs) so far has only been shown in *Drosophila* (Schuettengruber et al., 2007). The mechanism of silencing is also not completely understood, but could involve repression of chromatin remodelling and promoter blocking, as well as the formation of subnuclear silencing compartments (Schuettengruber et al., 2007). Interestingly, it has been shown that EZH2 can directly recruit DNA methyltranferases which could stabilize silencing at target genes (Vire et al., 2006).

In conclusion, the combination of histone variants and PTMs increases the diversity and structural complexity of chromatin. This allows for the dynamic regulation of gene expression and other processes such as recombination and repair. The broad focus of this dissertation is on how histone H2A.Z, its isoforms and acetylated forms, contribute to chromatin structure and gene regulation. Chromatin structure and function are extremely active, challenging and fascinating areas of research because they are not only relevant to

those who specialize in these areas, but also to those studying stem cells, cancer and cell signalling among many others.

Chapter 1: Histone H2A.Z: An essential histone variant with multiple functional and structural roles

Deanna Dryhurst and Juan Ausio

Department of Biochemistry and Microbiology, University of Victoria, Victoria, British Columbia, Canada V8W 3P6

Partially adapted from:

Dryhurst, D., Thambirajah, A.A., and Ausio, J. (2004). New twists on H2A.Z: a histone variant with a controversial structural and functional past. Biochem. Cell Biol. *82*, 490-497

Contributions: All material contained within this chapter was written by Deanna Dryhurst.

Introduction:

H2A.Z is highly conserved throughout evolution, sharing approximately 90% sequence identity between organisms as diverse as yeast, trypanosomes, insects, nematodes, frogs, mice, humans and plants (Thakar et al., 2009). This replication-independent histone variant shows approximately 60% protein sequence homology with the canonical H2A family members (Eirin-Lopez and Ausio, 2007). Importantly, H2A.Z has been shown to be essential for survival in several model organisms including *Tetrahymena thermophila* (Liu et al., 1996), *Drosophila melanogaster* (Clarkson et al., 1999; van Daal and Elgin, 1992), *Xenopus laevis* (Iouzalen et al., 1996; Ridgway et al., 2004), and *Mus musculus* (Faast et al., 2001). Whereas the lack of H2A.Z expression is not tolerated in these organisms, neither is its overexpression at least in developing *Xenopus laevis* embryos (Ridgway et al., 2004), indicating that expression levels of this histone must be tightly controlled. Homozygous H2A.$Z^{-/-}$ mouse embryos die approximately 4-5 days postcoitum (Faast et al., 2001). In the yeast *Saccharomyces cerevisiae*, deletion of H2A.Z (termed *HTZ1*) is tolerated but results in growth defects (Jackson and Gorovsky, 2000). This evidence points toward a role for H2A.Z in mediating chromatin structures and/or functions that are important for very basic cellular processes and consequently H2A.Z has received much research attention within the chromatin field.

Why is H2A.Z so important, what does it do? So far, there is no one simple answer to these questions. H2A.Z has been convincingly shown to play a role in many cellular processes including but not limited to gene expression, chromosome segregation, cell cycle progression, heterochromatin maintenance and epigenetic transcriptional memory.

Moreover, there are likely very significant species- and developmental stage-specific differences in H2A.Z function that have made consensus within the field difficult and have contributed to the rather controversial standing of this protein within the ranks of histones. It is for these reasons that H2A.Z remains a fascinating protein whose functional and structural features will be highlighted in the text that follows.

Genomic localization patterns of H2A.Z

In order to help understand the function of H2A.Z, many laboratories have investigated its localization pattern within the genomes of several species using different techniques. Immunofluorescence data from yeast indicate that H2A.Z is distributed in a non-random pattern and occupies thousands of discreet loci in euchromatin throughout the entire genome (Guillemette et al., 2005; Li et al., 2005b; Millar and Grunstein, 2006; Raisner et al., 2005; Zhang et al., 2005). Similarly, in differentiated mouse fibroblasts H2A.Z is distributed throughout the interphase nucleus but is relatively depleted from pericentric and centric heterochromatin (Bruce et al., 2005; Dryhurst et al., 2009; Sarcinella et al., 2007). However, small amounts of H2A.Z have been seen to occupy centromeric chromatin in differentiated mouse cells in other studies (Dryhurst et al., 2009; Greaves et al., 2007). The localization pattern of H2A.Z may also change depending on developmental stage since in trophoblast cells of the developing mouse embryo, H2A.Z associates with the heterochromatin of the pericentric and centric regions and to colocalize with Heterochromatin Protein 1 α (HP1α), which is considered a hallmark of heterochromatin (Rangasamy et al., 2003). Therefore, it appears that at least in regard to the localization pattern of H2A.Z, there are certain features that are common between

yeast and cells of higher eukaryotes; however, there exists an additional complexity to the pattern that could be partly related to the developmental stage in higher organisms.

Advances in the techniques of Chromatin Immunoprecipitation (ChIP) combined with either tiling microarray or massively parallel sequencing technologies have greatly expanded our knowledge of H2A.Z localization within genomes. Using these techniques, several groups determined that the non-random pattern of H2A.Z occupancy within the yeast genome was due to the association of this protein with the 5' ends of genes (Guillemette et al., 2005; Li et al., 2005b; Raisner et al., 2005; Zhang et al., 2005). In fact, the study by Guillemette and colleagues (2005) estimated that approximately 65-75% of yeast promoters associate with H2A.Z. Furthermore, owing to the high resolution of the aforementioned techniques, it was possible to map individual H2A.Z-containing nucleosomes to positions that flank the known nucleosome-free region (NFR) that exists approximately 150-200 bp upstream of the translation start codon in many yeast genes (Raisner et al., 2005). Interestingly, formation of the NFR is not dependent on H2A.Z, but rather the deposition of H2A.Z is dependent on the NFR that forms due to a specific DNA sequence pattern (Raisner et al., 2005). This suggests that deposition of H2A.Z is, at least in part, dependent on the underlying DNA sequence. Indeed, the DNA sequence preference of H2A.Z nucleosomes has been documented in human CD4(+) T cells (Tolstorukov et al., 2009).

Similar experiments in mammalian cells indicate that H2A.Z also localizes to promoter regions (Barski et al., 2007; John et al., 2008), and although there is evidence supporting

the existence of an NFR upstream of some human Pol II-transcribed genes, H2A.Z is not solely localized to the nucleosomes that flank these regions, rather it is present in several nucleosomes upstream and downstream of this region (Barski et al., 2007; Schones et al., 2008). In fact, recent evidence suggests that the NFR in human cells is not devoid of nucleosomes but is occupied by those containing both H2A.Z and the H3.3 variant resulting in a destabilized conformation (Jin et al., 2009). This unfolded organization possibly allows access to the underlying DNA sequence by transcription factors. However, the mechanisms responsible for this destabilization are completely unknown as nucleosomes reconstituted with recombinant H2A.Z and H3.3 exhibit no change in stability (Thakar et al., 2009).

In higher eukaryotes, H2A.Z is also found to be enriched within nucleosomes at other gene regulatory regions, namely at enhancers and insulators (Barski et al., 2007; Bruce et al., 2005). The molecular details of its action at these regions is not clear, but it is possible that either H2A.Z in conjunction with its nucleosomal partners and PTMs has a structural effect that is important for the function of these genomic regions, or that the positioning of H2A.Z serves as a signal for the recruitment of additional proteins that then mediate the required effects. Clearly, these options are not mutually exclusive. Recently, the insulator binding protein CTCF (CCCTC-binding factor) has been shown to bind specific linker DNA regions and mediate the positioning of the flanking nucleosomes that are enriched in H2A.Z (Fu et al., 2008). Insulators function in both the regulation of gene expression as well as in acting as barriers to prevent the spread of heterochromatin (Gaszner and Felsenfeld, 2006), thus establishing a potential role for

H2A.Z in both these processes. Finally, an important overall trend observed by ChIP-sequencing in *Arabidopsis thaliana* is that the presence of H2A.Z nucleosomes and DNA methylation are mutually exclusive (Zilberman et al., 2008). This supports the notion that H2A.Z functions mainly within euchromatic regions (Kobor and Lorincz, 2009).

Examination of the cellular localization pattern of H2A.Z paints a complex picture of how this histone variant may function. On the one hand, its presence at promoters points to an involvement in regulation of gene expression, but on the other hand its presence in heterochromatin suggests another yet-unknown function in silenced regions. The many proposed functions of H2A.Z will be described next.

The role of H2A.Z in gene expression

The presence of H2A.Z at enhancers and promoters, genomic loci that play pivotal roles in the regulation of gene expression, suggests an involvement of H2A.Z in this process. Indeed, the first evidence of this came from observations in *Tetrahymena thermophila*. In this organism, H2A.Z (termed hv1) is present only within the transcriptionally active macronucleus, and not within the transcriptionally inactive micronucleus (Allis et al., 1986). Early studies in yeast showed that *Saccharomyces cerevisiae* strains deleted for H2A.Z were unable to grow on medium containing galactose as the sole carbon source due to defects in the expression of the *GAL1-10* genes (Adam et al., 2001; Larochelle and Gaudreau, 2003). The cause of the defective gene expression was further shown to be dependent on the C-terminal region of H2A.Z, possibly due to the association of this region with Rbp1, the largest subunit of the RNA Pol II complex (Adam et al., 2001;

Larochelle and Gaudreau, 2003). Furthermore, *S. cerevisiae* H2A.Z deletion mutants showed an increased dependency on the SAGA histone acetyltransferase complex and the SWI/SNF chromatin remodelling complex for transcription over non-mutant strains (Santisteban et al., 2000), indicating that H2A.Z could facilitate transcription. When cDNA sequences from an *S. cerevisiae* H2A.Z deletion strain were hybridized to a whole-genome yeast microarray and compared to non-mutant strains, 214 genes that were activated by H2A.Z and 107 genes that were repressed were identified (Meneghini et al., 2003). Interestingly, the genes that were activated tended to cluster near telomeres and the silent mating type locus *HMR* (discussed below), while the repressed genes were randomly distributed throughout the genome (Meneghini et al., 2003). Most of this evidence suggests that H2A.Z functions to facilitate transcription, however the existence of genes that are repressed by H2A.Z in yeast combined with mammalian data from the Gaudreau lab indicating that H2A.Z may play a repressive role at the *p21* gene (Gevry et al., 2007) indicate that, depending on the gene, H2A.Z may positively or negatively regulate expression. Furthermore, another yeast study indicated that H2A.Z functions to silence chromatin regions near telomeres and the *HMR* locus (Dhillon and Kamakaka, 2000).

Direct role of H2A.Z in transcription

Given the capacity of H2A.Z to regulate gene expression, does this histone variant play a direct role in increasing or decreasing the transcription of the genes whose promoters it occupies? As mentioned above, knockdown of H2A.Z in human cells by small-hairpin RNA resulted in increased expression of the *p21* gene, suggesting that H2A.Z is involved

in transcriptional repression (Gevry et al., 2007). However in yeast, H2A.Z was also shown to physically associate with the RNA Pol II complex (Adam et al., 2001) arguing for a role in transcriptional activation. Several other yeast reports indicated that the presence of H2A.Z is inversely correlated with transcriptional rate (Guillemette et al., 2005; Li et al., 2005b), while another group found no correlation with transcription (Raisner et al., 2005). In human cells, H2A.Z was shown to be displaced from the *c-myc* gene upon transcriptional activation (Farris et al., 2005), exchanged from glucocorticoid-responsive genes during hormone induction (John et al., 2008), and depleted from gene promoters under activating conditions in human T cells (Sutcliffe et al., 2009). However, the requirement for eviction of H2A.Z at active promoters does not appear to be universal since H2A.Z is enriched at the active TFF1 gene promoter after induction with estradiol (Gevry et al., 2009). Most of this evidence could point toward a role for H2A.Z in transcriptional repression; however, an alternative hypothesis is that H2A.Z is involved in facilitating transcription by creating an appropriate chromatin architecture ahead of the active transcriptional state. Indeed, this hypothesis is supported by work indicating that the presence of H2A.Z in the inactive state is essential for optimal gene activation in yeast, thus creating a 'transcriptionally poised' state (Li et al., 2005b).

Another important piece of this puzzle lies in that H2A.Z may function in part to influence the post-translational modification state of other nearby histones and in doing so, influence the transcriptional read-out of downstream genes. In this way, the presence of H2A.Z acts in *trans* to direct a function that could be required for the assembly of an active transcription complex but is no longer needed for subsequent events. Evidence

supporting this comes not only from the overlap in the genomic localization patterns of H2A.Z and Tri Me K4 H3, but also from purified H2A.Z-containing mononucleosomes shown to be enriched in Tri Me K4 H3 over those containing H2A (Dryhurst et al., 2009; Sarcinella et al., 2007; Viens et al., 2006). The Tri Me K4 H3 mark is a euchromatic histone modification consistently present at promoters and the 5' end of genes that is thought to mediate protein interactions to enable transcription (Kouzarides, 2007). The enrichment of this modified form of H3 within H2A.Z nucleosomes implies that either Tri Me K4 H3 influences H2A.Z deposition, or that H2A.Z influences H3 methylation at K4. Either way, the downstream effect enables transcriptional activation.

Antisilencing and Poising

Genes that were activated due to the presence of H2A.Z did not exhibit a random localization throughout the yeast genome, rather they tended to cluster near telomeres and the silent mating type locus *HMR* (Meneghini et al., 2003). Telomeres and the *HMR* locus are kept in highly condensed states of heterochromatin by the actions of many factors, including the histone deacetylase enzymes Sir2 and Sir3. The activity of these enzymes spreads from the normal sites into the surrounding euchromatin in the absence of H2A.Z, producing changes in the acetylation levels of H3 and H4 (Meneghini et al., 2003). Furthermore, this defect could be circumvented by deleting the *sir2* gene (Meneghini et al., 2003). This evidence strongly supports the involvement of H2A.Z in maintaining the boundary between heterochromatin and euchromatin, hence acting as an antisilencing factor. A more recent analysis by the same group further suggests that H2A.Z and the Set1 enzyme (which catalyzes methylation at H3 K4) cooperate to prevent

the action of Sir3 at many regions across the yeast genome (Venkatasubrahmanyam et al., 2007). As previously mentioned, evidence suggestive of a boundary function for H2A.Z in vertebrates comes from studies indicating the presence of this protein at insulator regions (Barski et al., 2007; Bruce et al., 2005; Fu et al., 2008). Given this information, it is tempting to think that antisilenced and transcriptionally poised chromatin may in fact be, if not the same, very similar states. Thus, if we think of chromatin as existing as silenced condensed heterochromatin, active open euchromatin, or an intermediate poised state, it becomes easier to reconcile how H2A.Z can facilitate transcription while being removed from promoters once transcription is actually occurring. Moreover, evidence of the poised state suggests that it can be associated with assembled, but stalled complexes containing RNA Pol II (Hargreaves et al., 2009), thus explaining observations of an association of H2A.Z with Rbp1 (Adam et al., 2001; Hardy et al., 2009). Nevertheless, the 'poising hypothesis' does not necessarily assume poising for the sake of transcriptional activation, since poising for the purpose of repression and heterochromatin formation could also be possible.

Epigenetic transcriptional memory

Another recent and extremely interesting function proposed for H2A.Z is in mediating epigenetic transcriptional memory. Evidence for this function so far comes from yeast studies where it was shown that when the inducible *INO1* and *GAL1* genes are activated for the first time after having been repressed long term, this activation results in their physical translocation to the nuclear periphery (Brickner et al., 2007). This localization is maintained throughout several cell divisions and is mediated by the placement of H2A.Z

within the promoters (Brickner et al., 2007). Furthermore, once the genes have become short term repressed, their reactivation is much more rapid than when they are long term repressed, and this rapid reactivation also requires H2A.Z (Brickner et al., 2007). This model suggests that there is a difference in the way that genes are activated for the first time after long term repression, and how they are reactivated after short term repression. To this end, H2A.Z serves a marker function where it could indicate which genes have been activated recently within a given cell type and pass this information on to daughter cells. Given that H2A.Z has been shown to interact with the nuclear pore complex (NPC)-associated protein Nup2 (Dilworth et al., 2005) and that interaction with the NPC has been shown to increase gene transcription as well as prevent the spread of silent telomeric domains (Ishii et al., 2002), it is very possible that the functions of H2A.Z as a transcriptional activator, a boundary element maintainer, and an epigenetic marker could all be related. An interesting area of research will most definitely prove to be how H2A.Z placement is inherited, and whether these mechanisms are conserved in higher organisms.

The role of H2A.Z in heterochromatin

Despite significant evidence that H2A.Z may play several roles in euchromatin, evidence also suggests that it functions in heterochromatin and in chromosome segregation. In 2003, Rangasamy and colleagues examined trophoblast cells of the developing mouse embryo by immunofluorescence and determined that H2A.Z localized to the highly condensed constitutive heterochromatin of the pericentric region. They also saw that H2A.Z was present, but relatively depleted from the facultative heterochromatin of the inactive X chromosome (Rangasamy et al., 2003). Furthermore, the same authors found

that H2A.Z interacts with the centromere-interacting passenger protein INCENP (Rangasamy et al., 2003). It was later shown that in mature cells, the small amount of H2A.Z seen in the pericentric chromatin is likely due to its localization surrounding one side of the centromere which is found buried within the surrounding pericentric region (Greaves et al., 2007). Depletion of H2A.Z by RNAi revealed severe defects in chromosome segregation that were attributed to improper centromere chromatin architecture (Greaves et al., 2007), and purified centromeric nucleosomes containing the histone H3 variant Cenp-A were shown to be associated with H2A.Z (Foltz et al., 2006). Moreover, studies in yeast also indicate that depletion of H2A.Z results in increased chromosomal loss (Krogan et al., 2004). All together, these studies suggest that H2A.Z is involved in promoting the appropriate chromatin architecture that is required at centromeres to allow for the faithful transmission of genetic material, a function that could underlie its indispensability for survival in many organisms. Perhaps it is even possible that this function at centromeres could be very broadly related to another potential function of H2A.Z, marking regions of the genome to be brought to the nuclear periphery. This function would then presumably be employed when the spindle apparatus attaches to kinetochores and separates sister chromatids during mitosis. Indeed, mutations in H2A.Z and its deposition machinery (SWR1 complex) have been shown to partially recapitulate the effects of mutations in several kinetochore proteins (Krogan et al., 2004).

Post-translational modifications of H2A.Z

An interesting observation was made by Peter Cheung's group when they examined the relatively small amount of H2A.Z present within the facultative heterochromatin of the

inactive X chromosome in mouse cells. They determined that this H2A.Z was ubiquitinated at one of several possible lysine residues in the C-terminal tail (Sarcinella et al., 2007). As ubiquitinated H2A.Z was not seen at other regions of the genome, they concluded that this post-translational modification marks and defines a population of H2A.Z for the unknown function it serves on the inactive X chromosome. This raises the possibility that other PTMs could also perhaps specify fractions of H2A.Z for designated function, either by altering the structure of the H2A.Z-containing nucleosome, or by recruiting different interacting partners to mediate downstream effects.

Besides ubiquitination, two other PTMs have been identified on H2A.Z, N-terminal tail acetylation, and C-terminal SUMOylation. Of these, by far the best studied is acetylation which was shown to be present on lysines K3, K8, K10 and K14 of yeast H2A.Z, with K14 being the most predominant site (Babiarz et al., 2006; Keogh et al., 2006; Millar and Grunstein, 2006). So far, two enzymes have been shown to acetylate H2A.Z in yeast; Esa1 is the catalytic HAT of the NuA4 complex, and Gcn5 is the HAT within the SAGA complex. That acetylation plays an important role in H2A.Z biology is demonstrated by it being essential for viability in *Tetrahymena* (Ren and Gorovsky, 2001) and in yeast when combined with mutations in H4 at lysine residues that are also acetylated by NuA4 (Babiarz et al., 2006). Genome-wide localization of K14 acetylated H2A.Z in yeast indicates that this form is associated with the promoters of actively transcribing genes, while the unacetylated form is present at non-transcribing genes (Millar and Grunstein, 2006). Therefore it is possible that like ubiquitination, acetylation specifies a population of H2A.Z for an unknown function in transcription. Indeed, this notion is corroborated by

studies in chicken cells where acetylated H2A.Z was shown to be present at the 5' ends of active genes (Bruce et al., 2005).

In an effort to determine the stability of native H2A.Z-containing nucleosomes, our lab has shown that when oligonucleosomes are adsorbed to hydroxyapatite and eluted with a salt gradient, the H2A.Z/H2B dimers elute at higher salt along with the H3/H4 tetramers compared to canonical H2A/H2B dimers (Thambirajah et al., 2006). This indicates H2A.Z-containing nucleosomes are slightly more stable than those containing H2A; however, this increased stability was abolished when the histones were acetylated by treatment of the cells with sodium butyrate to inhibit histone deacetylases (Thambirajah et al., 2006). In a later study, our group also determined that acetylation of the N-terminal tail of H2A.Z is necessary, in combination with acetylation of the other core histones, to destabilize the H2A.Z-containing nucleosome (Ishibashi et al., 2009b) (see chapter 2). Furthermore, it was shown in yeast that H2A.Z is acetylated only after it has been incorporated into chromatin (Millar and Grunstein, 2006), supporting the notion that once H2A.Z is present at a promoter, its subsequent acetylation could decrease the stability of the nucleosome rendering them more amenable to chromatin remodelling machineries.

H2A.Z SUMOylation has only recently been described in yeast (Kalocsay et al., 2009). Little is known about this modification on H2A.Z except that it can occur at either K126, K133 or both residues, and that it is involved in the double-stranded break (DSB) repair pathway (Kalocsay et al., 2009). Interestingly, this group determined that in response to a persistent DNA DSB, the broken chromosome becomes associated with the nuclear

periphery and this association is dependent on H2A.Z and its SUMO modification (Kalocsay et al., 2009). This again suggests that H2A.Z is involved in localizing specific regions of the genome to the nuclear periphery and that a PTM can specify a population of H2A.Z for a specific function, namely DSB repair. The existence of SUMOylated H2A.Z in higher organisms and whether it also functions in DSB repair will no doubt be addressed very soon.

Deposition of H2A.Z into chromatin

How does H2A.Z become incorporated into chromatin? The discovery of the SWR1 complex as a specific deposition vehicle of H2A.Z/H2B dimers greatly increased our understanding of histone variant exchange in yeast. SWR-C is a 13 subunit complex that is required for the recruitment and exchange of H2A.Z into chromatin, and that interacts with a panoply of other proteins and complexes involved in transcription by RNA Pol II and in chromatin modification and remodelling (Kobor et al., 2004; Krogan et al., 2004; Mizuguchi et al., 2004). One of the subunits of the SWR1 complex, Swr1, is a member of the Swi2/Snf2 family and has ATPase activity (Mizuguchi et al., 2004). Other members of the complex, Act1 and Arp4, are both components of the NuA4 histone acetyltransferase complex and the Ino80 remodelling complex (Krogan et al., 2004). The SWR1 complex specifically catalyzes the ATP-dependent exchange of H2A.Z/H2B dimers with the canonical H2A/H2B dimer within the nucleosome (Mizuguchi et al., 2004) and the specificity of the interaction with the H2A.Z/H2B dimer occurs via the C-terminal region of H2A.Z and the Swc2 subunit (Wu et al., 2005) and through interactions between H2A.Z and Swr1 (Wu et al., 2009). The direct effects of Swr1

complex-mediated recruitment and exchange of H2A.Z on transcription indicate that both activation and repression are possible outcomes (Krogan et al., 2004; Meneghini et al., 2003; Mizuguchi et al., 2004). Interestingly, the genes that are activated by the SWR1 complex and H2A.Z tend to cluster near telomeres, whereas SWR1- and H2A.Z-repressed genes are not preferentially located at these regions (Krogan et al., 2004; Meneghini et al., 2003). Moreover, sites of H2A.Z recruitment into non-transcribed regions are near telomeres and correspond to places where Sir proteins are present (Krogan et al., 2004).

One of the proteins that both the SWR1 complex and H2A.Z were shown to interact with was the bromodomain-containing protein, Bdf1 (Krogan et al., 2004). Bdf1 binds the acetylated tails of histones H3 and H4 and stimulates gene expression near silent heterochromatin (Ladurner et al., 2003). The presence of H2A.Z, SWR-C, and Bdf1 at boundary regions between heterochromatin and euchromatin provide evidence that these proteins may function as barriers against histone deacetylation and the formation of heterochromatin mediated by Sir proteins (Figure 1). It is perhaps not surprising to see that proteins involved in preventing the spread of heterochromatin are linked to transcriptional activation in these regions since basic and gene-specific transcription factors would need to associate at the promoters, and this area of the genome would require special boundary elements to inhibit the formation of Sir-silenced heterochromatin.

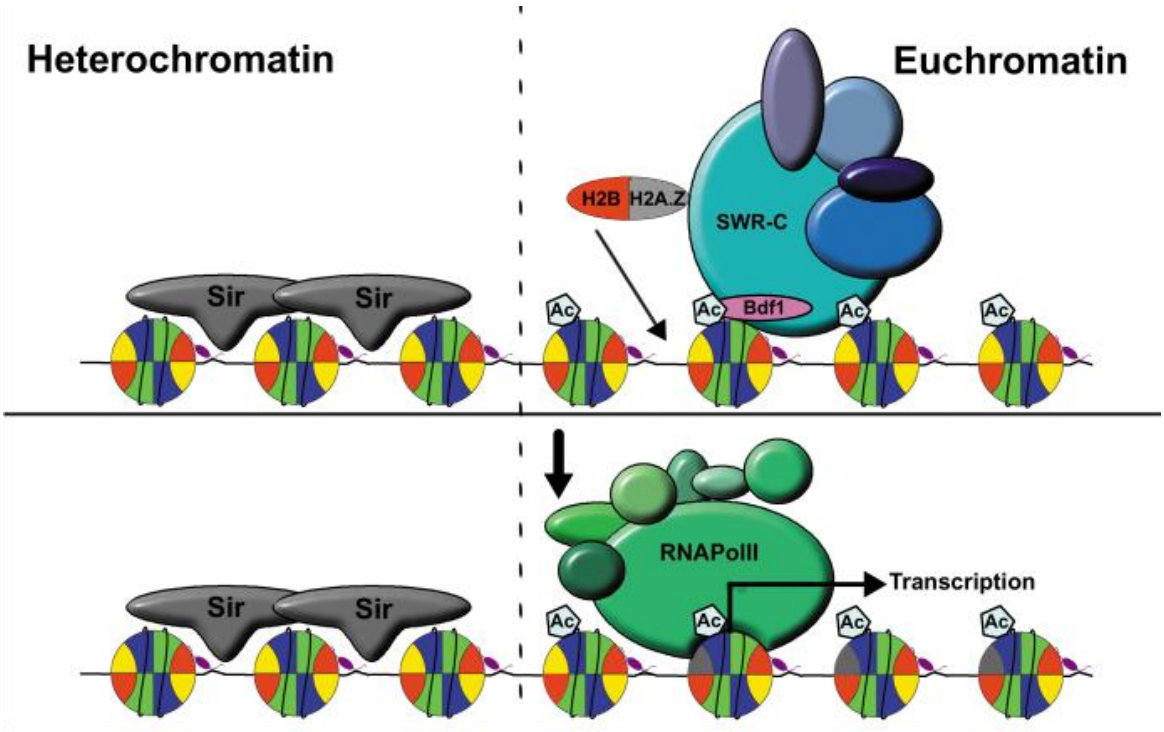

Figure 1: H2A.Z involvement at boundary elements.

Hypothetical involvement of H2A.Z (grey), Bdf1 (pink) and the SWR1 complex (blue) in poising chromatin for transcription at a boundary between heterochromatin and euchromatin in yeast. Heterochromatin is schematically represented as nucleosomes associated with silencing proteins (i.e. Sir proteins). Euchromatic chromatin is acetylated (Ac); Bdf1 is shown binding acetylated H3 (blue). The SWR1 complex is shown binding an H2B (red) H2A.Z (grey) dimer and mediating its exchange within the nucleosome with the H2A (yellow) H2B dimer. In the next frame, RNA polymerase II and associated factors (green) is recruited to H2A.Z-containing chromatin, probably through interactions between Rbp1 and the C-terminal tail of H2A.Z, to initiate transcription. H4 is shown in green and H1 is shown in purple.

In humans, there appears to be more than one complex responsible for depositing H2A.Z at appropriate chromosomal locations. There are two ATPases that are homologues of Swr1, p400 and the Snf-2-related CREB-binding protein activator protein (SRCAP). It has been proposed that the complex containing p400 is the human Tip60 complex that is a fusion between the yeast NuA4 and SWR1 complexes, while the SRCAP complex is distinct (Cai et al., 2005; Doyon et al., 2004; Fuchs et al., 2001). The human Tip60 complex also contains the bromodomain containing protein Brd8 that is a homologue of yeast Bdf1, as well as the Tri-Me H3 K4 binding protein ING3 which is homologous to Yng2 of the yeast NuA4 complex (Altaf et al., 2009). However, a very recent report indicates that SRCAP and p400 are present within the same complex and another complex that contains TIP 48 and TIP 49 as the ATPase that catalyzes exchange of H2A.Z/H2B dimers also exists in HeLa cells (Choi et al., 2009). These observed differences could be a result of the different cell types used in the experiments or they could reflect the dynamic nature of complex assembly as required by the cell. They also suggest that there is more than one mechanism that directs H2A.Z to chromatin that could be regulated by the presence of different subunits within the deposition complex. It is possible that in this way H2A.Z could be directed to different regions of the genome depending on complex assembly and the needs of the cell.

Recently, a specific chaperone for yeast H2A.Z was discovered. This protein, called Chz1, was shown to preferentially bind H2A.Z/H2B dimers over H2A/H2B dimers and to deliver them for incorporation into chromatin by the SWR1 complex (Luk et al., 2007). The interaction between Chz1 and the H2A.Z/H2B dimer was determined to be mostly

electrostatic by NMR (Zhou et al., 2008). Also, H2A.Z/H2B dimers *in vivo* were shown to be roughly equally partitioned between Chz1 and Nap 1, another histone chaperone best known for its ability to bind H2A/H2B (Luk et al., 2007). Nap 1 also co-purified with the SWR1 complex (Mizuguchi et al., 2004), although its role in H2A.Z deposition is unclear. Interestingly, the FACT (facilitates chromatin transcription) complex was shown to bind H2A.Z/H2B dimers in yeast strains harboring genetic deletions of *chz1* and *nap1*, indicating there could be a partially redundant role played by several proteins to provide H2A.Z/H2B dimers for exchange. It will be very interesting and informative to determine if the human homologues of these proteins function in a similar manner and with which human H2A.Z remodeling complexes they associate.

H2A.Z: The structure behind the function

Studies concerning the structural characterization of chromatin complexes containing H2A.Z paint a fairly complex picture of the way in which the variant affects the condensation state and folding stability of these complexes. The crystal structure of the H2A.Z-containing nucleosome core particle shows few differences in overall structural features compared to the major H2A-containing nucleosome (Suto et al., 2000). However, the substitution of Glu 104 in H2A for Gly 106 in H2A.Z was proposed to have a slight destabilizing effect between the H2A.Z/H2B dimer and the H3/H4 tetramer (Suto et al., 2000). Also, a slightly extended acidic patch corresponding to residues in the C-terminal region of H2A.Z and exposed on the surface of the nucleosome was proposed to interact with the N-terminal tail of H4 from a neighbouring nucleosome, or to provide a surface for the interaction of other factors (Suto et al., 2000). Evidence that H2A.Z

slightly destabilizes the NCP also came from early studies in our lab using recombinant histones. These biophysical studies indicated that the H2A.Z-containing NCP had a less compact conformation and was less stable than the H2A-containing particle as determined by analytical ultracentrifuge analysis (Abbott et al., 2001). This finding was also corroborated in yeast using different methods (Zhang et al., 2005). However, using fluorescence resonance energy transfer (FRET), it was demonstrated that H2A.Z stabilizes the nucleosome (Park et al., 2004). Moreover, a later analysis by our lab also indicated that NCPs reconstituted with purified native H2A.Z exhibited a more compact conformation and an enhanced stability compared to those reconstituted with canonical H2A (Thambirajah et al., 2006). The adsorption of native chromatin to hydroxyapatite and elution with an increasing salt gradient also corroborated the biophysical data and showed that H2A.Z/H2B dimers dissociate from the nucleosome at higher salt than H2A/H2B dimers, which indicates that the H2A.Z/H2B dimer is held more tightly to the H3/H4 tetramer (Thambirajah et al., 2006). The contradictory nature of these findings is perplexing but it could be attributed to several things, including the origin of the histones used in the different experiments (recombinant or native) and also the possible influence of post translational modifications on native histones.

An interesting question arises when considering the composition of an NCP containing any histone variant. Are both molecules within the NCP replaced with the variant, or is only one copy replaced? In the case of H2A.Z, the question becomes whether the NCP contains one or two H2A.Z/H2B dimers, with the other dimer in a heterotypic NCP presumably being H2A/H2B. Interestingly, the H2A.Z/H2B dimer has been shown to be

significantly less stable than the H2A/H2B dimer (Hoch et al., 2007; Placek et al., 2005; Thambirajah et al., 2006), though the functional meaning of this observation is unknown. It was initially suggested from the crystal structure that the heterotypic H2A.Z nucleosome would be unlikely to exist (Suto et al., 2000). Later studies proved this to not be the case since nucleosomes containing one H2A.Z/H2B dimer and one H2A/H2B dimer could be assembled *in vitro* (Chakravarthy et al., 2004; Ishibashi et al., 2009b). Immunoprecipitated Flag epitope-tagged H2A.Z-containing NCPs also demonstrate the existence of a heterotypic particle in transfected cell line experiments (Dryhurst et al., 2009; Sarcinella et al., 2007; Viens et al., 2006). It is therefore unknown whether a heterotypic particle truly exists *in vivo,* and the question of the conformation and stability of such particle is an open one.

Biophysical characterization of *in vitro* reconstituted chromatin fibers containing H2A.Z as the sole H2B partner has also had conflicting results. Abbott and colleagues (2001) showed by sedimentation velocity experiments that these fibers are less folded than their H2A-containing counterparts, while another group showed that they have a higher degree of intramolecular folding (Fan et al., 2002). The authors of this latter study also showed that H2A.Z-containing chromatin fibers show reduced fiber-fiber interactions, but that the degree of fiber folding of these was greater in the presence of HP1α than with H2A-containing fibers (Fan et al., 2002; Fan et al., 2004). This was taken as evidence to support a role for H2A.Z in mediating the binding of HP1α at pericentric heterochromatin, a genomic location shown to be enriched in H2A.Z in the developing mouse embryo (Rangasamy et al., 2003). Interpretation of the biophysical results and

their potential *in vivo* relevance is complicated by our lack of knowledge concerning: 1) the homo- or heterotypic nature of the H2A.Z-containing NCP *in vivo*, 2) the likelihood of having large tracks of successive H2A.Z nucleosomes *in vivo*, and 3) the contribution of post-translational modifications of H2A.Z and/or the other histones to the structure of the fiber. Indeed, several studies have indicated that H2A.Z preferentially associates with H3 Tri-Me K4 compared to H2A (Dryhurst et al., 2009; Sarcinella et al., 2007; Viens et al., 2006) and that these nucleosomes protect less DNA (Fu et al., 2008).

Finally, another important structural feature of H2A.Z-containing nucleosomes is their ability to preferentially occupy distinct positions along a DNA sequence. While all nucleosomes adopt a major location along a defined positioning sequence, a percentage of those nucleosomes adopt an alternate position. It was shown that when tandemly repeated arrays of a portion of the 5S ribosomal RNA gene from *Lytechinus variegatus* were reconstituted with H2A.Z nucleosomes, they tended to prefer the major position over H2A-containing nucleosomes (Fan et al., 2002). In another study, it was shown that the thermal mobility of H2A.Z nucleosomes was greater than that of H2A nucleosomes (Flaus et al., 2004). Together these results could imply that H2A.Z nucleosomes are more translationally mobile so that they can find and subsequently assume a DNA sequence-defined position. The biological relevance of these observations could be that H2A.Z serves in part to regularly space the nuclesomes containing it because the spacing itself is somehow relevant for the process in which it is playing a part. This concept is supported by the biological evidence indicating that H2A.Z nucleosomes flanking the NFR are very

well-positioned (Guillemette et al., 2005), as are those surrounding CTCF binding sites (Fu et al., 2008), and at the estrogen inducible TFF1 gene (Gevry et al., 2009).

Conclusions:

In conclusion, it is clear that H2A.Z biology in general is complex. Not only are there many proposed functions for this protein, some that could be more related to one another than others, but there could also be a diversity of structures containing H2A.Z, each with slightly different properties. What is clear is that H2A.Z does not direct nuclear events in isolation; rather, it cooperates with modified forms of other histones and many other proteins to participate in the orchestration of nuclear events. It is within this broader context that we will ultimately understand the function of this extremely interesting histone variant.

Chapter 2: Acetylation of vertebrate H2A.Z isoforms and its effect on the conformation and stability of the nucleosome core particle

Deanna Dryhurst and Juan Ausio

Department of Biochemistry and Microbiology, University of Victoria, Victoria, British Columbia, Canada V8W 3P6

Partially adapted from:

Coon JJ, Ueberheide B, Syka JE, Dryhurst DD, Ausio J, Shabanowitz J, Hunt DF. (2005). Protein identification using sequential ion/ion reactions and tandem mass spectrometry. Proc Natl Acad Sci U S A. 2005 Jul 5;102(27):9463-8.

Thambirajah AA, Dryhurst D, Ishibashi T, Li A, Maffey AH, Ausió J. (2006). H2A.Z stabilizes chromatin in a way that is dependent on core histone acetylation. J Biol Chem. 2006 Jul 21;281(29):20036-44.

Ishibashi T, Dryhurst D, Rose KL, Shabanowitz J, Hunt DF, Ausió J. (2009). Acetylation of vertebrate H2A.Z and its effect on the structure of the nucleosome. Biochemistry. 2009 Jun 9;48(22):5007-17.

Dryhurst D, Ishibashi T, Rose KL, Eirín-López JM, McDonald D, Silva-Moreno B, Veldhoen N, Helbing CC, Hendzel MJ, Shabanowitz J, Hunt DF, Ausió J. (2009). Characterization of the histone H2A.Z-1 and H2A.Z-2 isoforms in vertebrates. BMC Biol. 7,86.

Contributions:

Deanna Dryhurst wrote the chapter. Protein purification for Figures 2 and 3 was performed by Deanna Dryhurst and the mass spectrometry analysis was performed by Joshua Coon and Jeffrey Shabanowitz (Figure 2) and Kristie Rose (Figure 3) in Donald Hunt's lab at the University of Virginia. Deanna Dryhurst performed protein purifications and production and reconstitutions for Figures 4, 5 and 6. Operation of the analytical ultracentrifuge and data analysis was performed by David Bond (Figure 4) and Toyotaka Ishibashi (Figure 5 and 6). All the work associated with Figure 7 was performed by Deanna Dryhurst.

Introduction:

The replication independent histone variant H2A.Z is involved in many cellular processes including transcription, epigenetic memory, chromosomal stability and heterochromatin maintenance (Draker and Cheung, 2009). The structural effect of incorporating H2A.Z into the nucleosome is not entirely clear, since some reports suggest that it could destabilize the NCP (Abbott et al., 2001; Zhang et al., 2005), while others suggest a stabilizing role (Fan et al., 2002; Park et al., 2004; Thambirajah et al., 2006). As a result, how H2A.Z-containing chromatin structures translate into H2A.Z-mediated functions is equally unclear. The general assumption that if H2A.Z were to destabilize the NCP then it could allow greater access to the underlying DNA sequence for purposes like transcription initiation has not yet been conclusively validated. Conversely, if H2A.Z stabilizes the NCP it could support a role for this protein in condensed heterochromatin structures and possibly gene silencing. Genome-wide localization studies of H2A.Z indicate that it can associate with both euchromatin and heterochromatin (Barski et al., 2007; Greaves et al., 2007). Several possibilities that could reconcile these concepts include that the stability of NCPs containing H2A.Z could be DNA sequence- or histone complement-dependent, or it could be dependent on post-translational modification of H2A.Z itself and/or the histone complement. In this regard, acetylation of H2A.Z in conjunction with acetylation of the histone complement could act to destabilize the NCP and thus mediate the increased lability of promoter nucleosomes.

Acetylation of histones occurs by the action of HAT enzymes and its presence is positively correlated with transcription (Choi and Howe, 2009). There is a definite link

between H2A.Z and histone acetylation in several regards. In yeast, the NuA4 acetyltransferase and SWR1 remodelling complex that catalyzes the exchange of H2A/H2B dimers for H2A.Z/H2B dimers share several subunits and these complexes are combined as one within the human Tip60 complex which is a known transcriptional coactivator complex (Altaf et al., 2009). In fact, it has been proposed that one of the mechanisms for directing H2A.Z deposition into chromatin involves recognition of acetylated lysine residues within H3 and H4 by the yeast Bdf1 (human Brd8) protein (Dryhurst et al., 2004; Raisner et al., 2005; Zhang et al., 2005). Furthermore, in yeast acetylation of H4 lysine 16 is required for incorporation of H2A.Z at subtelomeric regions (Shia et al., 2006), and in humans a signature mark of promoters includes multiple acetylated lysine residues within histones as well as the presence of H2A.Z (Wang et al., 2008). The H2A.Z protein itself is also acetylated at lysine residues within the N-terminus in yeast by Esa1 and Gcn5, the catalytic subunits of the NuA4 and SAGA complexes, respectively. Also, a hyperacetylated form of H2A.Z was shown to be present at the promoters of active genes in the chicken (Bruce et al., 2005).

In *Tetrahymena*, H2A.Z was shown to be preferentially associated with active genes of the macronucleus (Allis et al., 1986) and to be acetylated at six possible sites (K4, K7, K10, K13, K16 and K21) within the N-terminal region (Ren and Gorovsky, 2003). In yeast, H2A.Z can be acetylated at K3, K8, K10 and K14, with K14 being the most predominant site (Babiarz et al., 2006; Keogh et al., 2006; Millar et al., 2006). In humans, H2A.Z was also shown to be acetylated; three sites (K4, K7 and K11) have been identified so far (Beck et al., 2006; Bonenfant et al., 2007) but their relative abundances

were not determined. In the present work, we used a mass spectrometry approach to characterize the sites and abundances of N-terminal acetylation on H2A.Z isolated from chicken erythrocytes and a chicken erythroleukemic cell line (MSB cells) treated with sodium butyrate to inhibit histone deacetylases. An unexpected result of this work proved to be the identification of two protein isoforms of H2A.Z present within these cells, now called H2A.Z-1 and H2A.Z-2 (discussed more thoroughly in Chapter 3). The sites of acetylation have thus been determined for both protein isoforms.

Our group has shown that acetylation of H2A.Z by itself and/or in conjunction with acetylation of other core histones destabilizes the association of H2A.Z with native chromatin (Thambirajah et al., 2006). We wanted to extend these findings by characterizing the effect of acetylation on the conformation and stability of reconstituted NCPs containing H2A.Z using the analytical ultracentrifuge. In accordance with our previous results and those concerning the destabilizing role played by acetylation on the nucleosome and chromatin (Ausio and van Holde, 1986; Dunker et al., 2001; Garcia-Ramirez et al., 1995), we hypothesize that acetylation of H2A.Z-containing NCPs will also result in a more open conformation and a destabilized particle compared to non acetylated NCPs.

Materials and Methods:

Native histone H2A.Z purification:

Native H2A.Z in its non-acetylated and acetylated forms was purified from chicken erythrocytes and from chicken MSB cells (chicken erythroleukemic cells transformed by Marek's virus) grown in the presence of 5mM sodium butyrate, respectively (Wang et al.,

2000). Histones were prepared from the isolated nuclei of these two tissues upon HCl extraction (Wang and Ausio, 2001). Nuclei were isolated by washing three times in Buffer A (250mM sucrose, 60mM KCl, 15mM NaCl, 10mM MES (pH 6.5), 5mM $MgCl_2$, 1mM $CaCl_2$, 0.5% Triton X-100) and twice in Buffer B (50mM NaCl, 10mM Pipes (pH 6.8), 5mM $MgCl_2$, 1mM $CaCl_2$) supplemented with 1:100 protease inhibitor cocktail (Roche) with all centrifugations performed at 3000xg. The histones were then acid extracted with 0.4N HCl and the supernatant was precipitated with 6 volumes of cold acetone overnight at -20°C. Approximately 30-40mg of the HCl protein extracts were loaded onto a 1.5 x 120 cm BioGel P-60 (Bio Rad) column and eluted in 50mM NaCl, 20mM HCl at 5 ml/3 fractions/hour. In this chromatographic fractionation, H1 and H5 elute first followed by an H2A/H2A.Z peak and subsequent H2B/H3 and H4 peaks. An H2A.Z-enriched H2A fraction corresponding to the late eluting part of the H2A/H2A.Z peak was dialyzed and lyophilized, and H2A.Z was purified by several rounds of reverse phase HPLC fractionation which combined preparative 1 x 25 cm (300Å and 5µm) C_4 and analytical 0.46 x 25 cm (300Å and 5µm) C_{18} columns from Vydac. Elution was with a gradient from buffer A (0.1% trifluoroacetic acid in water) to buffer B (100% acetonitrile).

Recombinant H2A.Z-1:

The coding region of *HsH2AFZ* (NM_002106) was cloned into the pET11 expression vector (Novagen). For protein expression, the vector was introduced into BL21 (DE3) *E. coli* (Novagen), and the bacteria were grown in 1L Luria broth medium. Cells were grown to an A_{600} of 0.8, and isopropyl β-d-thiogalactoside was added to a final

concentration of 1mM. Cells were harvested after 3 hours by centrifugation at 5,000 x g for 10 min at 4°C. Cell pellets were resuspended in lysis buffer (6M GuHCl, 1mM EDTA, 1mM DTT, 50mM Tris-HCl (pH7.5)), and homogenized for 40 strokes in a Dounce homogenizer. The homogenized sample was dialyzed against 100mM NaCl, 50mM Tris-HCl (pH7.5), 1mM EDTA for 2 hours at 4°C. After dialysis, HCl was added to a final concentration of 0.5N and the cells were centrifuged at 10,000 x g for 15 min at 4°C. Six volumes of cold acetone were added to the supernatant and proteins were precipitated overnight at -20°C. The next day, the sample was centrifuged at 12,000 x g for 10 min at 4°C followed by reverse phase HPLC fractionation using a C18 column.

Nucleosome core particle reconstitution:

Native histones H2A, H2B, H3 and H4 used for NCP reconstitutions were obtained from HeLa cells grown in the absence or presence of 5mM sodium butyrate and subsequently fractionated by reverse phase HPLC (Ausio and Moore, 1998). DNA was obtained from (155 ± 5 bp) DNA nucleosome core particles prepared from micrococcal nuclease-digested chicken erythrocyte chromatin for the experiments in Figure 5 and Figure 6 and represents random sequence DNA (Ausio et al., 1989). The DNA for reconstituted nucleosomes in Figure 4 was (145 ± 5 bp) from the same source. DNA purification was carried out by repeated phenol/chloroform extractions and recovered by ethanol precipitation. A histone protein titration was carried out using SDS-PAGE to ensure that all histones in the final mixture were present in equimolar amounts. The histone mixture thus obtained was dialyzed overnight against 2M NaCl, 10mM Tris-HCl (pH 7.5), 10mM β-mercaptoethanol, and 0.1mM EDTA at 4°C, and was mixed with 155 bp random

sequence chicken erythrocyte DNA in the same buffer, at a histone : DNA ratio of 1.13:1.0 (w/w). Nucleosome core particle reconstitution was carried out using salt gradient dialysis (Ausio and Moore, 1998). The integrity of the core particles was analyzed by 4% native PAGE and sedimentation velocity in the analytical ultracentrifuge (see below). Table 1 summarizes the different reconstituted NCPs used in this work.

Table 1: Summary and nomenclature of the reconstituted NCPs used in this work according to their histone composition.

Name	H2A variant	Histone complement
2A-N	H2A[(1)]	Native (N)[(1)]
r2AZ-N	rH2A.Z[(2)]	Native (N)
2A*-N*	Ac*H2A[(3)]	Acetylated (N*)
2AZ*-N*	Ac*H2A.Z[(4)]	Acetylated (N*)

[(1)] Native (N) histones obtained from HeLa cells.

[(2)] Recombinant human H2A.Z.

[(3)] Native-acetylated (N*) histones obtained from butyrate-treated HeLa cells.

[(4)] Native (H2A.Z) obtained from butyrate-treated chicken MSB cells.

(*) The asterisks denote acetylation.

Analytical ultracentrifuge:

Reconstituted NCPs were dialyzed against buffers of varying ionic strengths and were subjected to analytical ultracentrifuge analysis (Ausio et al., 1989). Briefly, sedimentation velocity runs were performed in a Beckman XL-I analytical ultracentrifuge (Beckman-Coulter Instruments, CA, USA) in an An-55 Al aluminum rotor using cells with double sector aluminum-filled Epon centerpieces. A value of 0.650cm/g was used for the partial specific volume of the NCP (Ausio et al., 1989). Absorbance scans were routinely

obtained at 260nm and the boundaries were analyzed as described in (Ausio and Moore, 1998) with the help of UltraScan 8.0 sedimentation data analysis software (Borries Demeler, Missoula, MT, USA).

Top-down mass spectrometry using sequential ion/ion reactions to identify H2A.Z isoforms:

Histone H2A.Z purified from chicken erythrocytes (~10pmol) (see above) was pressure-loaded onto a monolithic capillary column (360 × 100μm i.d., 5cm column length, LC Packings, Sunnyvale, CA) equipped with a 30μm SilicaTip electrospray ionization emitter (New Objective, Woburn, MA) and gradient-eluted with a linear gradient of 0–60% B for 12min and 60–100% B for 2min (A = 0.1 M formic acid, B = 70% acetonitrile in 0.1 M formic acid, flow rate = 1 μl/min). An Agilent Technologies (Palo Alto, CA) 1100 Series binary HPLC system was interfaced with the linear quadrupole ion trap mass spectrometer for online protein/peptide separations. Sequential ion/ion reactions were performed as detailed in (Coon et al., 2005). Briefly, the H2A.Z proteins were reacted for 15ms with the radical anions of fluoranthene in an electron transfer dissociation (ETD) reaction that results in extensive peptide backbone dissociation. The multiply charged peptides were then reacted with benzoic acid in a proton transfer charge reduction (PTR) reaction. All mass spectrometry analysis was performed using a commercial RF linear quadrupole ion trap (LTQ), the Finnigan LTQ mass spectrometer (Thermo Electron) equipped with either a modified factory nano-flow electrospray ionization source (chromatography experiments) or a nanospray robot (Advion Biosciences, Ithaca, NY; infusion). The LTQ was modified to accept a Finnigan 4500 chemical ionization source

(Thermo Electron) placed at the rear of the instrument (Syka et al., 2004). A batch inlet was used to volatilize molecules of both fluoranthene and benzoic acid into the chemical ionization source, where an electron beam generated anions of both species. The instrument control software (itcl) was modified to accommodate the following sequence after precursor ion selection (isolation width 4 *m*/*z* units) and storage: (*i*) anion injection (≈2 ms); (*ii*) fluoranthene anion isolation (*m*/*z* 202, 10 ms); (*iii*) ion/ion reaction of anion and precursor cation (≈10–15 ms); (*iv*) removal of excess fluoranthene anions and storage of ETD products; (v) injection of anions (≈2 ms); (*vi*) application of selective waveform to remove *m*/*z* 202 and other background anion species (≈5 ms); (*vii*) ion/ion reaction of purified benzoic acid anions (*m*/*z* 121) with ETD product ions (≈100–150 ms); and (*viii*) removal of excess benzoic acid anions and mass analysis of product ions.

Mass spectrometry to identify sites of H2A.Z acetylation:

Upon purification of H2A.Z as described above, the H2A.Z fraction purified from sodium butyrate treated MSB cells was lyophilized and reconstituted in 100mM ammonium bicarbonate, pH 8. An aliquot (10%) of each fraction was treated with propionic anhydride to derivatize unmodified ε-amino groups of lysine residues. Chemical derivatization with propionic anhydride converts the amino groups to their corresponding propionyl amides, and these methods have been detailed previously (Garcia et al., 2007). In brief, equal volumes of propionylation reagent (15µL) and H2A.Z (15µL) were reacted, and derivatization was performed twice to ensure full conversion. The sample was vacuum-dried after each derivatization. The two derivatized H2A.Z samples were then digested with 4ng trypsin (Promega) for 8 hours at 37°C.

Derivatization blocks lysine residues from cleavage, and thus trypsin cleaves C-terminal to arginine residues only. Following digestion, the samples were again reacted with propionic anhydride to derivatize the amino-termini of the trypsin-generated H2A.Z peptides. Both samples were dried a final time in a speed-vac concentrator, and were subsequently reconstituted in 0.1% acetic acid.

The resulting H2A.Z peptide mixtures were analyzed via tandem mass spectrometry. Each sample was pressure-loaded onto a capillary pre-column (360μm O.D. x 75μm I.D. fused silica) packed with 4cm of C18 reverse phase resin (5-20μm diameter). After washing for 5 min with 0.1% acetic acid, the pre-column was connected to an analytical column (360μm O.D. x 50μm I.D. fused silica) packed with 8cm of C18 (5-μm diameter) resin and equipped with an electrospray emitter tip as previously described (Martin et al., 2000). H2A.Z peptides were eluted using nanoflow HPLC with an 1100 series HPLC pump (Agilent Technologies), and a 60nL/min flow rate was achieved by splitting the flow from the HPLC. The gradient consisted of 0-60 %B in 50 min and 60-100 %B in 10 min (solvent A: 0.1 M acetic acid, solvent B: 70 % acetonitrile, 0.1 M acetic acid). Gradient-eluted peptides were ionized using an electrospray ionization source, modified for nanospray, and were analyzed using a hybrid quadrupole linear ion trap Fourier transform (LTQ-FT) mass spectrometer (Thermo Scientific). The LTQ-FT instrument was operated with a data-dependent method, which consisted of acquisition of a full scan mass spectrum using the FT as analyzer followed by ten MS/MS scans of the ten most abundant ions in the initial full scan. Full scan mass spectra were acquired for m/z 300-2000 using a resolution of 100,000. Upon collision-activated dissociation (CAD) of

precursor ions, MS/MS spectra were acquired using the ion trap as the analyzer. Dynamic exclusion was enabled by which precursor ions were selected for dissociation two times within 20s before they were added to the exclusion list for 30s. All CAD MS/MS spectra were interpreted via manual validation for identification of the N-terminal peptides of both H2A.Z isoforms. Accurate mass measurements acquired in the FT were utilized to generate selected ion chromatograms (SICs). A window of +/- 0.005 Da around the theoretical monoisotopic m/*z* values of the $[M+2H]^{+2}$ and $[M+3H]^{+3}$ ions was used to generate the SICs for the N-terminal peptides of H2A.Z-1 and H2A.Z-2.

Polyacrylamide gel electrophoresis:

Proteins were analyzed by 15% SDS-PAGE. Gels were then stained with 0.2% (w/v) Coomassie blue in 25% (v/v) isopropanol/10% (v/v) acetic acid and destained in 10% (v/v) isopropanol/10% (v/v) acetic acid. DNA and nucleosome core particles were analyzed by 4.5% native-PAGE (acrylamide;bis acrylamide 29:1) in 0.5 x TBE (45mM Tris-HCl (pH 7.5), 45mM boric acid 1mM EDTA).

Chromatin fractionation, Western blot analysis and PCR:

HeLa S3 cells were grown in suspension to a density of $5x10^5$ cells/ml in the presence or absence of 5mM sodium butyrate. S1, SE and P chromatin fractions were obtained by isolating nuclei at a DNA concentration of 2mg/ml in 50mM NaCl, 1mM $CaCl_2$, 5mM $MgCl_2$, 10mM PIPES (pH 6.8) buffer and digesting with micrococcal nuclease (Worthingon) at 30U per mg of DNA for 5 min at 37ºC. The reaction was stopped by addition of EDTA to a final 10mM concentration on ice and the sample was centrifuged

at 10,000 x g for 10min at 4 ºC to yield an S1 supernatant and a pellet. The pellet was resuspended and lysed in 0.25mM EDTA (pH 8.0) and stirred for one hour at 4ºC. Upon centrifugation as before, a supernatant SE and a final pellet P were thus obtained. Under the experimental conditions used here approximately S1, SE and P correspond to 5-10%, 25-30% and 60-65% of the total nuclear DNA. Western blotting was performed on the protein components of these fractions using SDS-PAGE and transferred to polyvinylidene fluoride (PVDF) membrane for 3 hours at 100V using standard procedures. Histone H3 Tri Me K27 antibody was from Abcam and was used at 1: 5000 dilution, the H4 antibody was produced in house and was used at 1:10,000 dilution, the tetra-acetylated H4 (H4 Pan Ac) antibody was from Millipore and used at a 1:5000 dilution, and the acetylated H2A.Z antibody (Bruce et al., 2005) was a kind gift from Dr. Crane-Robinson and was used at a 1:1000 dilution.

For the PCR analysis, a 147 bp fragment of the human protamine 1 gene was amplified from equal amounts of DNA from the S1, SE and P fractions using the following two primers: Forward: CTT TGC CCT CAC AAT GAC C; Reverse: GGC TTG GCT GAA TGC TCA. The fragment was selected from the chromatin organization of the rat protamine 1 gene (Adroer and Oliva, 1998) but using the DNA sequence of the highly homologous human counterpart. It encompasses a full NCP at the promoter region. Amplification was carried out with 32 cycles of: 95 ºC, 30 sec; 60 ºC, 30 sec; 72 ºC, 30 sec and final extension: 72 ºC, 7 min. The enzyme was platinum *Taq* DNA polymerase (Invitrogen).

Results:

Native H2A.Z from chicken is composed of two protein isoforms, H2A.Z-1 and H2A.Z-2

Total H2A.Z isolated from chicken erythrocytes was shown to be composed of two protein isoforms. Figure 2A shows the online chromatographic elution profile of this protein mixture, while Figure 2B shows the *m/z* spectrum for the two distinct protein forms with masses of M_r~13,380 Da and 13,456 Da. The lighter protein (13,380 Da) corresponds to the mass of H2A.Z described in the chicken. To identify these proteins by mass spectrometry and to determine the cause of the 76 Da increase in mass of the heavier protein, precursor *m/z* peaks were selected for sequential ion/ion reaction (15ms ETD/150ms PTR). The spectrum of the ions generated in this way identified the lower mass species as unmodified histone H2A.Z (H2A.Z-2). The c- and z-type ion series define approximately 30 residues from both the N- and C-termini of this protein (Figure 2C). The product ion spectrum for the heavier species shows a *m/z* shift of 30 units at residues 12 and 14 compared to the H2A.Z-2 sequence (Figure 2D). The replacement of alanine by threonine at residues 12 and 14 of the heavier species corresponds to this mass shift. A mass shift of 28 units was also seen in the z-type ion series which can be located to the first 3 amino acids from the C-terminus of the protein. A BLAST search (Altschul et al., 1990) was conducted to identify other H2A.Z isoforms in chicken with the expected amino acid changes. A protein was returned from this search with the same amino acid sequence as that identified by sequential ion/ion reactions having threonine residues at position 12 and 14. This protein was annotated as a hypothetical protein from chicken and was not described as an H2A.Z isoform. We refer to this protein as H2A.Z-1

(see discussion). Four amino acid substitutions were revealed in the sequence of hypothetical protein (H2A.Z-1) compared to H2A.Z-2: A12T, A14T, T38S, A128V. The substitution of valine for alanine at residue 128 corresponds to the mass increase of 28 units observed in the z-type ion series. The changes in these 4 amino acids corresponds to a mass change of 74 Da which agrees with the overall shift in mass of 76 Da observed by the full *m/z* scan. Tandem mass spectrometry of peptides generated by Glu-C digest confirmed that the isolated protein contained the described amino acid changes (data not shown).

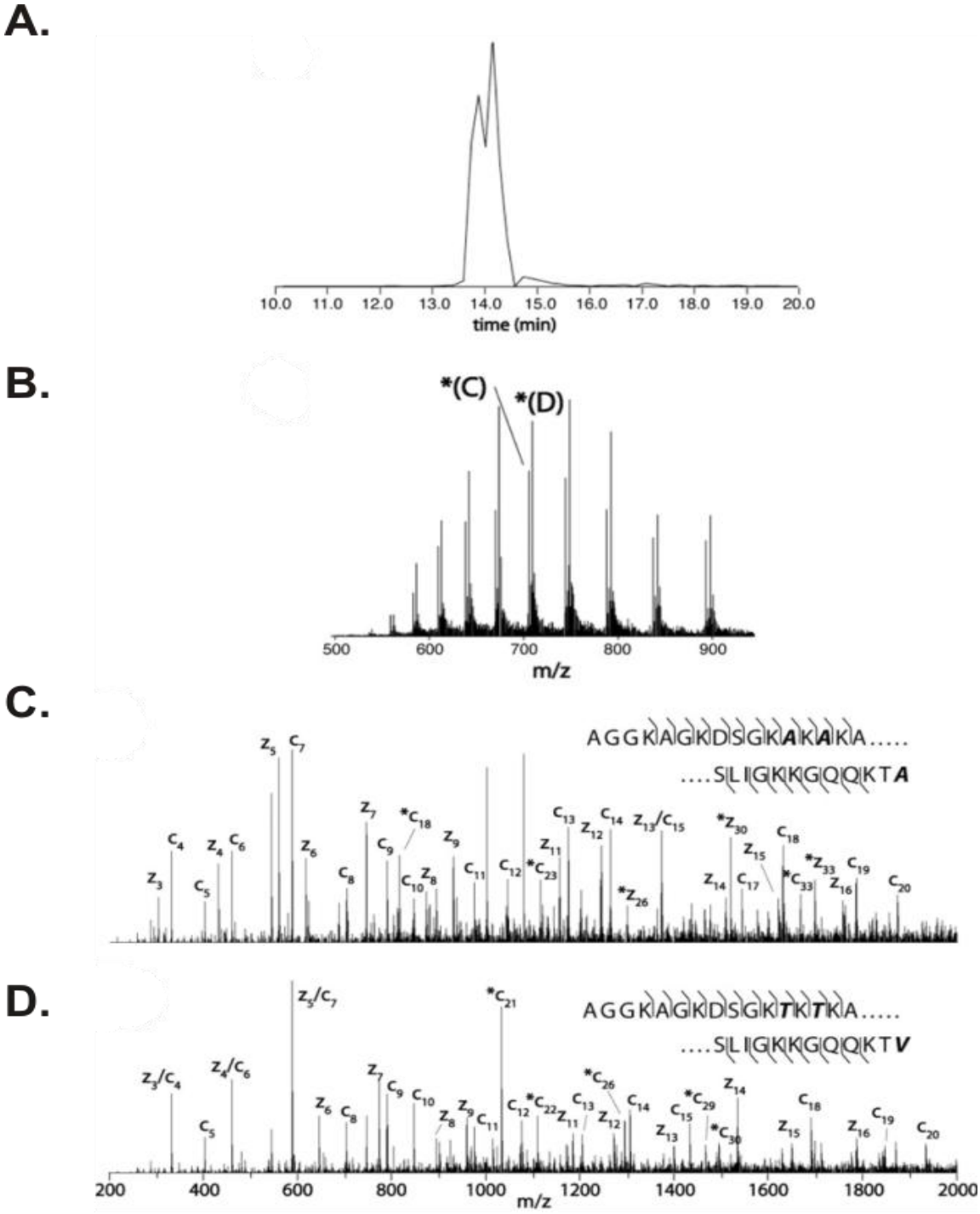

Figure 2: Analysis of a mixture of chicken H2A.Z isoforms by on-line chromatography and sequential ion/ion reactions.

A.) Chromatogram of the protein separation. B.) The protein charge envelope of two coeluting proteins and the corresponding *m/z* values that were selected for interrogation. C.) The resulting tandem mass spectrum after dissociation of the lighter *m/z* species, unmodified histone H2A.Z. D.) The resulting tandem mass spectrum after dissociation of the heavier protein. Comparison of the c- and z-type fragment series indicates the presence of a new H2A.Z isoform with four amino acid substitutions. The y-axis indicates the relative ion abundance; the asterisk (*) denotes a doubly charged c- or z-type fragmentation.

The N-terminal tails of H2A.Z-1 and H2A.Z-2 are acetylated *in vivo* in chicken cells

In order to determine the acetylated residues within the N-termini of both H2A.Z isoforms, purified total H2A.Z from chicken erythrocytes and sodium butyrate-treated chicken erythroleukemic cells was analyzed by tandem mass spectrometry. Chicken erythrocytes were used to give an indication of the acetylated species present within an intact tissue, while sodium butyrate-treated cells were used to determine which residues can be acetylated when histone deacetylases are inhibited. Purified H2A.Z was derivatized with propionic anhydride to limit trypsin digestion to arginine residues. The H2A.Z peptides were next analyzed by LC-coupled tandem mass spectrometry which enabled sequence determination of the first 19 residues of both H2A.Z-1 (AGGKAGKDSGKTKTKAVSR) and H2A.Z-2 (AGGKAGKDSGKAKAKAVSR). This technique also afforded the identification of multiple acetylation sites on both of the N-terminal peptides from the sodium butyrate-treated sample. Figure 3A and B illustrate the MS/MS spectra of the most abundant form of the N-terminal peptide identified in the sodium butyrate-treated sample which was a triply-acetylated form with acetylation present on K4, K7 and K11. In fact, four different forms of the H2A.Z-1 and H2A.Z-2 N-terminal peptides were detected. Selected ion chromatograms, shown in Figure 3C, illustrate the presence and abundance of the unmodified, singly-acetylated, doubly-acetylated, and triply-acetylated peptides from both H2A.Z isoforms.

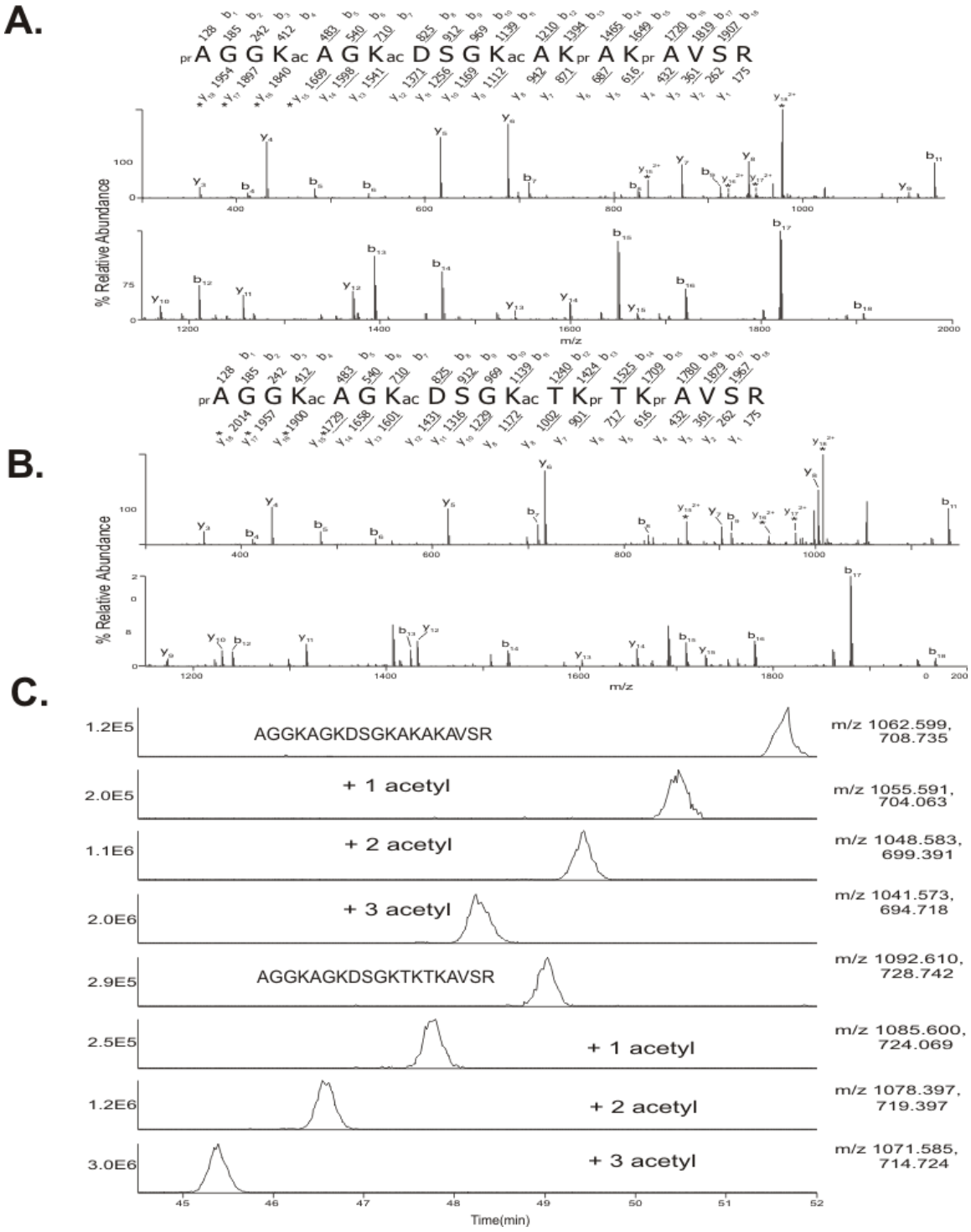

Figure 3: Tandem mass spectrometry analysis of acetylated H2A.Z-2 and H2A.Z-1 N-terminal peptides isolated from chicken.

A.) MS/MS spectrum of the N-terminal H2A.Z-2 peptide, AGGKAGKDSGKAKAKAVSR. The peptide is modified with three acetyl groups on lysines 4, 7, and 11. B.) MS/MS spectrum of the triply-acetylated N-terminal peptide, AGGKAGKDSGKTKTKAVSR, of H2A.Z-1. The acetyl groups were again identified on lysines 4, 7, and 11. The precursor ions selected for dissociation were the $[M+2H]^{+2}$ ions, and are *m/z* 1041.1 (A.) and *m/z* 1071.1 (B.), respectively. The amino acid sequences are shown above the spectra, and the masses above and below the sequences correspond to the theoretical b- and y-type product ions. The masses provided are the monoisotopic, nominal masses of the product ions. The observed, singly-protonated b- and y-type ions are underlined and are assigned to their corresponding *m/z* peaks in the spectra. The observed, doubly-protonated ions are denoted with asterisks. The acetylated lysines (K4, K7, and K11) are indicated with "ac". The unacetylated amino groups were derivatized with propionic anhydride and are denoted with "pr". C.) Selected ion chromatograms (SICs) for the N-terminal peptides of H2A.Z-2 and H2A.Z-1. The theoretical *m/z* values of the $[M+2H]^{+2}$ and $[M+3H]^{+3}$ ions for each peptide were used to generate the SICs, and these values are adjacent to each chromatogram. Note that the retention time decreases with increasing number of acetyl groups due to the loss of propionylated lysine. The ion count intensities for each SIC are located on the y-axis and are provided on the left adjacent to each chromatogram.

A comparison of the relative abundances of each ion species was performed for the N-terminal peptide of the H2A.Z-2 isoform in native chicken erythrocytes and the sodium butyrate-treated cells since this is the isoform that has been known as H2A.Z in the chicken. Table 2 indicates that 90% of the H2A.Z-2 N-terminus is unmodified in chicken erythrocytes, whereas the unmodified N-terminal peptide has a relative abundance of 40% in the butyrate-treated cells. While all five lysine residues were found to be singly-acetylated, the incidence of acetylation on K4 occurs with approximately the same frequency as that on K7, and these are both more abundant than single acetylation on K11, K13, or K15 (Table 2). This pattern of acetylation on the H2A.Z-2 N-terminal lysine residues can be seen in both the native erythrocytes and the sodium butyrate-treated erythroleukemic MSB cells. The doubly acetylated forms of the N-terminal peptide that were identified included the following: K4 + K7, K7 + K11, and K4 + K11 (Table 2). These forms were identified in both the untreated and treated cells. Furthermore, triply acetylated N-terminal peptides were also identified, with the predominant species containing acetyl groups on K4, K7 and K11; this form accounts for more than 95% of all triply acetylated species detected. In the native chicken erythrocytes, the triply acetylated species are present at less than 0.1%, whereas these species account for 20% of the N-terminal peptide forms in the sodium butyrate-treated cells.

Table 2: Sites of chicken H2A.Z-2 acetylation and their relative abundances.

A) N-terminal peptide of H2A.Z-2 from native chicken erythrocytes

AGG**K**AG**K**DSG**K**A**K**A**K**AVSR

Modification	**Percent of total sample**	**Modified lysine residues**
Unmodified	90%	
Singly-acetylated	9%	K4=K7 >K11 >K13 >>K15
Doubly-acetylated	<1%	(K4+K7), (K7+K11), (K4+K11)
Triply-acetylated	<0.1%	(K4+K7+K11)

B) N-terminal peptide of H2A.Z-2 from sodium butyrate-treated MSB cells

AGG**K**AG**K**DSG**K**A**K**A**K**AVSR

Modification	**Percent of total sample**	**Modified lysine residues**
Unmodified	40%	
Singly-acetylated	20%	K4=K7 >K11 >K13 >>K15
Doubly-acetylated	20%	(K4+K7), (K7+K11), (K4+K11)
Triply-acetylated	20%	(K4+K7+K11)

While unmodified, singly-acetylated, doubly-acetylated, and triply-acetylated peptides of H2A.Z-1 were also shown to exist in the sodium butyrate-treated cells (Figure 3C), the existence of these species was not determined in the chicken erythrocytes due to low abundances. However, doubly acetylated species of the N-terminal peptide of H2A.Z-1 in the sodium butyrate-treated cells included species concurrently modified at K4 + K7, K7 + K11 and K4 + K11, the same as those identified for H2A.Z-2. Similarly, the predominant triply acetylated species had acetyl groups at K4 + K7 + K11 (Figure 3A and B). Singly-acetylated species of H2A.Z-1 were also detected but were present at significantly lower abundances, and as a consequence the acetylation sites were not able to be determined for these forms. However, it is likely that they are very similar to those determined for H2A.Z-2 since all other modified forms are also very similar for both isoforms.

H2A.Z compacts the NCP and enhances its stability regardless of its acetylated state or that of the core histone complement

In order to determine the effects of H2A.Z and its acetylation on the conformation of NCPs, we prepared several forms of reconstituted mononucleosomes by salt gradient dialysis. Figure 4A-1 and 4A-2 show SDS-PAGE and AUT-PAGE, respectively of mononucleosomes reconstituted with purified H2A.Z from chicken erythrocytes that represents a roughly equal mixture of H2A.Z-1 and H2A.Z-2 as determined by mass spectrometry (Figure 2). All nucleosomes were also analyzed on 4.5% native acrylamide gels of which a representative example is shown in Figure 4A-3. Here it can be seen that the reconstituted H2A.Z-containing particles migrate slightly faster in the gel compared

to those containing H2A which suggests that the H2A.Z particle is more compact. Indeed, this observation is corroborated by analysis of the salt dependence of the sedimentation coefficient (Figure 4B) which indicates that at any given salt concentration, the sedimentation coefficient of the H2A.Z-containing NCP is greater than that of the H2A-containing NCP. It can also be observed in Figure 4B that the sedimentation coefficient value decreases as the concentration of NaCl increases, as previously seen (Ausio et al., 1989). Also as expected, the relative concentration of free DNA increases as the concentration of NaCl increases which is shown in Figure 5A for human recombinant H2A.Z-1-containing nucleosomes.

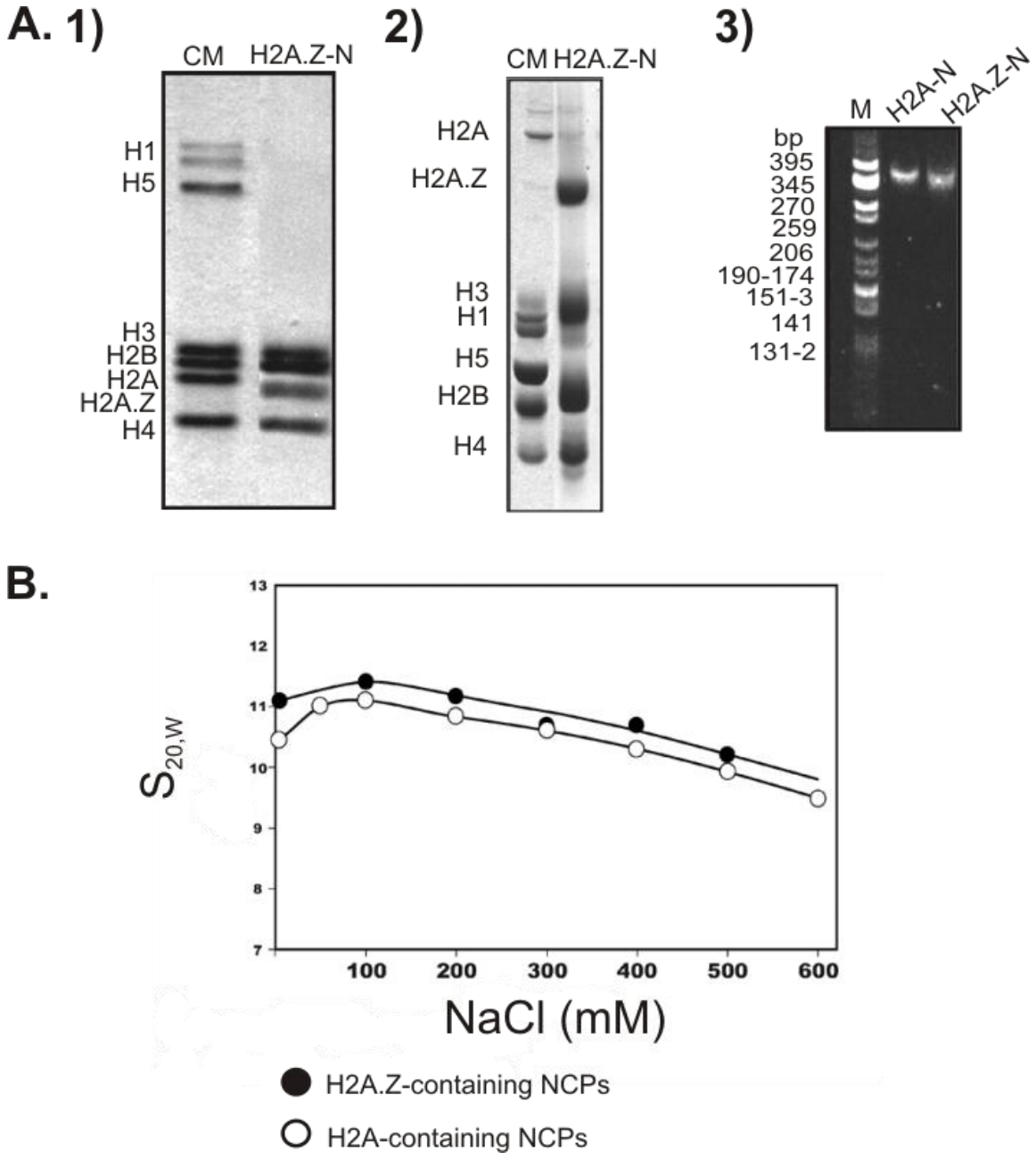

Figure 4: Sedimentation velocity analysis of H2A.Z-containing NCPs.

A.) Electrophoretic analysis of NCPs reconstituted with purified native H2A.Z. 1) SDS-PAGE, 2) AUT-PAGE, 3) 4.5% Native PAGE of H2A-containing and H2A.Z-containing NCPs. CM is chicken erythrocyte histone marker and M is Cfo1-digested pBR322 plasmid as a DNA marker. B.) Salt dependence of the sedimentation coefficient ($S_{20,w}$) of H2A-containing and reconstituted H2A.Z-containing NCPs.

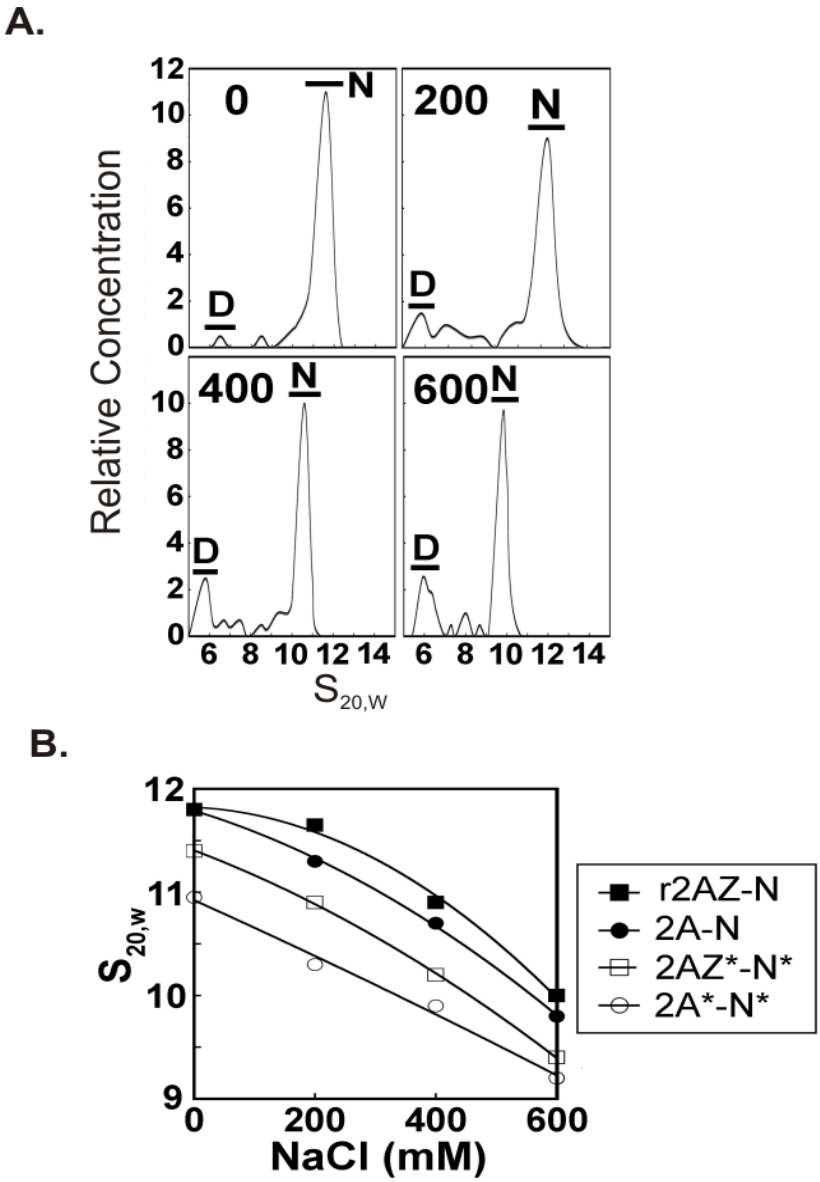

Figure 5: Sedimentation velocity analysis of acetylated nucleosomes.

A.) Profile of analytical ultracentrifuge analysis of nucleosomes containing human recombinant H2A.Z-1 and native HeLa cell non-acetylated histone complement. The graphs show plots of the relative sample concentration vs the sedimentation coefficient at four different NaCl concentrations (0, 200, 400, 600mM). Data were obtained using the histogram envelope analysis from the UltraScan software (see Materials and Methods). D is free 155 bp DNA and N is the NCP. B.) Ionic strength dependence of the sedimentation coefficient ($S_{,20w}$) of reconstituted NCPs that were dialyzed against 20mM Tris-HCl (pH 7.5), 0.1mM EDTA buffer containing different NaCl concentrations and analyzed by sedimentation velocity at 44,000 rpm and 20°C.

To examine the effect of acetylation on the conformation of the nucleosomes, we plotted the $S_{20,w}$ values versus NaCl concentration of several NCP constructs (Figure 5B). In agreement with the results obtained with reconstituted NCPs containing H2A.Z purified from chicken erythrocytes, the human recombinant H2A.Z-1-containing particle exhibits slightly higher sedimentation coefficients, especially at low salts, which is indicative of a slightly more compact conformation compared to the H2A-containing NCP.

Also in agreement with previous data (Ausio and van Holde, 1986; Garcia-Ramirez et al., 1995) it can be observed in Figure 5B that when all components of the histone octamer are acetylated, the NCP displays a significantly more relaxed and open conformation than that of the non-acetylated NCP regardless of whether the particles are reconstituted with H2A or H2A.Z. However, despite this, the trend towards a more compact conformation of the H2A.Z nucleosome persists when H2A.Z and the histone complement is acetylated (Figure 5B, open squares).

Analytical ultracentrifuge analysis was also used to measure the salt dependent stability of the various nucleosome constructs by determining the relative amounts of nucleosomes compared to free DNA. Figure 6A shows the profile of H2A with non-acetylated histone complement nucleosomes (2A-N, top 2 panels) and native acetylated H2A with acetylated histone complement nucleosomes (2A*-N*, bottom 2 panels) at 0 and 600mM NaCl. In both cases, the relative amount of nucleosomes is decreased at high salt; however, this decrease is much more apparent in the case of the acetylated particles. Acetylation of the histones decreased the stability of the nucleosome irrespective of the

presence of H2A or H2A.Z (Figure 6B) and in keeping with what was seen in the conformation analysis, the acetylated H2A.Z with acetylated histone complement (2AZ*-N*) nucleosomes were more stable compared to their acetylated H2A counterparts (shown at 600mM NaCl).

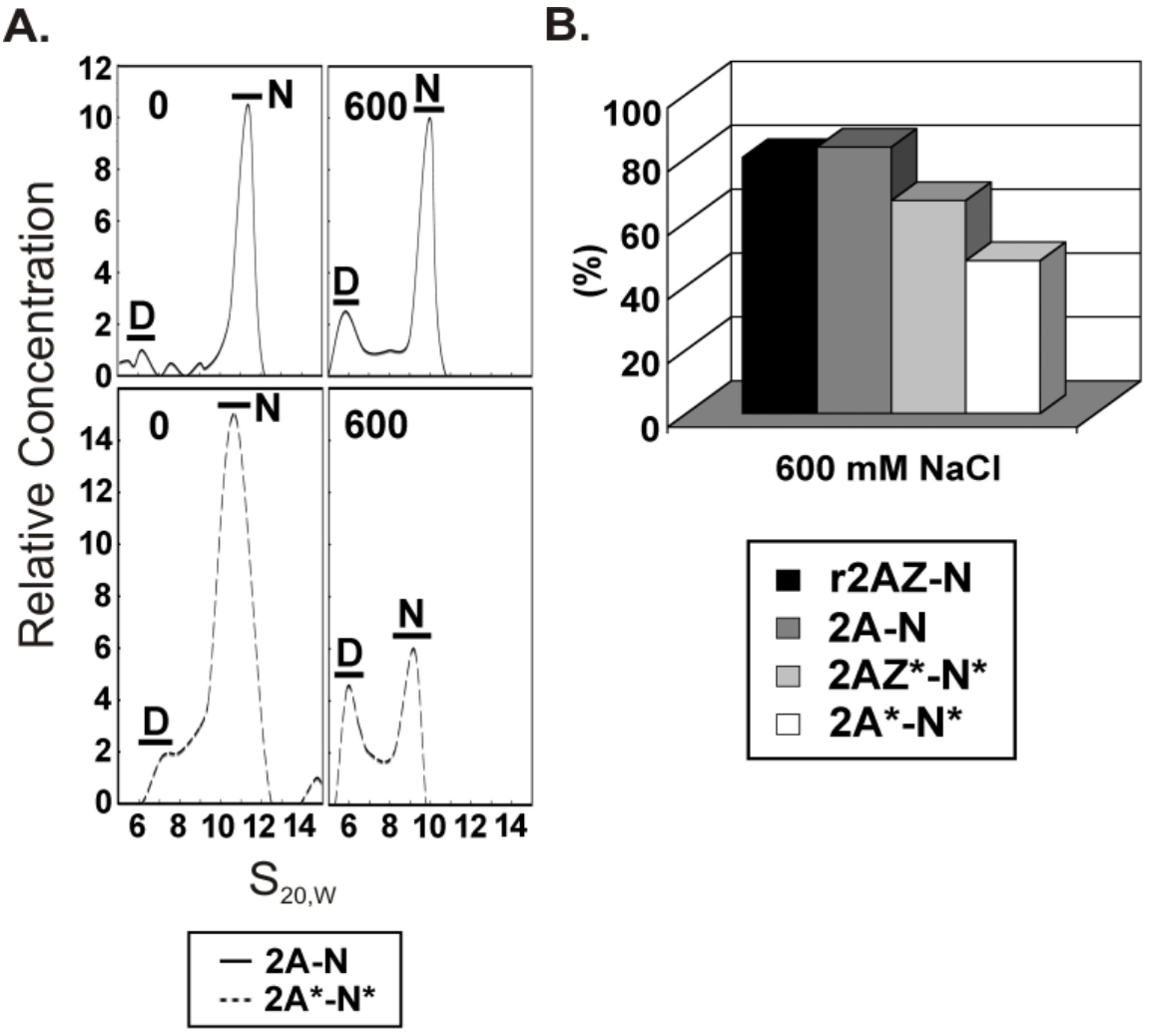

Figure 6: Salt-dependent stability of acetylated and nonacetylated H2A- and H2A.Z-containing NCPs.

A.) Profile of the analytical ultracentrifuge analysis of nucleosomes containing H2A with a non-acetylated histone complement or acetylated H2A with an acetylated histone complement at 0 and 600mM NaCl. D is free 155 bp DNA and N is the NCP. B.) Nucleosome stability analysis of H2A or H2A.Z with non-acetylated histone complement, acetylated H2A or acetylated H2A.Z with acetylated complement. Results show the percentage of undissociated NCPs containing a full histone octamer (calculated from the ratio (%) of the area under N in panel A at a given salt concentration to the area under N at 0 mM salt).

Characterizing the chromatin distribution of acetylated H2A.Z before and after sodium butyrate treatment.

Micrococcal nuclease digestion of chromatin under the conditions described in the Materials and Methods section leads to a partitioning in three different fractions; S1, SE and P, the first one of which is highly enriched in active genes (Henikoff et al., 2009; Huang et al., 1986; Rose and Garrard, 1984) and basically corresponds to the euchromatin fraction. Fraction SE is less readily accessible to nuclease and, as indicated by the western blot with an anti-trimethyl K27 H3 antibody which is a known marker of facultative heterochromatin (Liu et al., 2007) it consists mainly of chromatin fragments from transcriptionally inactive regions. The pellet P represents insoluble chromatin material that is resistant to nuclease digestion and is not associated with heterochromatin markers. Analysis of chromatin fractions generated in this way by Western blot using an antibody against triply-acetylated H2A.Z at K4, K7, K11 (Bruce et al., 2005) indicates that the levels of this modified histone are very low in the S1 fraction, slightly increased in the SE fraction and are more abundant in the P fraction of untreated HeLa cells (Figure 7B, lower panel). However, once the cells have been treated with sodium butyrate to inhibit histone deacetylase enzymes, a significant portion of the acetylated H2A.Z fractionates with the active chromatin of the S1 fraction while a smaller portion is present in the trimethyl-H3 K27-enriched SE fraction (Figure 7B). In contrast, the presence of acetylated H2A.Z increases gradually from the S1 to the P fraction (Figure 7A, bottom panel) in native non-butyrate-treated cells. As expected, the global acetylation of H4 also increases dramatically upon butyrate treatment (Vidali et al., 1978). Interestingly, the acetylated forms of H2A.Z and H4 are also prominent in the P fraction which exhibits an

almost complete absence of the trimethyl K27 H3 heterochromatin mark indicating that this fraction most likely contains active regions of chromatin that are insoluble as well as very highly condensed heterochromatin. It is likely that it consists of oligonucleosomes that are directly bound to components of the nuclear matrix, the nuclear pore or to large protein complexes such as the RNA Pol II and/or histone acetyltransferase complexes (Brown et al., 2008; Henikoff et al., 2009).

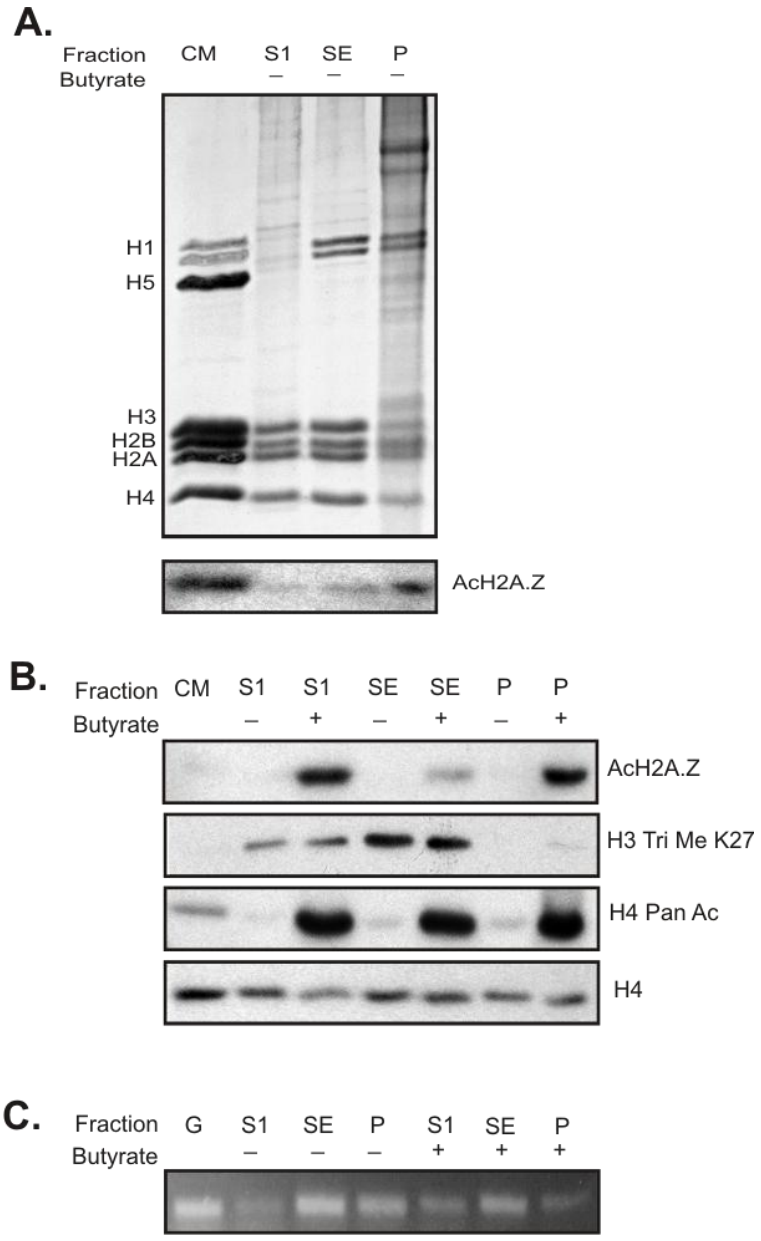

Figure 7: Chromatin partitioning of acetylated H2A.Z.

A.) SDS-PAGE of HeLa cell chromatin S1, SE, and P fractions and Western blot analysis using an antibody against acetylated H2A.Z. B.) Western blot analysis of chromatin fractions obtained from HeLa cell nuclei grown in the presence (+) or absence (-) of 5mM sodium butyrate using antibodies against acetylated H2A.Z (AcH2A.Z), methylated H3 (H3 Tri Me K27), tetra-acetylated H4 (H4 Pan Ac), and total H4 as a loading control. CM: chicken erythrocyte histone marker. C.) PCR analysis of the S1, SE, and P fractions using primers for a 147 bp fragment of the human protamine 1 gene. G: HeLa genomic DNA.

PCR analysis of DNA isolated from the chromatin fractions indicates that the human protamine 1 gene, which is inactive in HeLa cells, as expected is present mainly in the SE chromatin fraction and in the insoluble fraction (Figure 7C). The human protamine genes are present in a cluster that is associated with the nuclear matrix (Martins et al., 2004). Notice however, that a small amount of gene redistribution takes place (Figure 7C) upon treatment with butyrate in agreement with the genomic redistribution already described after treatment with HDAC inhibitors (Brown et al., 2008; Rada-Iglesias et al., 2007).

Discussion:

Our ability to purify significant quantities of histone H2A.Z from cells and tissues has allowed us to characterize the sites and abundances of acetylation present on the N-terminal tail of this protein. An unexpected result of this work was the finding that total H2A.Z from chicken cells represents a mixture of two protein isoforms, now called H2A.Z-2 and H2A.Z-1. The reason for this nomenclature will be discussed in the introduction to Chapter 3. The development of the sophisticated top-down mass spectrometry techniques of sequential ion/ion reactions enabled the identification of these isoforms and demonstrated the power of this technique in top-down sequencing of protein mixtures (Coon et al., 2005). An examination of the evolutionary history of histone H2A.Z indicates that the two protein isoforms share a common origin in early chordates but have become distinct proteins in vertebrates (Eirin-Lopez et al., 2009). While the protein sequence of the two isoforms is very similar, differing by 3-4 amino acid residues depending on the species, it is possible that they have acquired a degree of functional

independence that could help to explain in part the diverse and seemingly contradictory functions of H2A.Z in higher organisms.

The exact sites and abundances of N-terminal tail acetylation of either isoform of vertebrate H2A.Z have not previously been determined by mass spectrometry though they were hypothesized to be at K4, K7 and K11 of chicken H2A.Z-2 based on sequence homology with yeast H2A.Z (Bruce et al., 2005). The mass spectrometry analyses reported here provide the first quantitative determination of the acetylation sites in chicken H2A.Z-2 and underscore the notion that a portion of this acetylation occurs as dimers and trimers of K4, K7, and K11 (Table 2) in contrast to H2A.Z in yeast, where K14 represents the most abundantly acetylated site (Millar et al., 2006). Furthermore, in chicken the incidence of H2A.Z-2 peptide species having one acetyl group at K4 is relatively equal to that having one acetyl group at K7. In *Tetrahymena*, the retention of one acetylatable lysine is sufficient to provide the essential function of H2A.Z acetylation (Ren and Gorovsky, 2001). The fact that part of the acetylation pattern in vertebrates involves the presence of doubly and triply acetylated forms indicates that the function of H2A.Z acetylation in higher organisms may involve the neutralization of more than one charge in the N-terminal region. It is also possible that different combinations of acetylation could be part of a signaling mechanism to specify distinct downstream events.

The patterns of acetylation appear to be the same for both H2A.Z isoforms, where a triply-acetylated (K4, K7 and K11) form as well as doubly-acetylated (K4 + K7, K7 + K11, and K4 + K11) forms of the N-terminal peptides were identified in the sodium

butyrate-treated sample. Singly-acetylated N-terminal peptides of H2A.Z-1 were also detected; however, the sites of acetylation were not able to be determined owing to the low abundances of these species. We expect the singly-acetylated forms of H2A.Z-1 to be the same as those of H2A.Z-2 (see Table 2), owing to the similarity of the other acetylated species between the isoforms.

Purification of H2A.Z from native tissue (chicken erythrocytes) also allowed us to determine the effects of this histone variant on reconstituted NCPs. Our analyses of the salt dependence of the sedimentation coefficient of these particles indicate that H2A.Z-containing NCPs are slightly more compact than those containing H2A purified from native tissue (chicken erythrocytes) (Figure 4B). This is also the case for NCPs containing human recombinant H2A.Z-1 compared to NCPs reconstituted with purified human H2A (from HeLa cells) (Figure 5B). Increasing the amount of acetylation of the histone octamer by reconstituting NCPs with histones purified from sodium butyrate-treated cells results in a less compact and more open NCP; however the acetylated H2A.Z-containing NCP is still more compact than that containing H2A (Figure 5B). Similarly, our analyses of the stabilities of H2A and H2A.Z-containing particles indicates that acetylation destabilizes the NCP as previously shown using atomic force microscopy (Dunker et al., 2001), but acetylated H2A.Z-containing particles are still more stable than those containing acetylated H2A (Figure 6B). Interestingly, our lab has also shown that particles containing non-acetylated H2A.Z with an acetylated histone complement do not exhibit the highly decreased stability of the fully acetylated particle, indicating that acetylation of H2A.Z (or H2A) is required to completely destabilize these nucleosomes

(Ishibashi et al., 2009b). It is important to note that while sodium butyrate treatment increases the levels of histone acetylation as confirmed here by our mass spectrometry analysis of H2A.Z and while no other PTMs were observed on H2A.Z, it is nevertheless possible that increased levels of other PTMs could be present on the other core histones that could also contribute to the more open structure and decreased stability of the acetylated NCPs.

From a functional perspective, on the one hand these observations indicate that one purpose of acetylating H2A.Z-containing NCPs could be to cause them to adopt a more open and less stable conformation that could potentially allow greater access to the DNA of promoters and enhancers or allow H2A.Z nucleosomes to be more easily remodeled by chromatin remodeling machines. On the other hand, the fact that H2A.Z-containing NCPs are slightly more compact and stable than those containing H2A indicates that the placement of H2A.Z at promoters and enhancers likely does not solely serve a nucleosome stability-based structural role. Indeed, the role of H2A.Z at promoters and enhancers has been shown to involve nucleosome positioning (Fu et al., 2008; Raisner et al., 2005). Furthermore, recent evidence suggests that nucleosomes containing both H2A.Z and the H3.3 variant are located at promoters and are very unstable (Jin et al., 2009), while particles containing H2A.Z and H3 trimethylated at K4 protect less DNA (Fu et al., 2008). This indicates that other histone variants and PTMs besides acetylation can also influence the structure of H2A.Z-containing nucleosomes. Therefore, it is possible that the combined effects of acetylation, other PTMs, H3.3 and probably DNA sequence (Tolstorukov et al., 2009) could contribute properties to a nucleosome that

would allow it to be more permissive to transcription. Indeed, recent evidence suggests that fluctuations in the association of DNA with the nucleosome govern pause density, recovery and the pause-free velocity of transcribing RNA Pol II (Hodges et al., 2009).

Our analysis of the chromatin distribution of triply-acetylated H2A.Z indicates that it is present at low levels and mainly within the insoluble fraction (P) in untreated HeLa cells. This is likely consistent with evidence indicating that this hyperacetylated form of H2A.Z is a feature of active, and presumably actively transcribing genes in the chicken (Bruce et al., 2005; Myers et al., 2006). Chromatin regions that are engaged by large complexes including the transcriptional machinery most likely fractionate into the insoluble P fraction (Henikoff et al., 2009). Treatment of HeLa cells with sodium butyrate greatly increases the amount of triply-acetylated H2A.Z in the active S1 and P fractions, but not significantly within the inactive SE fraction. This indicates that acetylation of H2A.Z can mark a portion of the H2A.Z population for its function within active regions of the genome. That PTMs specify certain populations of H2A.Z for a given function is supported by the presence of ubiquitinated H2A.Z within the facultative heterochromatin of the inactive X chromosome in human cells (Sarcinella et al., 2007).

Conclusions and Future Directions:

We have characterized the sites of N-terminal acetylation of the two protein isoforms of H2A.Z (H2A.Z-1 and H2A.Z-2) in the chicken. Our data indicate that there do not appear to be any major differences in the sites or abundances of acetylation between these isoforms. According to the evolutionary analysis, the emergence of two H2A.Z isoforms

occurred in vertebrates and they exhibit substantial synonymous variation at the nucleotide level despite a high conservation of amino acid sequence (Eirin-Lopez et al., 2009). This analysis further indicated that in the transition from chordates to vertebrates, H2A.Z-1 may have arisen to acquire a novel or most likely complementary function to H2A.Z-2, which is more closely related to the common early chordate ancestor (Eirin-Lopez et al., 2009). While these proteins likely have strongly overlapping functions, whether they have acquired a degree of functional independence awaits further research. We show that the presence of H2A.Z within the NCP stabilizes the particle relative to those containing H2A, regardless of acetylation. Our increasing knowledge of the combinations of PTMs that exist on NCPs at certain genomic loci, such as at promoters, should allow for detailed structural studies of how these PTMs act synergistically to modulate nucleosome structure. Furthermore, determining the sequence of events of H2A.Z deposition and its acetylation along with acetylation of the rest of the core histones could help us to understand more about why H2A.Z is incorporated at certain loci.

Chapter 3: Characterization of the histone H2A.Z-1 and H2A.Z-2 isoforms in vertebrates

Deanna Dryhurst and Juan Ausio

Department of Biochemistry and Microbiology, University of Victoria, Victoria, British Columbia, Canada V8W 3P6

Partially adapted from:

Dryhurst D, Ishibashi T, Rose KL, Eirín-López JM, McDonald D, Silva-Moreno B, Veldhoen N, Helbing CC, Hendzel MJ, Shabanowitz J, Hunt DF, Ausió J. (2009). Characterization of the histone H2A.Z-1 and H2A.Z-2 isoforms in vertebrates. BMC Biol. 7,86.

Contributions:

Deanna Dryhurst wrote the chapter and performed all experimental procedures unless otherwise mentioned. Darin McDonald produced the images for Figure 9 in Michael Hendzel's lab at the University of Alberta. Nik Veldhoen and Toyotaka Ishibashi helped with experimental design. Caren Helbing provided samples and equipment for Figure 14. Jose Maria Eirín-López produced the phylogenetic tree in Figure 15 B.

Introduction:

H2A.Z is the most extensively studied histone variant and it has been shown to be involved in several seemingly unrelated and divergent processes. Understanding how this protein participates in different cellular events has undoubtedly been further complicated by the use of different biological systems, since while certain general functions of H2A.Z may be universal in all organisms, the specific details and fine-tuning in higher eukaryotes may not be present or may be the work of other proteins in yeast or flies. Part of this fine-tuning of H2A.Z in vertebrates could be due to the co-existence in the cell of two H2A.Z protein isoforms (H2A.Z-1/H2A.Z-2) that was first determined by our group in total H2A.Z isolated from chicken erythrocytes using a novel mass spectrometric approach (Coon et al., 2005). We have also shown that both isoforms are acetylated at the same lysine residues with similar patterns in chicken erythroleukemic cells treated with sodium butyrate (see Chapter 2).

Our subsequent evolutionary and phylogenetic analysis of these isoforms revealed a substantial conservation at the protein level where they differ by only 3 amino acids (Figure 8), but a marked divergence at the nucleotide sequence level (Eirin-Lopez et al., 2009). The isoform that has been annotated as H2A.Z in humans has now been named H2A.Z-1 along with all the other H2A.Z sequences in vertebrates that form this group. The other isoform, which in the human database was labeled as H2A.V, has now been named H2A.Z-2. Interestingly, the protein that was historically known as H2A.Z in the chicken is in fact an H2A.Z-2 isoform. The H2A.Z isoform genes were located on different chromosomes in all organisms analyzed; in humans, the H2A.Z-1 gene is on the

long arm of chromosome 4 (4q24), while the H2A.Z-2 gene is on the short arm of chromosome 7 (7p13). The evolutionary analysis also revealed that the two H2A.Z isoforms had a common origin early in chordate evolution that was followed by a subsequent process of differentiation in the vertebrate groups (Eirin-Lopez et al., 2009). Indeed, it appears that the strength of the evolutionary constraints operating at the nucleotide level are not equal between the isoforms, with H2A.Z-2 being significantly more constrained than H2A.Z-1 (Eirin-Lopez et al., 2009).

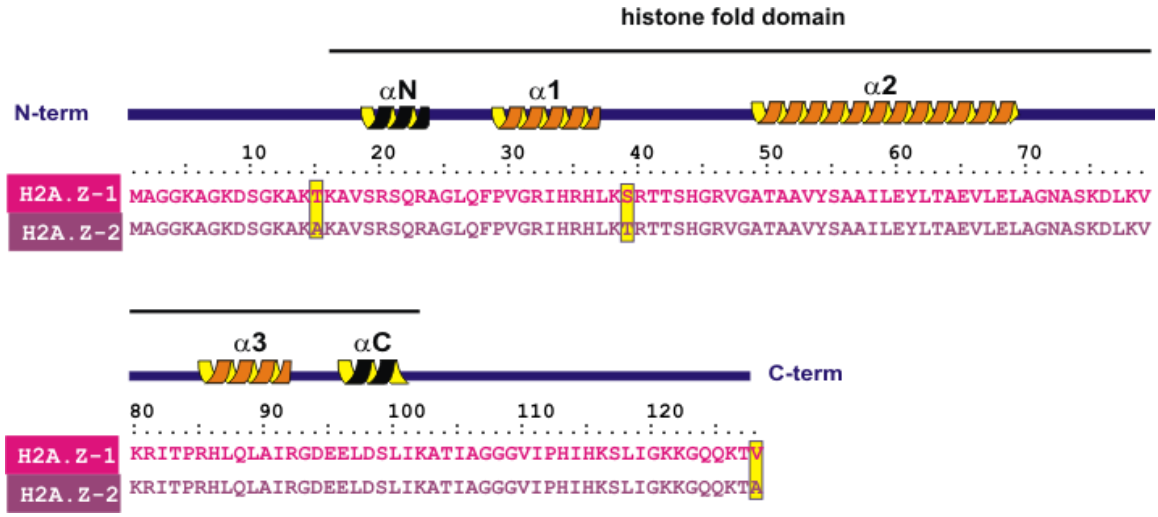

Figure 8: Protein sequence alignment of human H2A.Z-1 and H2A.Z-2 isoforms.

The alpha-helices of the histone fold domain are shown on top. Human H2A.Z-1 and H2A.Z-2 differ by three residues which are boxed in yellow.

Importantly, H2A.Z is the only histone variant that has been shown to be indispensable for survival in *Drosophila* (van Daal and Elgin, 1992) and mice (Faast et al., 2001); however in this latter study, only H2A.Z-1 was knocked out. This indicates that H2A.Z-2 is incapable of compensating for the loss of H2A.Z-1 in mice. Whether this is because of lower amounts of total H2A.Z or because of differences in the nuclear localization, post translational modification (besides acetylation), biochemical interactions or temporal expression of the H2A.Z-1 and H2A.Z-2 genes is unknown. Based on the evolutionary and genetic knockout studies, we hypothesize that the two H2A.Z isoforms in vertebrates may have different yet probably overlapping functional roles.

In the present work, we show that both isoforms are expressed across a wide range of human tissues and they display a similar nuclear distribution. Furthermore, we show that the distribution of H2A.Z-1 and H2A.Z-2 within chromatin differs, as does their association with histone H3 trimethylated at lysine 4. Despite the high degree of amino acid sequence similarity between these H2A.Z isoforms, they display very divergent promoter sequences that could result in temporal and tissue-specific differences in gene expression.

Materials and Methods:

Immunoflorescence:

Mouse embryonic fibroblasts were grown in DMEM with 10% fetal calf serum, plated on glass coverslips and allowed to attach and grow until between 40 and 80% confluent. The coding region of H2A.Z-1 was fused in frame to the 3’ end of cyan fluorescent protein (CFP) into the pAmCyan1-N1 vector (Clontech) and the coding region of H2A.Z-2 was

fused in frame to the 3' end of yellow fluorescent protein (YFP) into the pZsYellow1-N1 vector (Clontech). The cells were then co-transfected with H2A.Z-1-CFP and H2A.Z-2-YFP using Effectene transfection reagent (Qiagen) according to the manufacturer's instructions. The cells were grown for an additional 16-20 hours followed by replacement of the medium and the addition of 1 microgram/ml Hoechst 33342. After 10 minutes, the medium was replaced with fresh medium containing no Hoechst dye. The coverslips were then mounted onto glass slides after using vacuum grease to create a small reservoir for media and imaged immediately using a Zeiss Axiovert 200M inverted fluorescence microscope. Images were collected with a 100X 1.4 N.A. PlanApo objective and a Photometrics CoolSnap fx CCD.

Stable Transfection and Chromatin Fractionation:

H2A, H2A.Z-1 and H2A.Z-2 sequences were amplified from HeLa cell cDNA and Flag tags were added in frame to the 3' ends by PCR. The sequences were then cloned into pcDNA3.0 vector (Invitrogen) and the plasmid was linearized by digesting with Sca1. HEK 293 cells were transfected using PolyFect reagent (Qiagen) and cells stably expressing the Flag-tagged protein were selected for by the addition of G418 (Gibco) to cell culture medium (DMEM containing 10% FBS). After several weeks, stable colonies expressing similar levels of the proteins were selected. Nuclei were isolated and digested with Micrococal Nuclease (Worthington) at 30U/mg of DNA for 5 min. at 37°C. The reaction was stopped by the addition of EDTA to a final concentration of 10mM on ice, and the sample was centrifuged at 10000*g* for 10 min at 4 °C to yield an S1 supernatant and a pellet. The pellet was resuspended and lysed in 0.25 mM EDTA (pH 7.5) and

stirred for 1 h at 4 °C. Upon centrifugation as before, a supernatant SE and a final pellet P were thus obtained. Under the experimental conditions used here, S1, SE, and P correspond to approximately 5−10, 25−30, and 60−65%, respectively, of the total nuclear DNA. Western Blotting was performed on the normalized protein component of these fractions using SDS-PAGE and standard procedures. Flag antibody (Sigma) dilution was 1:5000, H2A.Z antibody (Abcam) dilution was 1:1000, H3 Tri-Me K4 antibody (Millipore) dilution was 1:5000, and H4 antibody was made in-house and used at a 1:10,000 dilution.

Preparation of Mononucleosomes and Immunoprecipitation:

Mononucleosomes were prepared from HeLa cells transiently transfected with H2A-Flag, H2A.Z-1-Flag or H2A.Z-2-Flag within the pcDNA3.0 vector following the procedure of Sarcinella and colleagues (Sarcinella et al., 2007). When required, cells were treated with 100mg/ml nocodazole for 16 hours after 24 hours of transfection and an aliquot was monitored by FACS after treatment with propidium iodide to ensure mitotic arrest. Briefly, isolated nuclei were digested with Micrococal Nuclease (Worthington) at a concentration of 100U/mg of DNA at 37°C for 30 minutes. The reaction was stopped by the addition of EGTA to a final concentration of 1mM and the suspension was centrifuged at 600g for 10 minutes. The resulting pellet was resuspended in 20mM Tris pH 7.5, 0.2mM EGTA, 420mM NaCl and 1.5mM $MgCl_2$ and incubated on ice for 1 hour then spun at 1000g for 10 minutes. The supernatant was then brought to 150mM NaCl by addition of 20mM Tris pH 7.5, 1.5mM $MgCl_2$, 0.2mM EGTA and 25% glycerol dropwise on the vortex. This suspension was centrifuged at 1000g for 10 minutes and monitored on

4% native acrylamide gels to ensure complete digestion of the chromatin to mononucleosomes. For the immunoprecipitation, 10ul of anti-Flag agarose beads (Sigma) was used to immunoprecipitate Flag-containing mononucleosomes from H2A-Flag, H2A.Z-1-Flag, H2A.Z-2-Flag or mock transfected control HeLa cells. The beads were washed 8 times in 1ml 20mM Tris pH 7.5, 150mM NaCl, 1.5mM $MgCl_2$, 0.2mM EGTA, 0.2% Triton X-100, resuspended in SDS sample buffer without β-mercaptoethanol, boiled, followed by the addition of β-mercaptoethanol to the supernatant. Immunoprecipitated nucleosomes were run on 15% SDS-PAGE and transferred to PVDF membrane (BioRad). Anti H3 AcK9K14, anti H3 Tri-MeK27, anti H3 PhosS10 and anti H4 AcK16 were all from Millipore and used at a 1:1000 dilution.

Two-dimensional PAGE:

Total histones from HeLa cell nuclei were extracted in 0.6N HCl as described in (Wang and Ausio, 2001). These histones were electrophoresed on a 10% polyacrylamide AUT gel (Abbott et al., 2001) in several lanes, one of which was cut out and soaked in 125mM Tris-HCl pH 6.8, 4% SDS, 20% glycerol and 1.43M β-mercaptoethanol for 10 min at room temperature while the other was stained with Coomassie blue solution. The unstained gel strip was laid horizontally and electrophoresed in a 6% polyacrylamide stacking, 15% polyacrylamide separating SDS gel prepared according to (Laemmli, 1970).

Quantitative PCR:

Samples from three human cDNA panels derived from various human fetal and adult tissues were obtained from Clontech Laboratories Inc. (CTL) (Mountain View, CA, USA). These included normal tissue from adult (CTL MTC panel I, CTL MTC panel II) and fetal (CTL MTC fetal MTC panel) sources. Each cDNA sample represented a pool of individuals of either gender. For QPCR analysis, cDNA was diluted 20-fold in RNase/DNAse free water. H2A.Z-1- and H2A.Z-2-specific primers were designed based on the 5' and 3' untranslated regions and amplicon sequences were confirmed by DNA sequencing. H2A.Z-1 forward primer: TTGCTTGAGCT TCAGCGGAATT, reverse primer: TTCCTTGTTATCTCAGGACTCT H2A.Z-2 forward primer: GCGGCCGAGCGGAGGCGGAG, reverse primer: TGCTTAGAGGGATGCTTTAAC. The levels of H2A.Z transcripts were analyzed by SYBR Green incorporation using a Stratagene MX3005P QPCR system and MXPro software. Each 15µl DNA amplification reaction consisted of 2µl of diluted cDNA and 13µl of Platinum SYBR Green qPCR SuperMix-UDG with Rox (Invitrogen) containing 2.5pmol of each primer. Thermocycling conditions for both primer sets were: 9 min 95°C followed by 40 cycles of 15 sec 95°C, 30 sec 60°C and 45 sec 72°C. Reactions were performed in quadruplicate and averaged cycle threshold (Ct) was converted to transcript copy number by interpolation from a standard curve. The standard curve was constructed using a dilution series of purified H2A.Z-1 or H2A.Z-2 amplicon.

Phylogenetic analysis:

Nucleotide sequences corresponding to promoter regions of H2A.Z-1 and H2A.Z-2 histones were retrieved from the GenBank database through recurrent BLAST searches performed on general nucleotide collections as well on completed genomes (Altschul et al., 1990). A total of 27 nonredundant sequences belonging to mammals were compiled and properly classified as either H2A.Z-1 or H2A.Z-2 (Appendix 1). Multiple alignments of the promoter sequences were conducted using the CLUSTAL_X and the BIOEDIT programs (Thompson et al., 1997). Conserved regulatory elements have been simultaneously identified from the alignments of mammalian H2A.Z-1 and H2A.Z-2 sequences by using the program Transcription Regulatory Element Search (TRES, http://bioportal.bic.nus.edu.sg/tres/) to perform searches in the object-oriented transcription factors database (ooTFD) (Ghosh, 2000). Phylogenetic relationships among H2A.Z promoter regions were reconstructed using the neighbor-joining method using uncorrected nucleotide *p*-distances using the complete deletion option. The reliability of the resulting topology was tested by both the bootstrap and the interior-branch test methods, producing the BP and CP values, respectively, for each interior node after 1000 replicates (Sitnikova, 1996). The tree was rooted with the H2A.Ze sequence from sea urchin, representing an early chordate in which H2A.Z-1 and H2A.Z-2 variants are not yet differentiated. The amino acid residues corresponding only to the three differential residues of the H2A.Z-1 and H2A.Z-2 isoforms from all 27 mammalian sequences were input into the WebLogo program (http://weblogo.berkeley.edu) to generate the Logo in Figure 6C (Crooks et al., 2004).

Results:

H2A.Z-1 and H2A.Z-2 are mainly distributed in euchromatin in mouse fibroblasts and in HEK 293 cells

To determine the pattern of H2A.Z-1 and H2A.Z-2 distribution within chromatin, asynchronous mouse embryonic fibroblasts were transfected with YFP-H2A.Z-2 and CFP-H2A.Z-1 and imaged live (Figure 9). Figure 9 indicates that YFP-H2A.Z-2 (top right panel) and CFP-H2A.Z-1 (bottom left panel) have a near identical distribution throughout chromatin. The composite image showing Hoechst DNA staining (green) and YFP-H2A.Z-2 (red) indicates H2A.Z-2 is preferentially located within regions of euchromatin (orange) but since both variants localize to the same regions, it stands that H2A.Z-1 would also be mainly present in euchromatic regions. However, both variants are also present within the DNA-dense chromocenters as shown by their yellow staining in the composite image. To ensure that the transfected proteins were able to be incorporated into nucleosomes, chromatin from these cells was isolated, digested with micrococcal nuclease and separated on sucrose gradients to obtain mononucleosomes (Gautier et al., 2004). Western blot analysis of these mononucleosomes with an anti-GFP antibody that also recognizes YFP confirmed the incorporation of transfected H2A.Z-2-YFP (Figure 10).

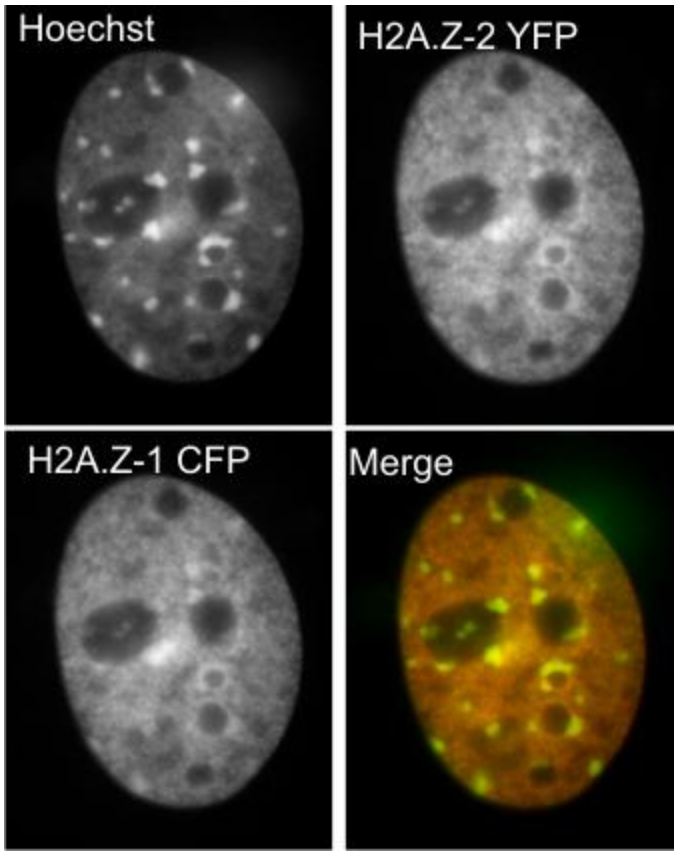

Figure 9: Fluorescence microscopy of H2A.Z-1 and H2A.Z-2 variants in mouse embryonic fibroblasts.

A mouse embryonic fibroblast nucleus is shown following transfection with H2A.Z-2-YFP and H2A.Z-1-CFP and imaged live. The top left panel shows cells stained with DNA binding dye Hoechst 33342. The top right panel shows the distribution of H2A.Z-2-YFP. The bottom left panel shows the distribution of H2A.Z-1-CFP while the composite image shows the Hoechst staining (green) relative to the distribution of H2A.Z-2-YFP. Sites that are enriched in H2A.Z-2 are orange and are predominantly euchromatin. The chromocenters appear yellow, indicating the presence of both DNA and H2A.Z-2-YFP.

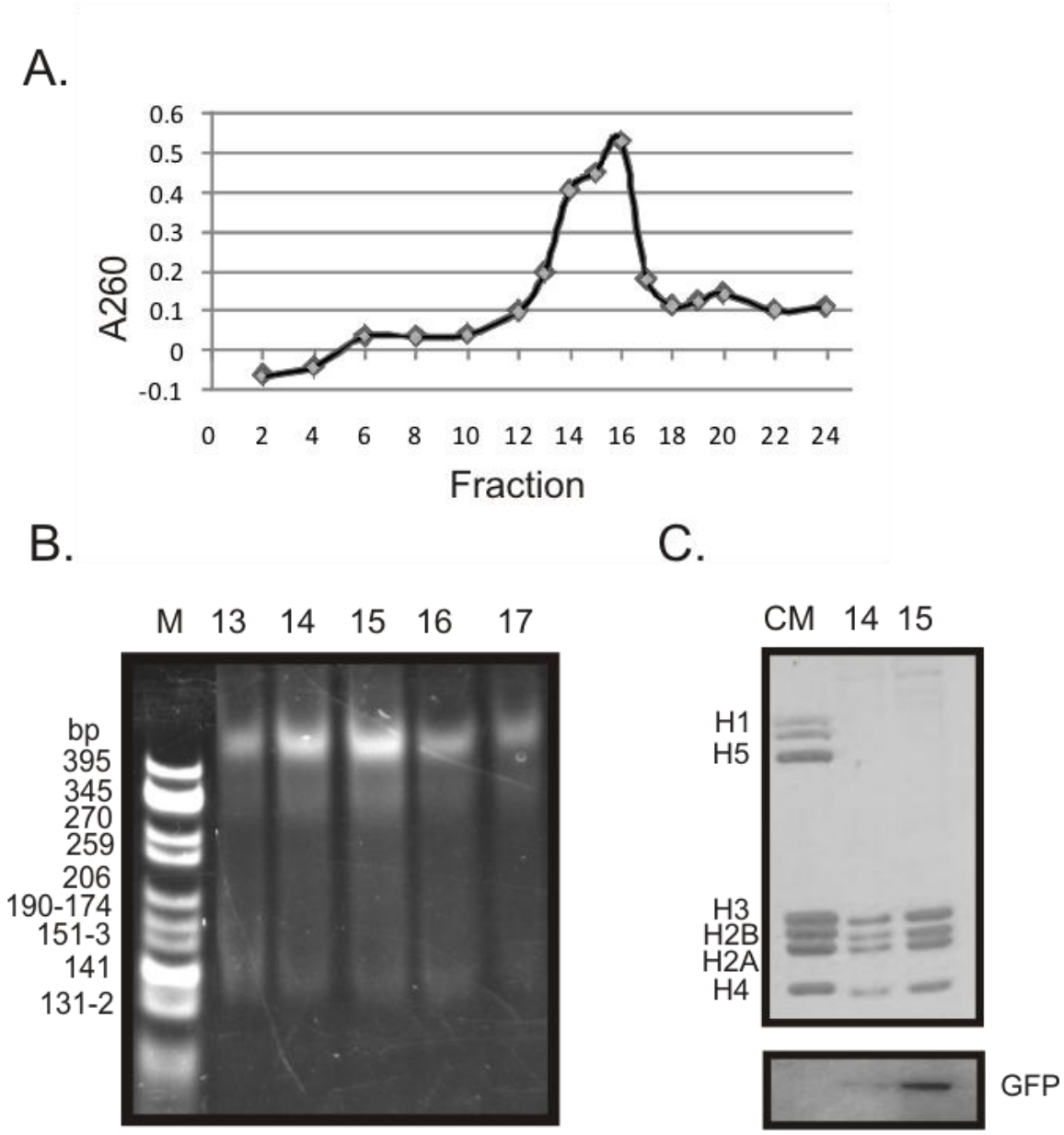

Figure 10: Transfected H2A.Z-2-YFP is incorporated into mononucleosomes.

A.) Profile of the sucrose gradient to purify mononucleosomes from mouse embryonic fibroblasts. B.) 4% native acrylamide gel of sucrose gradient fractions showing purified mononucleosomes. M is DNA marker. C.) SDS-PAGE and Western blot (bottom) analysis of fractions 14 and 15 from the sucrose gradient. CM is chicken erythrocyte marker. Western blot was performed with anti-GFP antibody that also recognizes YFP.

In order to analyze the distribution of H2A.Z variants within chromatin biochemically, C-terminal Flag epitope tagged H2A.Z-1 and H2A.Z-2 were stably transfected into HEK 293 cells, nuclei were isolated and digested with microccocal nuclease and the chromatin was separated into S1, SE and Pellet fractions. The stably transfected clones that were selected had nearly identical expression levels of the respective Flag-tagged H2A.Z that represented less than 30% of the total endogenous H2A.Z (Figure 11 and Figure 12A). The highly nuclease-accessible S1 fraction contains mainly mononucleosomes having a DNA length of approximately 146 bp that generally represents euchromatin, while the more nuclease-resistant SE fraction contains mainly heterochromatin with DNA of varying lengths (Figure 12B). The insoluble Pellet fraction most likely represents a mixture of heterochromatin and euchromatin that is insoluble due to its association with large protein complexes such as the RNA Pol II and chromatin remodelling complexes or components of the nuclear matrix (Figure 12B) (Henikoff et al., 2009). This fraction contains far fewer histones compared to other high molecular weight proteins. Western blot analysis of the histones extracted from these fractions using an antibody against H2A.Z that does not discriminate between the variants indicates that total endogenous H2A.Z (bottom band, arrow 1) is present in all three chromatin fractions but is more abundant in the S1 and SE compared to the P (Figure 12A). This antibody is also able to detect the Flag-tagged H2A.Z proteins (top band, arrow 2) and indicates that these forms fractionate similarly to the endogenous forms but that the H2A.Z-2-Flag protein is present in higher amounts in the S1 fraction. This pattern can also be seen when the blot is probed with an anti-Flag antibody (Figure 12A). These blots were further probed with an antibody against total H4 as a loading control and against H3 trimethylated at lysine 4

(H3 Tri-Me K4). Staining with the latter antibody indicates that this modification does not partition equally among the fractions, but is proportionally more abundant within the pellet fraction. Since H3 Tri-Me K4 is a marker of promoter regions of active genes, this result is in agreement with the notion that the Pellet fraction contains genomic regions that are actively being transcribed.

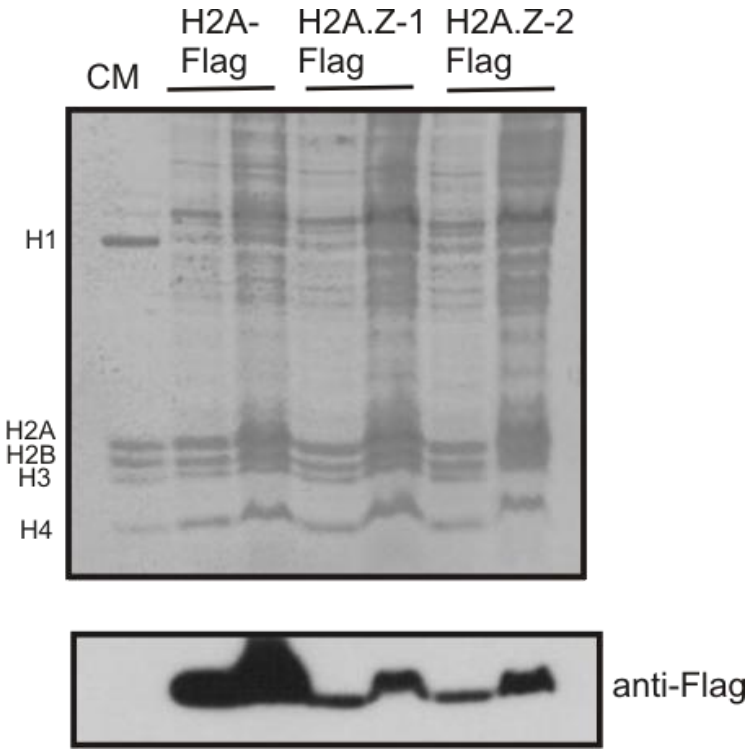

Figure 11: Expression of H2A-, H2A.Z-1-, and H2A.Z-2-Flag in stably transfected HEK 293 clones.

The top panel shows an SDS-PAGE of normalized histones that were extracted from isolated nuclei of HEK 293 cells stably transfected with the indicated construct, two loadings are shown for each. The bottom panel is the Western blot of the gel in the top panel probed with anti-Flag antibody.

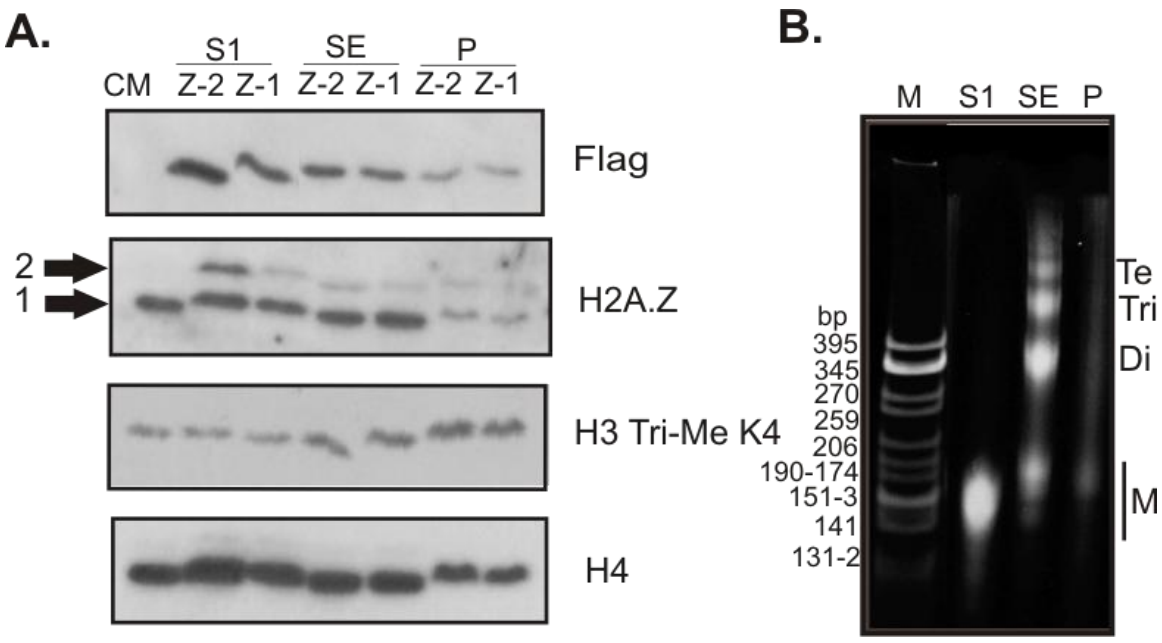

Figure 12: Distribution of H2A.Z-2 and H2A.Z-1 within chromatin fractions.

A.) S1, SE and P chromatin fractions were generated from HEK 293 cells stably expressing Flag epitope tagged H2A.Z-2 and H2A.Z-1, resolved by SDS-PAGE and analyzed by Western blot. The antibodies used for Western blotting are indicated on the right. The anti-H2A.Z antibody recognizes both isoforms in their endogenous (arrow 1) and Flag-tagged (arrow 2) forms. Probing with the anti-H3 Tri Me K4 antibody indicates that this modification is more enriched within the P fraction and therefore does not partition equally among the fractions. Total histone H4 was used as a loading control and CM indicates chicken erythrocyte histone marker. The trends seen were consistent across multiple experimental replicates. B.) 4% native acrylamide gel of purified DNA from the S1, SE and P chromatin fractions used in A. The S1 fraction contains mononucleosomes (M) with approximate DNA length 150 bp, while the SE and P fractions contain chromatin composed of mononucleosomes, dinucleosomes (Di), trinucleosomes (Tri), tetranucleosomes (Te) and longer chromatin. M is CFO-1 cut pBR322 DNA marker.

H2A.Z-1 and H2A.Z-2 associate with different forms of post-translationally modified H3 and H4 within the nucleosome

We sought to determine next whether the H2A.Z variants differentially associate with several post-translationally modified forms of other histones within the nucleosome. Following the protocol of Sarcinella and colleagues (Sarcinella et al., 2007), C-terminal Flag-tagged versions of H2A.Z-1, H2A.Z-2 and H2A as a control were transiently expressed in HeLa cells and the chromatin was digested to mononucleosomes using micrococal nuclease. Each preparation of mononucleosomes was analyzed on native acrylamide gels to ensure complete digestion of the chromatin (data not shown). The nucleosomes containing the Flag-tagged proteins were immunoprecipitated using anti-Flag agarose beads and the specificity of the immunoprecipitations was monitored by AUT-PAGE (Figure 13A). Figure 13A shows that the immunoprecipitations are specific for H2A-Flag, H2A.Z-2-Flag or H2A.Z-1-Flag containing nucleosomes and the identity of these histones was further confirmed by 2-dimensional PAGE with an AUT gel in the first dimension followed by an SDS gel in the second dimension (Figure 13B). Figure 13A also indicates that both the H2A.Z-1-Flag and H2A.Z-2-Flag nucleosomes most likely only contain one copy of the tagged protein in the histone octamer, as an H2A band with equal staining intensity is also present in the gel. The immunoprecipitated nucleosomes were then normalized with respect to total H4, resolved by SDS-PAGE and transferred to membranes which were probed with antibodies specific for several post-translationally modified forms of histones (Figure 13C). Both forms of H2A.Z nucleosomes are enriched in H3 trimethylated at lysine 4 compared to H2A nucleosomes as shown by other groups (Figure 13C) (Sarcinella et al., 2007; Viens et al., 2006).

However, this enrichment is greater in the case of the H2A.Z-2-Flag nucleosomes compared to the H2A.Z-1-Flag nucleosomes. The promoters of most protein coding genes contain nucleosomes that have the H3 Tri-Me K4 mark along with H3 acetylated at K9 and K14 (Guenther et al., 2007; Zhang et al., 2004). When the immunoprecipitated nucleosomes were probed with an antibody against this latter H3 modification, roughly equal amounts can be seen in the H2A-Flag, H2A.Z-2-Flag and H2A.Z-1-Flag nucleosomes (Figure 13C). H3 trimethylated at lysine 27 is a marker of inactive promoters and mediates transcriptional silencing (Fischle et al., 2003). The levels of this modification are relatively equal among all the Flag immunoprecipitated nucleosomes (Figure 13C). Similarly, the levels of H4 acetylated at lysine 16 are equal among nucleosomes. Interestingly, H2A.Z-1-Flag and H2A.Z-2-Flag nucleosomes are enriched in H3 phosphorylated at serine 10 compared to H2A-Flag nucleosomes. This pattern was also seen when the transfected cells were arrested in mitosis by nocodazole treatment before generation of mononucleosomes and immunoprecipitation. It is possible that the majority of the H3PhosS10 staining in the asynchronous cells could be due to the proportion of mitotic cells within that population. This is likely the case since the staining intensity is increased in mitotic H2A.Z-1 and H2A.Z-2 nucleosomes.

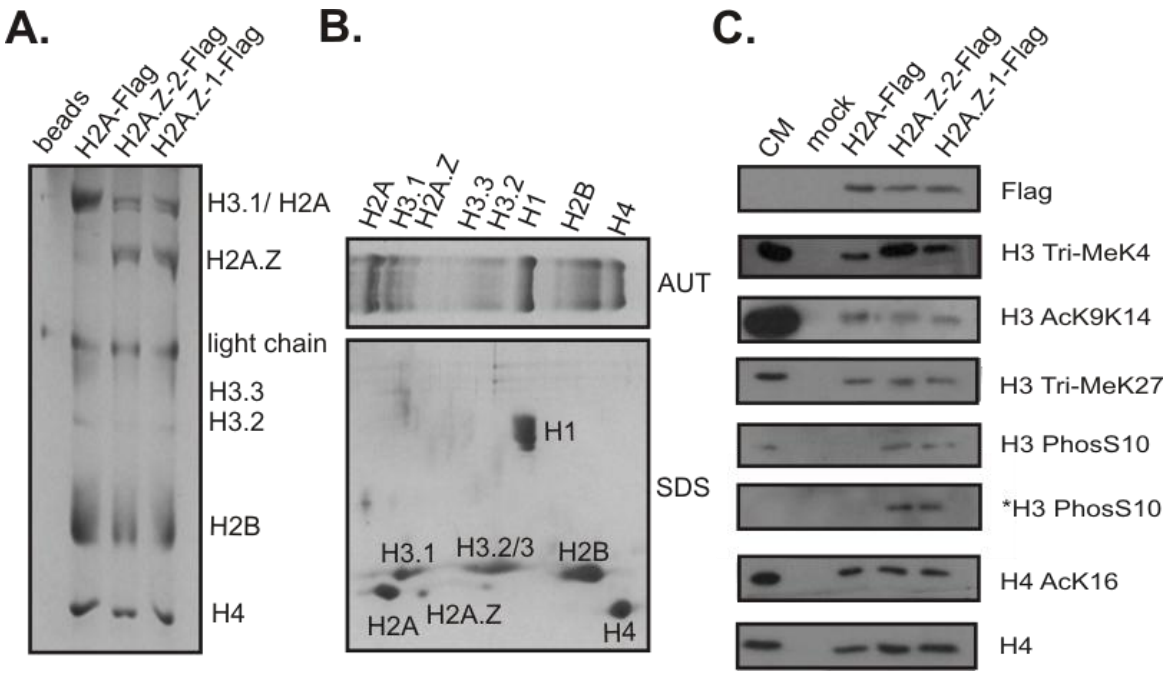

Figure 13: Immunoprecipitation of H2A.Z-2- and H2A.Z-1-containing mononucleosomes. A.) AUT-PAGE of HeLa cell mononucleosomes immunoprecipitated with anti-Flag agarose beads. Light chain refers to the immunoglobulin light chain from the anti-Flag agarose beads. B.) Two-dimensinal PAGE analysis of HeLa cell histones with the first dimension AUT shown on top and second dimension SDS gel shown below. C.) Western blots of anti-Flag agarose bead immunoprecipitated mononucleosomes electrophoresed on 15% SDS gels. Samples were normalized with respect to Flag and total H4 levels. Antibodies used to probe the Western blots are indicated on the right. The asterisk indicates the cells were arrested in mitosis by nocodazole treatment prior to immunoprecipitation. The trends in the association of the Flag-tagged proteins with post-translationally modified forms of H3 and H4 were consistent across multiple replicates of the experiment of which a representative example is shown.

H2A.Z-1 and H2A.Z-2 are differentially expressed among tissues

In order to compare the levels of H2A.Z-1 and H2A.Z-2 mRNA expression in different tissues and in HeLa cells, we performed quantitative PCR on a panel of adult and fetal human tissue samples. Primers were designed that specifically amplify the cDNA of either H2A.Z isoform based on substantial sequence differences within the UTR regions. The specificity of the PCR reaction was monitored by DNA sequencing of the amplicons and by melting curve analysis. The highest levels of H2A.Z transcripts were seen in HeLa cells and in the testes (Figure 14). Figure 14 also shows that the levels of H2A.Z-1 and H2A.Z-2 transcript expression were similar in several adult tissues including testes, ovary, prostate, peripheral blood leukocytes, small intestine, pancreas and HeLa cells. The adult brain showed approximately 4-fold more H2A.Z-1 transcript than H2A.Z-2. A 2-fold increase in H2A.Z-2 transcript levels over H2A.Z-1 was seen in the adult liver and kidney. The widest range of expression levels between tissues for each variant was 5-fold (liver vs testes) for H2A.Z-1 and 5-fold (brain vs testes) for H2A.Z-2. To determine if the expression levels of the H2A.Z variants differed depending on developmental stage, we also analyzed their expression in three fetal tissues for which there was an adult counterpart. When comparing the fetal H2A.Z variant transcript levels to one another, H2A.Z-1 was more abundant than H2A.Z-2 in the brain (2-fold) and they had similar levels in the fetal liver and kidney (Figure 5, compare hatched bars). While the fetal kidney showed a similar H2A.Z-1 and H2A.Z-2 expression pattern compared to adult kidney (Figure 14), the patterns observed in brain and liver were different between fetus and adult suggesting possible developmental regulation of transcript levels (Figure 14).

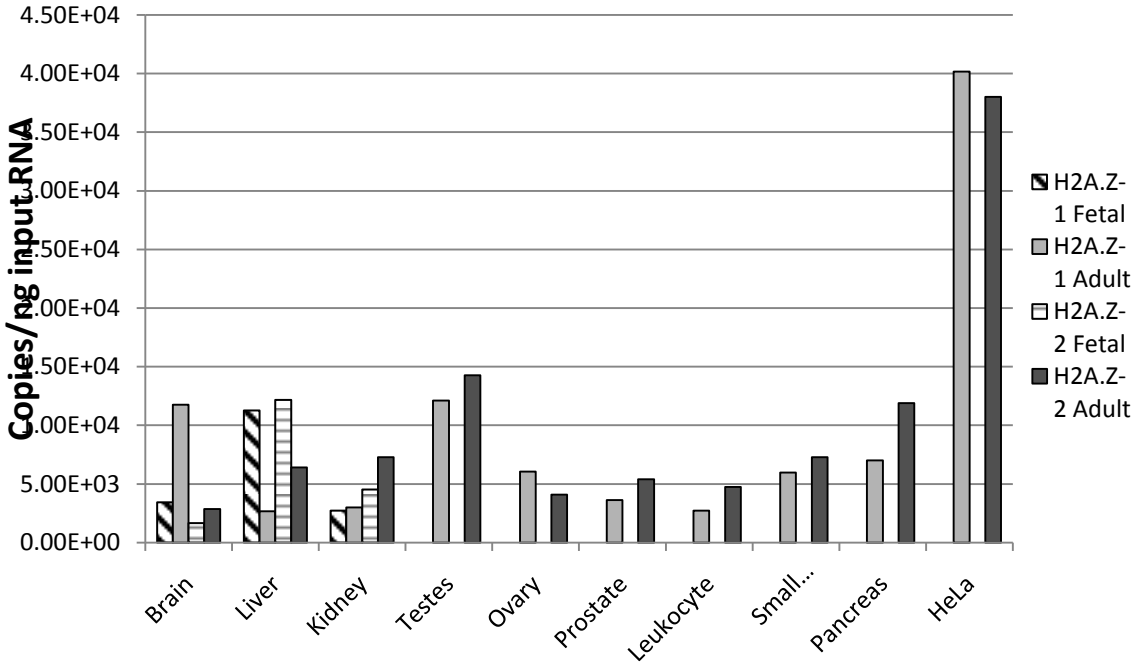

Figure 14: Quantitative PCR analysis of H2A.Z-1 and H2A.Z-2 mRNA transcript levels in adult and fetal human tissues.

The abundances of H2A.Z-1 and H2A.Z-2 transcript levels were determined relative to a standard curve of known DNA amount for each primer set. Fetal levels are denoted with hatched bars while adult levels are represented by solid bars.

The promoter sequences of the H2A.Z-1 and H2A.Z-2 genes are substantially different

The evolutionary process responsible for the differentiation between H2A.Z-1 and H2A.Z-2 has been described as a refined stepwise mutation change within the codons of the three differential residues (triresidue), leading to differences in the intensity of the selective constraints acting upon the two H2A.Z isoforms in vertebrates (Eirin-Lopez et al., 2009). To determine whether the variation in expression patterns of the H2A.Z variants could be attributed in part to differences in transcription factor binding sites in the promoters and therefore potential differential gene regulation, we dissected the proximal promoter regions of both H2A.Z variants in mammals (Figure 15A), where the evolutionary differentiation between H2A.Z-1 and H2A.Z-2 has reached its maximum. Recurrent search rounds for transcription regulatory elements were performed on H2A.Z promoter regions from human, rhesus monkey and mouse, leading to the identification of several putative promoter elements as well as to the localization of previously studied modules shown to be critical for H2A.Z-1 promoter activity (Hatch and Bonner, 1990). However, comparisons between H2A.Z-1 and H2A.Z-2 promoter regions revealed completely different promoter architectures. H2A.Z-1 shows the presence of typical elements common to other replication-independent histone variants as well as putative binding sites for other transcription factors. A perfect TATA box, three CAAT boxes and several putative GC-boxes (among which GC.1, GC.2 and GC.3 have been previously reported to form complexes with the Sp1 transcription factor) are observed in the proximal promoter region. Among these elements, one CAAT box (CAAT.2) and a GC-box (GC.2) are critical for H2A.Z promoter activity (Hatch and Bonner, 1995).

Furthermore, binding sites for c-myc are present within the upstream region of the H2A.Z-1 promoter (-459, -563) where they have been shown to specifically bind MYC and increase H2A.Z-1 transcription in response to estrogen (Hua et al., 2008).

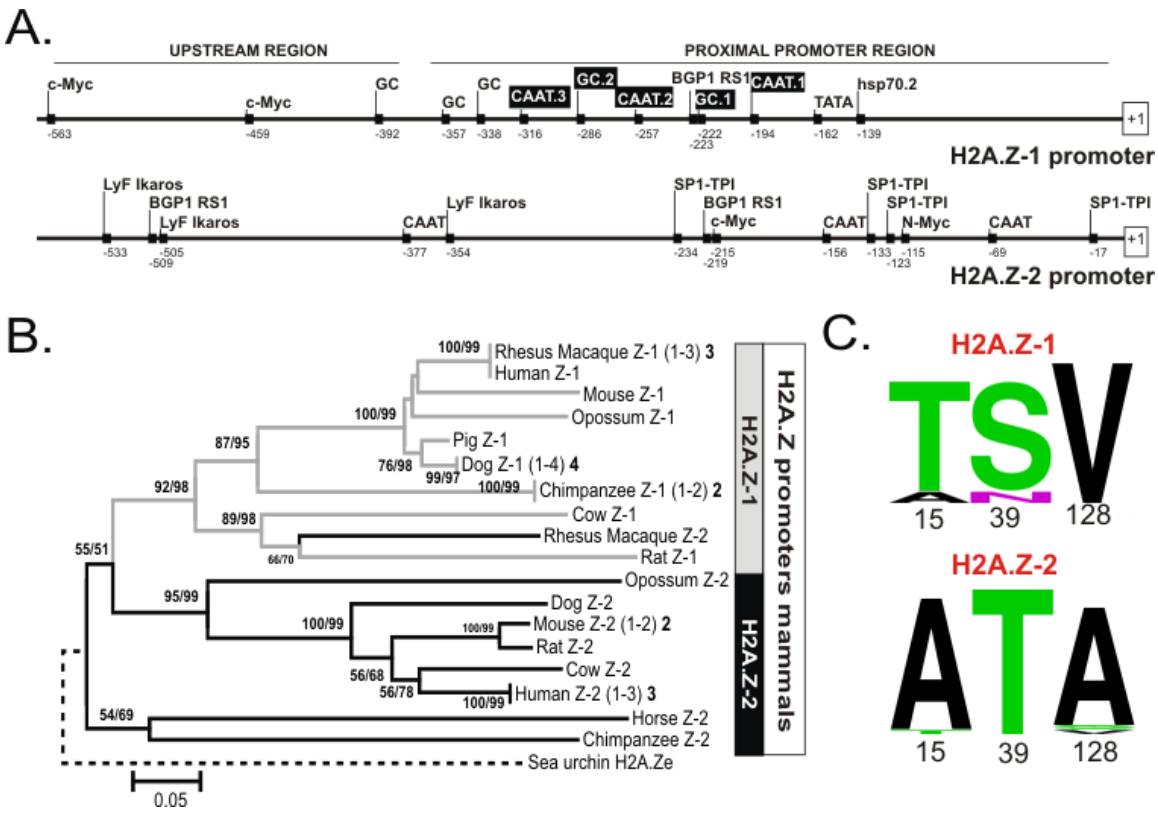

Figure 15: Phylogenetic analysis of the promoter regions of H2A.Z-1 and H2A.Z-2 in mammals.

A.) Dissection of the putative regulatory elements in the proximal and the upstream promoter regions of both H2A.Z variants. Elements whose relevance for H2A.Z promoter activity has been experimentally demonstrated are indicated in black boxes. B.) Phylogenetic relationships among H2A.Z promoter regions in mammalian representatives. The numbers for internal nodes in the topology indicate confidence values for the groups defined (BS/IBT), both based on 1000 replications and only shown when a value is greater than 50%. Numbers in parentheses and in boldface near species names indicate the sequence variant copy and the number of sequences analyzed, respectively (Appendix 1). The tree was rooted with the H2A.Ze sequence from sea urchin, representing an early chordate in which H2A.Z-1 and H2A.Z-2 variants are not yet differentiated. C.) Logos representation of the amino acid residues at postions 15, 39 and 128 in H2A.Z-1 and H2A.Z-2. The sequences used to create the logos were the same as in B.

Characterization of the H2A.Z-2 promoter emphasizes the existence of a clear differentiation between H2A.Z-1 and H2A.Z-2. The H2A.Z-2 promoter contains no TATA box and the positions of the CAAT elements and GC-boxes do not coincide with those identified in H2A.Z-1 (Figure 15A). Furthermore, it seems that H2A.Z-2 promoters show a lesser degree of conservation across the mammalian species studied, as indicated by less positional consensus in the elements identified. Searches for potential regulatory elements in the proximal promoter region resulted in the identification of three CAAT elements as well as several binding sites for transcription factors including c-Myc and N-Myc. However, the positioning of these latter binding sites at the proximal region suggests that they may function in constitutive gene expression rather than in inducible regulation in response to agents such as hormones (Hatch and Bonner, 1995; Hua et al., 2008).

The differentiation between the H2A.Z-1 and H2A.Z-2 promoters has also been analyzed from a phylogenetic perspective (Figure 15B). Our results reveal the differentiation of two major evolutionary lineages based on H2A.Z promoter sequences, one encompassing the H2A.Z-1 promoter sequences and the other including H2A.Z-2 promoter sequences (Figure 15B). Such topology is in agreement with the phylogenetic inferences reconstructed on the basis of H2A.Z protein sequences and nucleotide coding regions, which also show an evolutionary differentiation between H2A.Z-1 and H2A.Z-2 variants (Eirin-Lopez et al., 2009). The presence of such differentiation at promoter regions strongly supports the presence of evolutionary constraints which act with different direction and intensity on the H2A.Z-1 and H2A.Z-2 proteins. The conservation of the

three amino acid residues that differ between the isoforms in mammals is highlighted by the logos in Figure 15C.

Discussion:

Our results regarding the nuclear localization of the H2A.Z isoforms indicate that they are identically distributed mainly in the euchromatin of mouse embryonic fibroblasts, as seen by other groups (Bruce et al., 2005; Sarcinella et al., 2007). However, both H2A.Z-1 and H2A.Z-2 staining is also present within DNA-dense regions that represent the centers of chromosomes. This is most likely due to the known presence of H2A.Z in pericentric and centric chromatin (Greaves et al., 2007; Rangasamy et al., 2003). This distribution of H2A.Z is corroborated by our biochemical analysis of chromatin fractions indicating that endogenous H2A.Z is present in greater amounts within the S1 (euchromatin) and SE (heterochromatin) fractions compared to the Pellet (insoluble chromatin). In accordance with the distribution of endogenous H2A.Z within these fractions, we see that both stably transfected H2A.Z-1-Flag and H2A.Z-2-Flag are also present in all fractions; however, interestingly H2A.Z-2-Flag protein is present in greater amounts within the S1 fraction compared to H2A.Z-1-Flag. This suggests that H2A.Z-2 may play a greater role in the function of H2A.Z within the nuclease accessible euchromatin than does H2A.Z-1. It has been shown in several systems that H2A.Z functions in part to poise promoter chromatin for transcriptional activation, since it is remodeled from promoters of actively transcribing genes (Farris et al., 2005; Gevry et al., 2007; Gevry et al., 2009; John et al., 2008; Li et al., 2005b; Sutcliffe et al., 2009). H2A.Z functioning in this manner would likely fractionate within the S1 fraction since this chromatin would be in a more open

conformation. Furthermore, the low levels of H2A.Z present within the P fraction also agree with it not playing a significant role after the initiation stage of transcription. Therefore, in HEK 293 cells H2A.Z-2 may be playing a greater role than H2A.Z-1 in poising chromatin for transcription, which agrees with our results indicating that H2A.Z-2 also shows a greater association with H3 Tri-Me K4 than H2A.Z-1 (see below).

Genome wide distribution patterns indicate that H3 Tri-Me K4 and H2A.Z are both present at the promoters and 5' ends of genes in yeast and humans (Barski et al., 2007). It is therefore not surprising that H2A.Z and H3 Tri-Me K4 are present within the same nucleosome (Sarcinella et al., 2007; Viens et al., 2006). The fact that H2A.Z-2 associates with H3 Tri-Me K4 to a greater extent than H2A.Z-1 is interesting because it indicates that there is a greater overlap in the regions of chromatin where H2A.Z-2 is incorporated in conjunction with the H3 Tri-Me K4 mark than H2A.Z-1. This suggests that H2A.Z-1 and H2A.Z-2 could be incorporated at different locations within the genome in a manner that cannot be detected by our chromatin fractionation method. The remodelling of H2A.Z into chromatin in mammals is known to occur via the action of several distinct complexes that contain the SRCAP protein, p400 or TIP 48/49 as the ATP-dependent remodelling subunits and evidence suggests that the deposition patterns of these complexes may differ (Choi et al., 2009; Gevry et al., 2007; Ruhl et al., 2006; Wong et al., 2007). It is tempting to speculate that one complex may prefer a specific isoform over the other, or that one complex may be responsible for incorporating H2A.Z at low levels across the genome and another for the increased levels of H2A.Z that are necessary to promote appropriate chromatin architecture at promoters (Albert et al., 2007).

Furthermore, H2A.Z nucleosomes flank nucleosome free regions whose formation is DNA-sequence dependent in several organisms including humans (Barski et al., 2007). Whether one of the human complexes that integrates H2A.Z into chromatin contains a subunit that recognizes a specific DNA sequence is unclear but points to the potential for more than one mechanism to specify the location of H2A.Z nucleosomes (Hartley and Madhani, 2009). Indeed, a recent *in silico* analysis suggests that both genetic and epigenetic factors can predict whether a nucleosome will contain H2A.Z (Gervais and Gaudreau, 2009).

The functional output of the increased association of H2A.Z-2 with H3 Tri-Me K4 is unclear, but it is highly unlikely that it results in a structural alteration of the nucleosome that would otherwise not be observed in those containing H2A.Z-1 with H3 Tri-Me K4 given the high sequence similarity of the isoforms. At least one of the effects of having H2A.Z and H3 Tri-Me K4 within the same nucleosome could be related to the recruitment or function of the RNA Pol II complex, since both the C-terminal region of H2A.Z and H3 Tri-Me K4 have been shown to interact with components of this complex (Adam et al., 2001; Shilatifard, 2008). Another possibility is that nucleosomes containing both H2A.Z and the H3 Tri-Me K4 mark protect less DNA than other nucleosomes, making the DNA more accessible for transcription (Fu et al., 2008). Nevertheless, it is possible that any differences in the genomic localization and association with post translationally modified forms of other histones of the endogenous H2A.Z-1 and H2A.Z-2 could reflect spatial and temporal differences in their nuclear availability as determined by their levels of expression, or by their import into the nucleus.

Our results also reveal that H2A.Z-1 and H2A.Z-2 nucleosomes are enriched in H3 phosphorylated at S10 compared to H2A nucleosomes in asynchronous and mitotic HeLa cells. This association is interesting because like H2A.Z, H3 PhosS10 has been shown to be involved in processes requiring open and condensed chromatin, namely in transcription and chromosome condensation during mitosis (Prigent and Dimitrov, 2003). The structural and functional consequences of H3S10 phosphorylation are not entirely clear; however, this modification does correlate with increased expression of immediate early genes after induction of MAP Kinase cascades (Clayton et al., 2000; Thomson et al., 2001) and has been shown to be required for the release of RNA Pol II from promoter proximal pausing (Ivaldi et al., 2007). Furthermore, it is not surprising that H4AcK16 is found to associate with H2A.Z-1 and H2A.Z-2 nucleosomes because it has been shown that this modification of H4 is required for incorporation of H2A.Z into subtelomeric chromatin in budding yeast (Shia et al., 2006).

Our analysis of the transcript levels of H2A.Z-1 and H2A.Z-2 indicate that there is no one dominant form, rather they are both expressed across a wide range of human tissues and that the expression levels vary depending on developmental stage. This pattern of expression likely reflects the significant sequence variation within the promoter regions of these genes and the differences in abundance of specific transcription factors within the tissues; however, it could also reflect subtle changes in the requirements of the tissues for one isoform over the other based on any functional differences between H2A.Z-1 and H2A.Z-2. Indeed, recently it has been shown that H2A.Z-2 is specifically upregulated

during macrophage differentiation and activation (Baek et al., 2009). Also as previously mentioned, genetic knockout studies in mice show that H2A.Z-1 is essential for development, indicating that H2A.Z-2 cannot compensate for the loss of H2A.Z-1 at least at early stages of mouse embryo differentiation (Faast et al., 2001).

The evolutionary evidence presented here suggests that it is highly possible that H2A.Z-1 and H2A.Z-2 appeared in vertebrates as a result of the entire genome duplication that took place between the divergence of the prochordates from the ancestral chordate lineage and the evolution of vertebrates, as stated by the 2R hypothesis (Meyer and Van de Peer, 2005). While most of the genes arising from this duplication event were silenced, some of them were retained and their protein products either acquired a neofunctionalization (a completely new function) or a subfunctionalization in which the two new proteins acquired specialized functions (Lynch and Conery, 2000). This latter situation appears to be the case in going from H2A.Z-e to H2A.Z-1 and H2A.Z-2 in vertebrates.

Conclusions and Future Directions:

We present evidence that the two forms of H2A.Z present in mammals display similar genomic localization patterns mainly within euchromatin but that subtle differences in their association with post translationally modified forms of other histones exist. Thus, it is possible that throughout the course of vertebrate evolution, the two H2A.Z isoforms have acquired a degree of independent function that could contribute to the increased complexity and large diversity of roles for this histone variant in higher organisms. It is also likely that differences in chromatin localization patterns of the isoforms could be due

to the temporal regulation of their genes, especially considering the dissimilarity in the promoter regions. In order to perform a more extensive analysis of the genome-wide distributions of H2A.Z-1 and H2A.Z-2, it would be very informative to perform chromatin immunoprecipitation of the stably transfected HEK 293 cells followed by parallel sequencing. This approach would allow us to more specifically identify whether one isoform predominates over the other in certain regions or at certains types of gene promoters. It would also be very interesting to analyze the properties of NCPs reconstituted with either H2A.Z isoform along with a chemically homogeneous population of H3 Tri-Me K4 since it has been suggested that these nucleosomes protect less DNA than canonical nucleosomes (Tolstorukov et al., 2009)

Chapter 4: H2A.Z poises the Prostate Specific Antigen (PSA) gene promoter for androgen-dependent transcription

Deanna Dryhurst and Juan Ausio

Department of Biochemistry and Microbiology, University of Victoria, Victoria, British Columbia, Canada V8W 3P6

Contributions:

Deanna Dryhurst wrote the chapter and performed all experimental procedures unless otherwise mentioned. LNCaP xenograft tumours were produced at the Vancouver Prostate Centre by personnel in Paul Rennie's lab.

Introduction:

The structure of chromatin in general has a repressive effect on transcription because it limits access to the underlying DNA sequence. In order to overcome this barrier, the cell employs three interconnected processes to modify the chromatin template which are 1) post-translational modification of histones, 2) chromatin remodelling, and 3) incorporation of histone variants. That these three processes act synergistically to facilitate transcription is exemplified by incorporation of the histone variant H2A.Z into chromatin which occurs at many human promoters genome-wide via the action of complexes that contain at least one ATP-dependent chromatin remodelling subunit (SRCAP, p400, TIP48/49) as well as histone acetyltransferase enzymes including Tip60 (Altaf et al., 2009). Many studies have now shown that H2A.Z is found associated with gene regulatory regions including promoters and enhancers (Barski et al., 2007; Bruce et al., 2005) and while the exact mechanistic details of how it participates in facilitating transcription are not entirely clear, very recent evidence indicates that H2A.Z may help in directly recruiting RNA Pol II (Hardy et al., 2009). However, several studies show that H2A.Z may help to poise promoter chromatin for transcriptional activation since it does not appear to be required after the initiation stage of transcription (John et al., 2008; Sutcliffe et al., 2009). H2A.Z has been shown to play a role in other cellular processes including maintaining the boundaries between heterochromatin and euchromatin (Meneghini et al., 2003), mediating proper chromosome segregation (Rangasamy et al., 2004), and in estrogen receptor signalling (Gevry et al., 2009). Furthermore, several large-scale gene expression analyses in different cancers have identified H2A.Z as being

associated with cancer progression (Dunican et al., 2002; Hua et al., 2008; Rhodes et al., 2004; Zucchi et al., 2004).

The androgen receptor (AR) is a member of the steroid hormone receptor family of nuclear transcription factors that is crucial for male development and in the biology of prostate cancer (Heinlein and Chang, 2002). AR is normally held in an inactive state in the cytoplasm where it is complexed with heat shock proteins, but upon binding to androgen AR translocates to the nucleus where it binds as a homodimer to androgen response elements (AREs) usually located within enhancer sequences of androgen responsive genes (Devlin and Mudryj, 2009). Hormone-bound AR can recruit coactivator proteins, many of which have chromatin remodelling or histone modification abilities, as well as components of the basic transcriptional machinery that leads to increased gene expression. That most prostate tumours are dependent on a functional AR signalling pathway is exemplified by the fact that anti-androgen therapies are combined with chemotherapy and radiation therapy to treat disease that has spread too extensively locally or has developed distant metastases. However, these cancers inevitably progress to an androgen-independent or castration resistant stage when they no longer require androgen for growth and hence no longer respond to anti-androgen therapy. The AR is expressed in both androgen-dependent and –independent cancers and AR signalling pathways play an important role in both since knockdown of AR protein levels reduces the growth of both types of tumours in model systems (Cheng et al., 2006; Snoek et al., 2009).

Interestingly, two known coactivators of AR include the Tip60 enzyme which has been shown to acetylate AR itself (Sapountzi et al., 2006) as well as lysine residues within histones, and SRCAP. The SNF2-related CBP activator protein (SRCAP) is one of the human orthologs of the Swr1 protein in yeast and both have been shown to catalyze the ATP-dependent incorporation of H2A.Z/H2B dimers into chromatin (Krogan et al., 2004; Mizuguchi et al., 2004; Wong et al., 2007). Furthermore, the human Tip60 complex is generally considered to be orthologous to the yeast NuA4 histone acetyltransferase complex (Altaf et al., 2009). We therefore hypothesized that H2A.Z would be involved in AR-mediated transcription of the PSA (prostate-specific antigen) gene in prostate cancer cells. To investigate this possibility, we used three prostate cancer cell lines, the AR-negative PC3 cell line, the AR-positive and androgen-dependent LNCaP cell line, and the AR-positive but androgen-independent C4-2 cell line that was derived from long-term androgen deprived LNCaP cells (Thalmann et al., 2000). We also hypothesized that H2A.Z could be involved in the progression of prostate cancer to the castration resistant state. To this end, we have employed an *in vivo* mouse LNCaP tumour model of prostate cancer progression and examined H2A.Z expression levels.

Here we show that H2A.Z and N-terminally acetylated H2A.Z are mainly present at the PSA enhancer and proximal promoter when the gene is inactive. Furthermore, we provide evidence that the H2A.Z-1 isoform gene is specifically upregulated in response to androgen treatment, while the H2A.Z-2 isoform gene is not. Finally, our results indicate that total H2A.Z protein levels are increased in castration resistant LNCaP xenograft

tumours suggesting that H2A.Z may play a role in the androgen-independent phenotype of these tumours.

Materials and Methods:

Cell Culture:

PC3, LNCaP and C4-2 cells were from Dr. Rennie's lab at the Vancouver Prostate Centre. LNCaP and C4-2 cells were maintained in RPMI 1640 medium (Invitrogen) supplemented with 10% FBS (PAA laboratories), 1% penicillin/streptomycin (Invitrogen) while PC3 cells were maintained in DMEM (Invitrogen) with 10% FBS and 1% penicillin/streptomycin. All cells were transferred to phenol red-free medium supplemented with 5% charcoal-stripped FBS (PAA laboratories) for 3 days prior to induction with 10nM of synthetic androgen R1881 or ethanol control.

Histone acid extraction:

Nuclei were isolated from PC3, LNCaP and C4-2 cells or from LNCaP tumours by washing three times in Buffer A (250mM sucrose, 60mM KCl, 15mM NaCl, 10mM MES pH 6.5, 5mM $MgCl_2$, 1mM $CaCl_2$, 0.5% Triton X-100) and twice in Buffer B (50mM NaCl, 10mM Pipes pH 6.8, 5mM $MgCl_2$, 1mM $CaCl_2$) supplemented with 1:100 protease inhibitor cocktail (Roche) with all centrifugations performed at 3000xg. The histones were then acid extracted with 0.4N HCl and the supernatant was precipitated with acetone overnight at -20°C. The histones were dried under vacuum.

Western Blotting:

Acid extracted histones were resolved on 15% acrylamide SDS gels normalized with respect to total H4 and transferred to PVDF membrane for 3 hours at 100 volts. The membranes were probed with anti-H2A.Z (1:5000, Abcam), anti-Acetylated H2A.Z (1:1000, Abcam) and anti-H4 (1:10,000) that was produced in house.

LNCaP xenografts:

LNCaP cells (5×10^6) were inoculated subcutaneously with 0.1 mL Matrigel (Becton Dickinson Labware, Mississauga, Ontario, Canada) in two flank regions of 6- to 8-week-old male athymic nude mice (Harlan Sprague Dawley, Inc., Indianapolis, IN) under halothane anesthesia using a 27-gauge needle. When the tumours became palpable, their volumes were measured weekly. Blood was also collected from the tail vein at weekly intervals to monitor PSA. Tumour size was calculated by the formula length x width x depth x 0.5236 (Gleave et al., 1999), and serum PSA was measured by ELISA (ClinPro International, Union City, CA). When PSA values reached 50 to 75 ng/mL, tumours of one quarter of the mice were harvested as 'intact'. Three quarters of the mice were castrated and tumours were harvested after 7 or 14 days. Once the levels of PSA had returned to 50-75 ng/mL the tumours were considered castration resistant. All animal procedures were done according to the guidelines of the Canadian Council of Animal Care and with appropriate institutional certification.

RNA extraction and Quantitative reverse-transcriptase PCR:

Total RNA was extracted from cell lines and tumour tissues using the RNeasy kit (Qiagen) following the manufacturer's protocol. One microgram of RNA was converted to cDNA using Superscript II (Invitrogen). The cDNA was diluted 20-fold for analysis with the following primer sets: PSA mRNA Forward: GATGCTGTGAAGGTCATGGA, PSA mRNA Reverse: AGCACACAGCATGAACTTGG, H2A.Z-1 Forward: TTGCTTGAGCT TCAGCGGAATT, Reverse: TTCCTTGTTATCTCAGGACTCT H2A.Z-2 Forward: GCGGCCGAGCGGAGGCGGAG, Reverse: TGCTTAGAGGGATGCTTTAAC. The identity of the amplicons was confirmed by DNA sequencing. The transcript levels were analyzed by SYBR Green incorporation using a Stratagene MX3005P QPCR system and MXPro software. Each 15ul DNA amplification reaction consisted of 2ul of diluted cDNA and 13ul of Platinum SYBR Green qPCR SuperMix-UDG with Rox (Invitrogen) containing 2.5pmol of each primer. Thermocycling conditions for all primer sets were: 9 min 95°C followed by 40 cycles of 15 sec 95°C, 30 sec 60°C and 45 sec 72°C. Reactions were performed in quadruplicate and averaged cycle threshold (Ct) was compared to the invariant glyceraldehyde-3-phosphate dehydrogenase (GAPDH) transcript using the comparative Ct method ($\Delta\Delta$Ct) (REF). GAPDH forward primer: AAGGTCATCCCTGAGCTGAACGGG and reverse primer: CCAGGAAATGAGCTTGACAAAGTG. PSA, H2A.Z-1 and H2A.Z-2 primer sets satisfied the requirements for the comparative Ct method with the absolute value of the slope of log input amount versus Ct being less than 0.1 and the primer efficiency being greater than 99%. In the case of the LNCaP tumour tissue, to allow for direct comparison between sample types, a cDNA standard was included in the QPCR analysis

to be used as a comparator for data normalization. The standard represented an equivolume mixture of all the tumour tissue cDNA used in the analysis. The expression of H2A.Z-1 and H2A.Z-2 transcripts for each tumour type is therefore represented as fold change relative to this standard.

Chromatin Immunoprecipitation:

Control and 24 hr 10nM R1881 treated PC3, LNCaP and C4-2 cells were grown in 150mm dishes and were approximately 80-90% confluent at the time of crosslinking. Each plate contained approximately $1X10^7$ cells which were crosslinked by addition of 1% formaldehyde directly to the culture medium for 10 minutes at room temperature. The cross linking reaction was quenched with 1.25M glycine and cells were washed twice with cold PBS. Cells were then resuspended in SDS lysis buffer (50mM Tris pH 8.0, 10mM EDTA, 1% SDS) containing protease inhibitors, lysed on ice for 10 minutes or flash frozen and stored at -80°C. The cell lysate was then sonicated using a Fisher Scientific brand Model 100 sonicator and 15 second pulses at output 1 until an average DNA length of 500bp was obtained as measured by agarose gel electrophoresis. Insoluble material was removed by centrifugation and 100ul of sonicated chromatin, which represented approximately 60-80ug of chromatin in each case, was diluted in 1ml of ChIP dilution buffer (0.01% SDS, 1.1% Triton X-100, 1.2mM EDTA, 16.7mM Tris pH 8.0, 167mM NaCl). The chromatin was pre-cleared by incubation with protein A/G agarose (Pierce) for 1hr at 4°C and the resulting supernatant was incubated with an experimentally determined amount of the indicated antibody at 4°C overnight. Immunoprecipitated complexes were pulled down with protein A/G agarose beads and

beads were successively washed in low salt buffer (0.1% SDS, 1% Triton X-100, 2mM EDTA, 20mM Tris pH 8.0, 150mM NaCl), high salt buffer (0.1% SDS, 1% Triton X-100, 2mM EDTA, 20mM Tris pH 8.0, 500mM NaCl), LiCl buffer (0.25M LiCl, 1% NP-40, 1% sodium deoxycholate, 1mM EDTA, 10mM Tris pH 8.0) followed by two washes in Tris-EDTA buffer. Complexes were then eluted from the beads in elution buffer (1% SDS, 0.1M $NaHCO_3$) and heated to 65°C overnight to reverse crosslinks. The immunoprecipitated complexes were treated with RNase A and proteinase K and the DNA was purified using the QiaQuick DNA purification kit (Qiagen). One percent of the initial chromatin was purified as input.

Quantitative PCR:

ChIP DNA was analyzed by quantitative PCR on a Stratagene MX3005P thermocycler. For each ChIP experiment and primer set a standard curve of input DNA was generated and all values for immunoprecipitated DNA were interpolated from this standard curve. All reactions were performed in triplicate and averaged, then subsequently divided by the input value for the corresponding primer set. The standard errors of the means were propagated throughout all subsequent calculations using the application at http://statpages.org/erpropgt.html. All ChIP DNA generated by immunoprecipitation using histone antibodies was further normalized for nucleosome density by dividing by the corresponding total H4 value. The identity of each amplicon was confirmed by DNA sequencing. Error bars for each data point represent the standard error of the mean of two independent experiments. The primers sequences used are indicated in Table 3.

Table 3: PSA primer sequences used for ChIP.

Primer	Forward	Reverse
PSA A	CTGGCAGGATATTCCAAAGC	CTGTGAGGGAGACTGTGCAA
PSA B	ACTGGGACAACTTGCAAACC	TCTCAGATCCAGGCTTGCTT
PSA C	GCCAGCATCAGCCTTATCTC	TACAACCACATCCCCGTTCT
PSA D	CTGCCTTTGTCCCCTAGATG	AAACCTTCATTCCCCAGGAC
PSA E	AAACAGGGTATGGGGGAAAG	TGTGGGAGAGAAAAGGGAGA

Results:

H2A.Z and acetylated H2A.Z are present at the PSA enhancer and promoter under non-inducing conditions

PC3, LNCaP and C4-2 human prostate cancer cell lines were used as a system to investigate the occupancy of H2A.Z and AcH2A.Z under inducing (R1881) and non-inducing (EtOH) conditions at several PSA gene regions. In order to determine the transcript induction kinetics, we measured the relative levels of PSA mRNA by quantitative PCR after treatment with 10nM synthetic androgen R1881 for 24, 36 and 48 hours and compared them to the levels of the invariant GAPDH gene. Figure 16 indicates that the levels of PSA are increased approximately 10-, 20- and 50-fold after 24, 36 and 48 hours, respectively in LNCaP cells. The relative levels of PSA transcript also increase after treatment in C4-2 cells (5-, 10- and 30-fold) though to a lesser extent than LNCaP cells (Figure 16). No PSA transcript was able to be detected in PC3 cells at any time point, as expected.

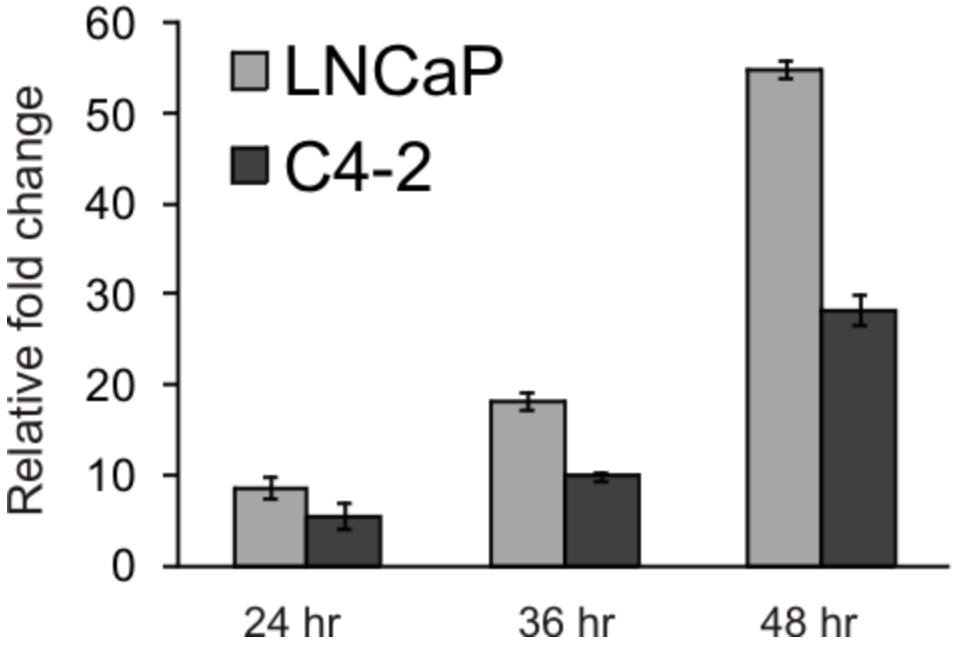

Figure 16: PSA mRNA transcript levels are upregulated in response to androgen.
LNCaP, C4-2 and PC3 cells were treated with 10nM synthetic androgen R1881 for 24, 36 and 48 hours. The relative fold change of PSA mRNA levels in androgen treated cells over the ethanol control treated cells is shown for LNCaP and C4-2 cells. No PSA expression was detected in PC3 cells. Error bars represent the standard error of the mean of 3 independent experiments.

ChIP experiments were performed to examine the location of H2A.Z-containing nucleosomes at an upstream region (PSA A), at the ARE within the enhancer (PSA B), at a position between the enhancer and the proximal promoter that encompasses a cyclic AMP response element (PSA C), at ARE 1 within the proximal promoter (PSA D), and within the transcribed region of the gene (PSA E). The organization of the PSA gene and the location of the primers are depicted in Figure 17A. Figure 17B shows the enrichment of several histones and histone PTMs across the PSA gene in all three cell lines which was calculated by dividing the percent input of histone antibody immunoprecipitation by the percent input of total H4 immunoprecipitation to normalize for nucleosome density. Non-immune IgG (rabbit and sheep) was included as a control for non-specific immunoprecipitation for each set of reactions and the levels were always a minimum of 10-fold lower than histone or PTM-specific antibody immunoprecipitation. The top 3 panels of Figure 17B show the enrichment of total H2A.Z at the PSA loci in all three cell lines. H2A.Z is present at low levels at all loci in PC3 cells and these levels do not change upon treatment with R1881 (Figure 17B, top left panel). In the androgen-responsive LNCaP cells, low levels of H2A.Z that do not change with androgen treatment can be seen at PSA A and PSA C, while a greater enrichment is seen at the enhancer region (PSA B), the proximal promoter (PSA D) and into the coding region of the gene (PSA E) in the absence of androgen (Figure 2B top middle panel). Under conditions where the PSA gene is undergoing rapid cycles of active transcription (24 hr R1881 treatment), the levels of H2A.Z enrichment are lower than in the uninduced state, particularly at PSA D and PSA E, which is a pattern that can also be seen in the C4-2 cells (Figure 17B, top right panel). This agrees with data of genes induced by the

glucocorticoid receptor which also show decreased association of H2A.Z with the promoter upon gene induction (John et al., 2008), as well as with recent genome-wide localization studies (Hardy et al., 2009).

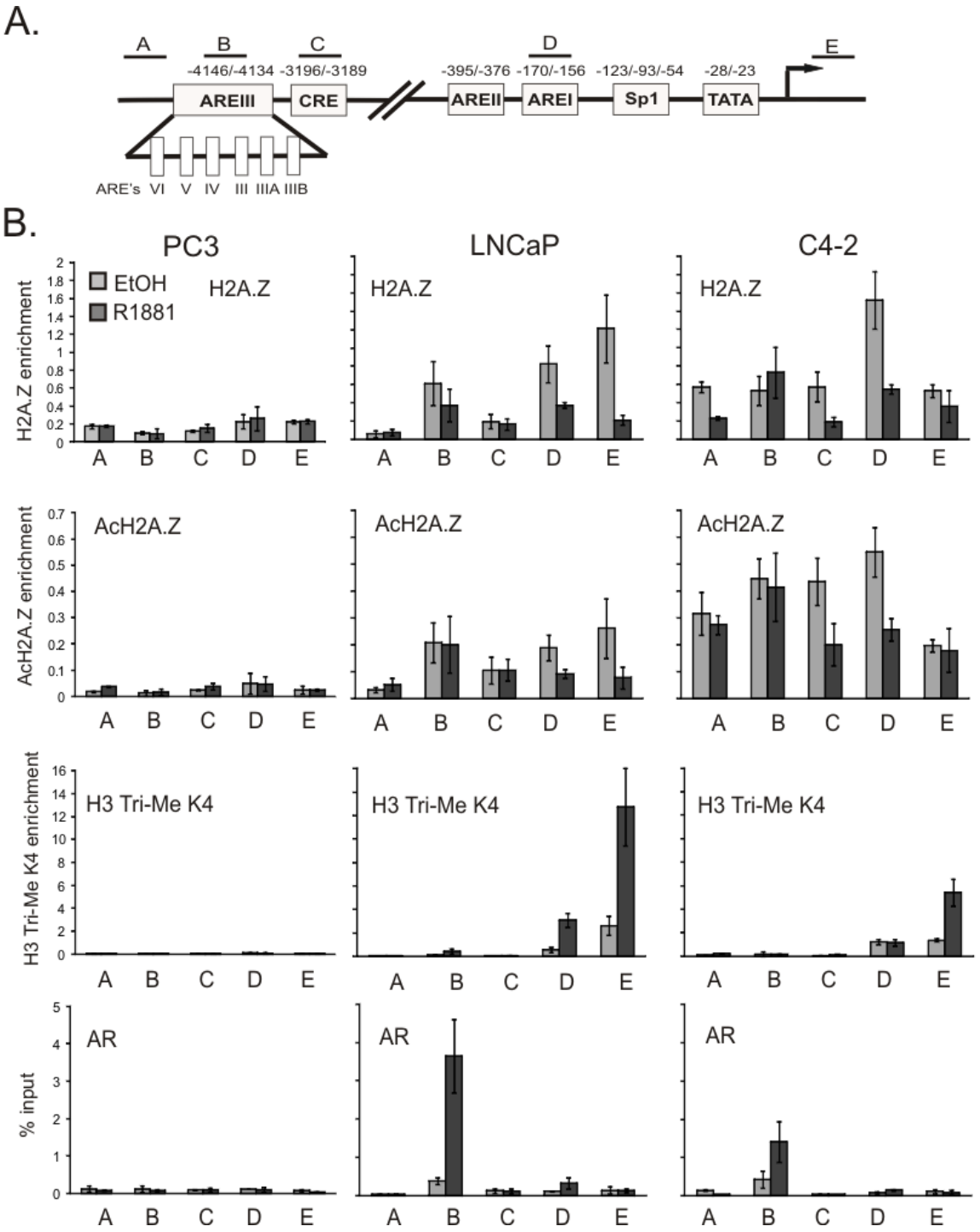

Figure 17: Chromatin immunoprecipitation at the PSA gene.

A.) Representation of the PSA gene, letters indicate the location of primer sets used for ChIP. B.) ChIP experiments using antibodies specific for H2A.Z, AcH2A.Z, H3 Tri-Me K4 and AR in PC3 (left column), LNCaP (middle column), and C4-2 (right column). Error bars represent the standard error of the mean of duplicate experiments.

We also performed ChIP reactions using an antibody that recognizes H2A.Z triply acetylated at K4, K7 and K11 within the N-terminal tail region of the protein (AcH2A.Z) (Bruce et al., 2005). Figure 17B top middle panels indicate that there are very low levels of acetylated H2A.Z at all PSA loci in PC3 cells. In keeping with the pattern seen for total H2A.Z, in the LNCaP and C4-2 cells the levels of acetylated H2A.Z are higher in the uninduced state compared to the induced (Figure 17B top middle panels). However, we see that for both H2A.Z and AcH2A.Z the relative levels present at the enhancer (PSA B) do not change significantly upon induction. Moreover, there are generally higher levels of AcH2A.Z across all loci in C4-2 cells compared to LNCaP (Figure 17B, top middle panels).

In order to examine the levels of H3 trimethylated at lysine 4 (H3 Tri-Me K4) at the different PSA loci, we used an antibody specific for this modification in ChIP reactions. As expected, we see that this modification specifically marks the proximal PSA promoter (PSA D) and the 5' coding region of the gene (PSA E), but only in LNCaP and C4-2 cells where the PSA gene is active. Furthermore, we see a large increase in H3 Tri-Me K4 in response to induction with synthetic androgen for 24 hours at these loci (Figure 17B, lower middle panels). This increase is greater in the case of LNCaP cells compared to C4-2.

Finally, in order to confirm binding of the androgen receptor to the PSA gene we measured its relative enrichment over input levels (% input) at all PSA loci in the three cell lines. As expected, we could not detect any significant levels of AR binding at any

location on the PSA gene in PC3 cells (Figure 17B, bottom left panel). Low levels of AR binding were seen only at the PSA enhancer (PSA B) in both LNCaP and C4-2 cells in the absence of androgen and these levels were greatly increased in the presence of androgen (Figure 17B, bottom center and right panels). A very slight increase in AR levels at ARE 1 within the proximal promoter was seen only in the LNCaP cells in the presence of androgen.

The H2A.Z-1 gene is induced upon treatment with androgen

Next we sought to determine if H2A.Z is upregulated in response to androgen treatment as it is after treatment with estrogen (Hua et al., 2008). PC3, LNCaP and C4-2 cells were treated with ethanol vehicle control or 10nM R1881 for 24, 36 and 48 hours and total histones were extracted (Figure 18A top panel). Western blots were probed with anti-H2A.Z antibody and indicate that the protein levels of this histone do not increase in response to treatment in PC3 cells but do in LNCaP cells, particularly after 24 and 36 hours (Figure 18A). Interestingly, the strength and kinetics of H2A.Z induction by androgen appears to be different in C4-2 cells, where the protein levels of H2A.Z increase slightly, and only after 48 hours of treatment (Figure 18A). However, the levels of triply acetylated H2A.Z do not increase with androgen treatment in any of the cell lines (Figure 18A).

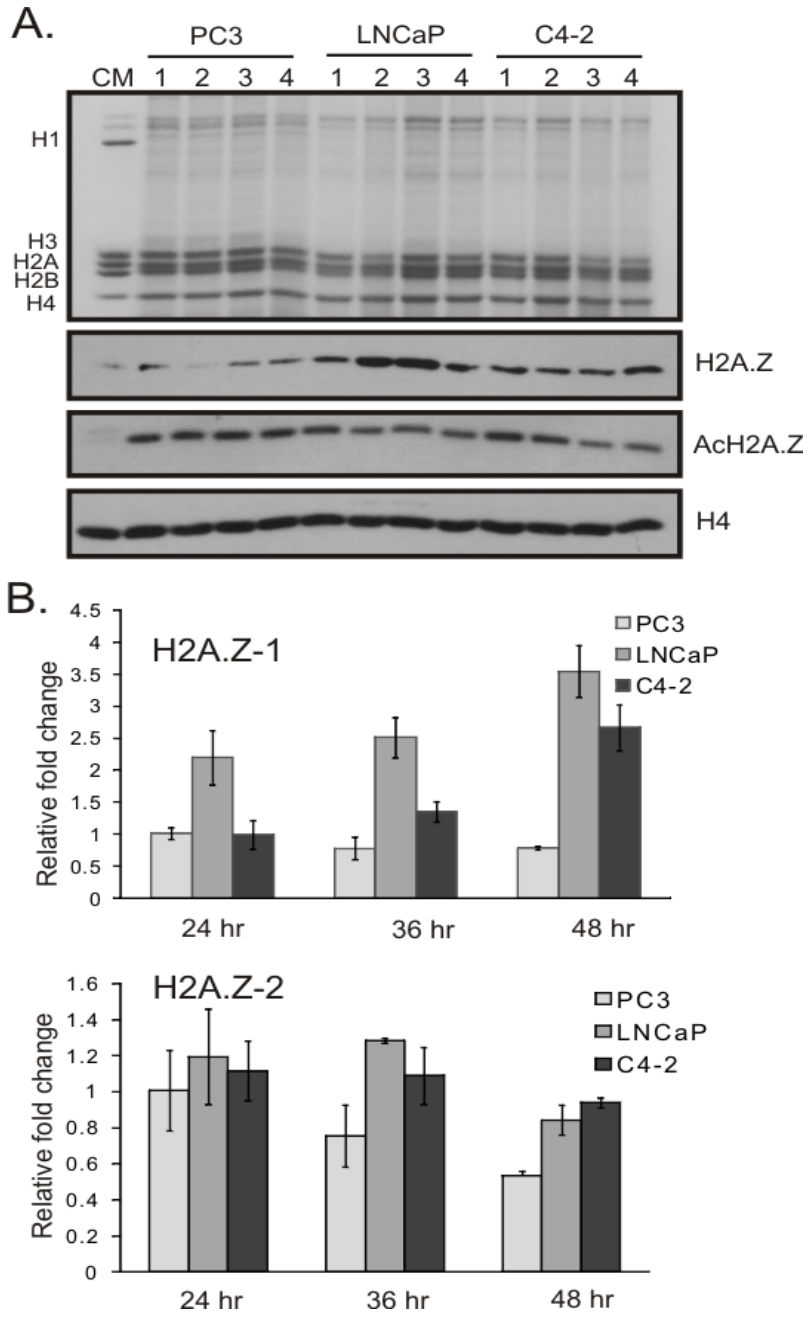

Figure 18: Total H2A.Z protein and H2A.Z-1 mRNA transcript levels are upregulated in response to androgen.

A.) SDS PAGE of histones extracted from PC3, LNCaP and C4-2 cells after treatment with ethanol control (1) or 10nM R1881 for 24 hrs (2), 36 hrs (3) or 48 hrs (4). The lower panels are Western blots with the antibodies indicated on the right. B.) Quantitative RT-PCR of H2A.Z-1 and H2A.Z-2 transcript levels in response to androgen treatment. The levels of transcript were assessed relative to the ethanol-treated control, error bars represent the standard error of the mean of triplicate experiments.

We also analyzed the relative mRNA transcript levels of both H2A.Z isoforms in PC3, LNCaP and C4-2 cells after treatment with androgen and compared them to the levels in uninduced cells. The top panel of Figure 18B indicates that H2A.Z-1 transcript levels increase approximately 2-fold after 24 and 36 hours and 3-fold after 48 hours of treatment with androgen in LNCaP cells, which is relatively consistent with the Western blot data of the protein levels. Treatment of PC3 cells with androgen has no effect on the transcript levels of H2A.Z-1 (Figure 18B). The relative expression of H2A.Z-1 transcript also increases in C4-2 cells but only significantly after 48 hours of treatment, as seen with the protein levels (Figure 18B). Conversely, no significant changes in the levels of H2A.Z-2 mRNA were observed in any cell line (Figure 18B, bottom panel).

The levels of H2A.Z-1 are increased in castration resistant LNCaP xenograft tumours

In order to examine whether the levels of H2A.Z change with the development of castration resistant (androgen independent) prostate cancer, we extracted total histones from the isolated nuclei of LNCaP tumours grown as subcutaneous xenografts in athymic nude mice and probed Western blots with anti-H2A.Z and anti-AcH2A.Z antibodies. Once LNCaP tumours were established (intact), they were either removed 7 days or 14 days after castration or were removed and considered castration resistant once the serum PSA levels of the mouse had returned to the levels measured when the tumour was considered intact (Snoek et al., 2009). Figure 19A shows that total H2A.Z protein levels are increased in castration resistant tumours compared to the intact, 7 day and 14 day tumours. The levels of AcH2A.Z also increase slightly in the castration resistant tumours.

This increase in H2A.Z protein level is mainly due to an approximate 2- to 3-fold increase in expression of the H2A.Z-1 gene, though small increases in H2A.Z-2 gene expression can also be observed (Figure 19B).

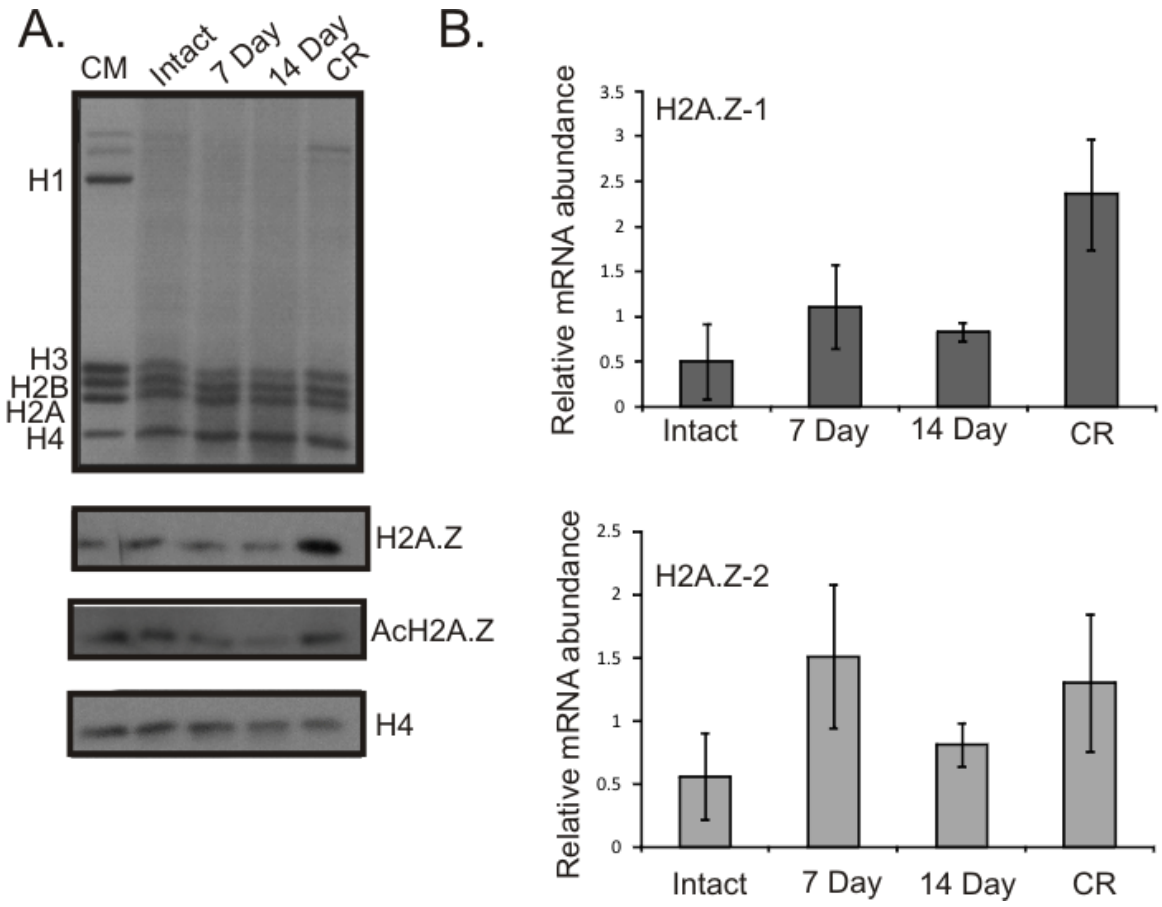

Figure 19: Total H2A.Z protein is increased in castration resistant LNCaP tumours.
A.) SDS PAGE of histones extracted from Intact, 7 Day, 14 Day, and CR (castration resistant) LNCaP tumours grown subcutaneously in mice. The lower panels are Western blots with antibodies indicated on the right. B.) Quantitative RT-PCR of H2A.Z-1 and H2A.Z-2 transcript levels in Intact, 7 Day, 14 Day and CR tumours. Error bars represent the standard error of the mean of duplicate experiments.

Discussion:

Like many other human cancers, the development and progression of prostate cancer has been shown to involve both genetic and epigenetic mechanisms. Many different genetic rearrangements have been characterized in prostate cancer, including a major translocation on chromosome 21 that fuses the androgen responsive promoter of the *TMPRSS2* gene to the ERG transcription factor, resulting in its aberrant activation (Kumar-Sinha et al., 2008). Epigenetic mechanisms involved in prostate cancer include hypermethylation of tumour suppressor genes, general hypomethylation of the genome, as well as deregulated expression of polycomb group (PcG) proteins including the EZH2 methyltransferase and BMI-1 (Schulz and Hoffmann, 2009). These latter proteins are considered crucial for the survival of adult multipotent stem cells and it is thought that their overexpression may contribute to the maintenance of a population of these cells that, according to the 'cancer stem cell hypothesis', could be responsible for initiating prostate cancer (Valk-Lingbeek et al., 2004). The regulation of histone variant replacement, generally considered an epigenetic mechanism, has so far not been examined in prostate cancer.

Here we show that the histone variant H2A.Z is present mainly at the enhancer, the proximal promoter, and the 5' region of the PSA gene in AR positive prostate cancer cells. The levels of H2A.Z decrease at the promoter and 5' gene region when transcription of the PSA gene is increased in response to treatment with androgen, which is consistent with what is seen upon dexamethasone induction of the glucocorticoid receptor (John et al., 2008) and during gene activation in T cells (Sutcliffe et al., 2009),

though interestingly H2A.Z levels increase at the *TFF1* gene during induction by the estrogen receptor (Gevry et al., 2009). The decrease in H2A.Z at the promoter and 5' region of the PSA gene is not due to loss of nucleosomes since the levels of total H4 remain fairly constant regardless of transcriptional status (data not shown). However, specific loss of H2A.Z/H2B dimers or their replacement by canonical H2A/H2B dimers cannot be discounted. On the other hand, H2A.Z levels are not significantly decreased after androgen induction at the PSA enhancer that is located more than 4 kb upstream of the promoter indicating that loss of H2A.Z at the promoter is somehow coupled to transcription. Similar localization patterns are seen for AcH2A.Z, indicating that it is likely not simply the unacetylated form that occupies the transcriptionally inactive promoter while the acetylated form occupies the highly active promoter. Finally, given that only comparatively low levels of H2A.Z were seen at the completely transcriptionally inactive PSA gene in PC3 cells, it is likely that H2A.Z serves to poise the PSA promoter chromatin for activation in LNCaP and C4-2 cells. In this manner, H2A.Z may also facilitate the reactivation of the PSA gene after hormonal stimulus is removed and the gene is silenced or it may function as an epigenetic tag that is maintained throughout cell division, as has been demonstrated in yeast (Brickner et al., 2007).

We also show that the expression of the H2A.Z-1 isoform is specifically upregulated in response to androgen treatment. This likely occurs indirectly by the action of MYC since MYC-binding sites exist within the promoter of H2A.Z-1 and have been shown to be bound by MYC in response to estrogen receptor signalling (Hua et al., 2008). The

H2A.Z-2 gene is not significantly upregulated in response to androgen at the timepoints measured here indicating perhaps that the transcriptional program initiated by androgen receptor signalling specifically requires the H2A.Z-1 isoform over H2A.Z-2. Indeed, data from our lab indicates that there are subtle differences in the chromatin fraction distribution and association with post-translationally modified forms of other histones between the two H2A.Z isoforms (Dryhurst et al., 2009). Androgen treatment results in an approximate 2-fold increase in H2A.Z-1 transcript levels in C4-2 cells, but only after 48 hours of treatment. This data, along with the smaller increase in PSA gene induction seen in C4-2 compared to LNCaP cells agrees with several reports showing that androgen signalling activity is significantly decreased in androgen-independent compared to androgen-dependent prostate cancer (Tomlins et al., 2007; Wang et al., 2009a).

Our results suggest that total H2A.Z protein is increased in castration resistant prostate cancer, and that this is likely due mainly to the upregulation of the H2A.Z-1 gene. Increased expression of this gene could be due to androgen receptor signalling and increased MYC levels, though it is quite likely that the increase in total H2A.Z protein could be a result of completely different signalling events. Indeed, it has been recently shown that the androgen receptor regulates a distinct transcription program in androgen-independent compared to androgen-dependent prostate cancer (Wang et al., 2009a). It is unknown whether increased levels of H2A.Z-1 expression are required to mediate a specific cellular function in castration resistant prostate cancer, or if they are simply a bi-product of a more aggressive and advanced stage of cancer. One interesting possibility is that increased incorporation of H2A.Z into chromatin could exacerbate the effects of

global DNA hypomethylation since H2A.Z and DNA methylation have been shown to be broadly antagonistic (Kobor and Lorincz, 2009; Zilberman et al., 2008). Alternatively, increased expression of H2A.Z-1 could lead to its random or aberrant incorporation into chromatin where it could increase the plasticity of castration resistant cancer cells causing them to become more de-differentiated. Further studies in this area will be a challenging area of research for the future.

Conclusions and future directions:

Considering H2A.Z levels have been shown to increase at the *TFF1*gene promoter in response to estrogen treatment (Gevry et al., 2009), it would be interesting to determine whether the decrease in H2A.Z seen here at the PSA promoter is also seen at other androgen responsive genes. The dependence of these genes on H2A.Z (-1 or -2) for expression should also be assessed by short term siRNA-mediated knockdown of H2A.Z protein levels. In order to determine if total H2A.Z protein levels are also upregulated in human androgen independent prostate cancer, we will perform immunohistochemistry on prostate tumour tissue microarrays available at the Vancouver Prostate Centre (Vancouver, BC Canada). These arrays contain tumour sections from patients who have not been treated with antiandrogen therapy, who have been treated for different amounts of time with antiandrogens, or whose cancer has progressed to an androgen independent stage. Furthermore, since extended knockdown of H2A.Z protein has been shown to result in defects in chromosome segregation and apoptosis (Rangasamy et al., 2004), it would be very interesting to determine what effect this knockdown could have on different stages of prostate cancer. This could be achieved by constructing a Lentivirus

that inducibly expresses an siRNA molecule for H2A.Z and infecting LNCaP cells. These cells could then be grown in mice as explained in the Materials and Methods section and the siRNA could be induced at different stages. Similar experiments have been performed using siRNA against the androgen receptor (Snoek et al., 2009). Further studies in this area will be an exciting and challenging area of research for the future.

Final Conclusions

The topic of histone H2A.Z is a very active area of research for two main reasons: 1) because at the chromatin level, the mechanisms of its action are not fully understood and 2) because it participates in so many different biological functions. The data presented in this dissertation mainly focus on the structures and functions of H2A.Z that most likely relate to its function at promoter regions.

In chapter 2, we indicate that purified native H2A.Z slightly compacts the NCP and our group has shown that it also slightly stabilizes this particle (Thambirajah et al., 2006). Combined with the potential propensity of H2A.Z nucleosomes to adopt a particular position along a DNA sequence (Fu et al., 2008), this could perhaps create a structurally favourable condition for assembly of the preinitiation complex and binding of RNA Pol II at the promoter. The stability of H2A.Z nucleosomes might then be disrupted by acetylation of H2A.Z itself and the histone core complement, as shown by our group (Ishibashi et al., 2009a). This could then result in the displacement of H2A.Z from the nucleosome once transcription ensues, as is the case at the PSA gene (chapter 4). Clearly there are many unresolved features of this potential mechanism, particularly in considering the timing of these events.

Furthermore, it could be that at particular genes or in specific cell types the H2A.Z-2 isoform plays a greater role at these promoter regions, based on its increased association within euchromatin and its greater association with H3 Tri-Me K4 (chapter 3). This might

be the result of a preference of a certain H2A.Z deposition complex for one isoform over the other, or more simply because of cell type-specific or environmental cue-specific expression of the H2A.Z-1 or H2A.Z-2 genes. Again, here there are still more questions than answers especially concerning whether the presence of H2A.Z within nucleosomes recruits the MLL complexes, or whether H3 Tri-Me K4 recruits H2A.Z deposition complexes.

Lastly, the potential involvement of H2A.Z in prostate cancer progression is very intriguing. Given that knock down of H2A.Z levels causes severe defects in chromosome segregation resulting in apoptosis (Rangasamy et al., 2004), perhaps targeting H2A.Z with siRNA-based therapies could also be detrimental to tumour cells. There are still many pieces of the puzzle to put together on the topic of H2A.Z biology which makes it, like so many other topics, very compelling to work on.

Bibliography

Abbott, D. W., Ivanova, V. S., Wang, X., Bonner, W. M., and Ausio, J. (2001). Characterization of the stability and folding of H2A.Z chromatin particles: implications for transcriptional activation. J Biol Chem *276*, 41945-41949.

Adam, M., Robert, F., Larochelle, M., and Gaudreau, L. (2001). H2A.Z is required for global chromatin integrity and for recruitment of RNA polymerase II under specific conditions. Mol Cell Biol *21*, 6270-6279.

Adroer, R., and Oliva, R. (1998). Nucleosome positioning in the rat protamine 1 gene in vivo and in vitro. Biochim Biophys Acta *1442*, 252-260.

Albert, I., Mavrich, T. N., Tomsho, L. P., Qi, J., Zanton, S. J., Schuster, S. C., and Pugh, B. F. (2007). Translational and rotational settings of H2A.Z nucleosomes across the Saccharomyces cerevisiae genome. Nature *446*, 572-576.

Allfrey, V. G., Faulkner, R., and Mirsky, A. E. (1964). Acetylation and Methylation of Histones and Their Possible Role in the Regulation of Rna Synthesis. Proc Natl Acad Sci U S A *51*, 786-794.

Allis, C. D., Richman, R., Gorovsky, M. A., Ziegler, Y. S., Touchstone, B., Bradley, W. A., and Cook, R. G. (1986). hv1 is an evolutionarily conserved H2A variant that is preferentially associated with active genes. J Biol Chem *261*, 1941-1948.

Altaf, M., Auger, A., Covic, M., and Cote, J. (2009). Connection between histone H2A variants and chromatin remodeling complexes. Biochem Cell Biol *87*, 35-50.

Altschul, S. F., Gish, W., Miller, W., Myers, E. W., and Lipman, D. J. (1990). Basic local alignment search tool. J Mol Biol *215*, 403-410.

Anderson, J. D., Lowary, P. T., and Widom, J. (2001). Effects of histone acetylation on the equilibrium accessibility of nucleosomal DNA target sites. J Mol Biol *307*, 977-985.

Annunziato, A. T., and Hansen, J. C. (2000). Role of histone acetylation in the assembly and modulation of chromatin structures. Gene Expr *9*, 37-61.

Ausio, J., and Abbott, D. W. (2002). The many tales of a tail: carboxyl-terminal tail heterogeneity specializes histone H2A variants for defined chromatin function. Biochemistry *41*, 5945-5949.

Ausio, J., Dong, F., and van Holde, K. E. (1989). Use of selectively trypsinized nucleosome core particles to analyze the role of the histone "tails" in the stabilization of the nucleosome. J Mol Biol *206*, 451-463.

Ausio, J., and Moore, S. C. (1998). Reconstitution of chromatin complexes from high-performance liquid chromatography-purified histones. Methods *15*, 333-342.

Ausio, J., and van Holde, K. E. (1986). Histone hyperacetylation: its effects on nucleosome conformation and stability. Biochemistry *25*, 1421-1428.

Babiarz, J. E., Halley, J. E., and Rine, J. (2006). Telomeric heterochromatin boundaries require NuA4-dependent acetylation of histone variant H2A.Z in Saccharomyces cerevisiae. Genes Dev *20*, 700-710.

Baek, Y. S., Haas, S., Hackstein, H., Bein, G., Hernandez-Santana, M., Lehrach, H., Sauer, S., and Seitz, H. (2009). Identification of novel transcriptional regulators involved in macrophage differentiation and activation in U937 cells. BMC Immunol *10*, 18.

Barski, A., Cuddapah, S., Cui, K., Roh, T. Y., Schones, D. E., Wang, Z., Wei, G., Chepelev, I., and Zhao, K. (2007). High-resolution profiling of histone methylations in the human genome. Cell *129*, 823-837.

Beck, H. C., Nielsen, E. C., Matthiesen, R., Jensen, L. H., Sehested, M., Finn, P., Grauslund, M., Hansen, A. M., and Jensen, O. N. (2006). Quantitative proteomic analysis of post-translational modifications of human histones. Mol Cell Proteomics *5*, 1314-1325.

Bonenfant, D., Towbin, H., Coulot, M., Schindler, P., Mueller, D. R., and van Oostrum, J. (2007). Analysis of dynamic changes in post-translational modifications of human histones during cell cycle by mass spectrometry. Mol Cell Proteomics *6*, 1917-1932.

Brickner, D. G., Cajigas, I., Fondufe-Mittendorf, Y., Ahmed, S., Lee, P. C., Widom, J., and Brickner, J. H. (2007). H2A.Z-mediated localization of genes at the nuclear periphery confers epigenetic memory of previous transcriptional state. PLoS Biol *5*, e81.

Brown, C. R., Kennedy, C. J., Delmar, V. A., Forbes, D. J., and Silver, P. A. (2008). Global histone acetylation induces functional genomic reorganization at mammalian nuclear pore complexes. Genes Dev *22*, 627-639.

Bruce, K., Myers, F. A., Mantouvalou, E., Lefevre, P., Greaves, I., Bonifer, C., Tremethick, D. J., Thorne, A. W., and Crane-Robinson, C. (2005). The replacement histone H2A.Z in a hyperacetylated form is a feature of active genes in the chicken. Nucleic Acids Res *33*, 5633-5639.

Cai, Y., Jin, J., Florens, L., Swanson, S. K., Kusch, T., Li, B., Workman, J. L., Washburn, M. P., Conaway, R. C., and Conaway, J. W. (2005). The mammalian YL1 protein is a shared subunit of the TRRAP/TIP60 histone acetyltransferase and SRCAP complexes. J Biol Chem *280*, 13665-13670.

Calestagne-Morelli, A., and Ausio, J. (2006). Long-range histone acetylation: biological significance, structural implications, and mechanisms. Biochem Cell Biol *84*, 518-527.

Cao, R., and Zhang, Y. (2004). The functions of E(Z)/EZH2-mediated methylation of lysine 27 in histone H3. Curr Opin Genet Dev *14*, 155-164.

Chakravarthy, S., Bao, Y., Roberts, V. A., Tremethick, D., and Luger, K. (2004). Structural characterization of histone H2A variants. Cold Spring Harb Symp Quant Biol *69*, 227-234.

Champagne, K. S., and Kutateladze, T. G. (2009). Structural insight into histone recognition by the ING PHD fingers. Curr Drug Targets *10*, 432-441.

Cheng, H., Snoek, R., Ghaidi, F., Cox, M. E., and Rennie, P. S. (2006). Short hairpin RNA knockdown of the androgen receptor attenuates ligand-independent activation and delays tumor progression. Cancer Res *66*, 10613-10620.

Choi, J., Heo, K., and An, W. (2009). Cooperative action of TIP48 and TIP49 in H2A.Z exchange catalyzed by acetylation of nucleosomal H2A. Nucleic Acids Res.

Choi, J. K., and Howe, L. J. (2009). Histone acetylation: truth of consequences? Biochem Cell Biol *87*, 139-150.

Choudhary, C., Kumar, C., Gnad, F., Nielsen, M. L., Rehman, M., Walther, T. C., Olsen, J. V., and Mann, M. (2009). Lysine acetylation targets protein complexes and co-regulates major cellular functions. Science *325*, 834-840.

Clapier, C. R., and Cairns, B. R. (2009). The biology of chromatin remodeling complexes. Annu Rev Biochem *78*, 273-304.

Clarkson, M. J., Wells, J. R., Gibson, F., Saint, R., and Tremethick, D. J. (1999). Regions of variant histone His2AvD required for Drosophila development. Nature *399*, 694-697.

Clayton, A. L., Rose, S., Barratt, M. J., and Mahadevan, L. C. (2000). Phosphoacetylation of histone H3 on c-fos- and c-jun-associated nucleosomes upon gene activation. Embo J *19*, 3714-3726.

Cloos, P. A., Christensen, J., Agger, K., and Helin, K. (2008). Erasing the methyl mark: histone demethylases at the center of cellular differentiation and disease. Genes Dev *22*, 1115-1140.

Coon, J. J., Ueberheide, B., Syka, J. E., Dryhurst, D. D., Ausio, J., Shabanowitz, J., and Hunt, D. F. (2005). Protein identification using sequential ion/ion reactions and tandem mass spectrometry. Proc Natl Acad Sci U S A *102*, 9463-9468.

Crooks, G. E., Hon, G., Chandonia, J. M., and Brenner, S. E. (2004). WebLogo: a sequence logo generator. Genome Res *14*, 1188-1190.

Devlin, H. L., and Mudryj, M. (2009). Progression of prostate cancer: multiple pathways to androgen independence. Cancer Lett *274*, 177-186.

Dhillon, N., and Kamakaka, R. T. (2000). A histone variant, Htz1p, and a Sir1p-like protein, Esc2p, mediate silencing at HMR. Mol Cell *6*, 769-780.

Dilworth, D. J., Tackett, A. J., Rogers, R. S., Yi, E. C., Christmas, R. H., Smith, J. J., Siegel, A. F., Chait, B. T., Wozniak, R. W., and Aitchison, J. D. (2005). The mobile nucleoporin Nup2p and chromatin-bound Prp20p function in endogenous NPC-mediated transcriptional control. J Cell Biol *171*, 955-965.

Dover, J., Schneider, J., Tawiah-Boateng, M. A., Wood, A., Dean, K., Johnston, M., and Shilatifard, A. (2002). Methylation of histone H3 by COMPASS requires ubiquitination of histone H2B by Rad6. J Biol Chem *277*, 28368-28371.

Doyon, Y., Selleck, W., Lane, W. S., Tan, S., and Cote, J. (2004). Structural and functional conservation of the NuA4 histone acetyltransferase complex from yeast to humans. Mol Cell Biol *24*, 1884-1896.

Draker, R., and Cheung, P. (2009). Transcriptional and epigenetic functions of histone variant H2A.Z. Biochem Cell Biol *87*, 19-25.

Dryhurst, D., Thambirajah, A. A., and Ausio, J. (2004). New twists on H2A.Z: a histone variant with a controversial structural and functional past. Biochem Cell Biol *82*, 490-497.

Dryhurst, D., Ishibashi, T., Rose, K. L., Eirin-Lopez, J. M., McDonald, D., Silva-Moreno, B., Veldhoen, N., Helbing, C. C., Hendzel, M. J., Shabanowitz, J., *et al.* (2009). Characterization of the histone H2A.Z-1 and H2A.Z-2 isoforms in vertebrates. BMC Biol *7*, 86.

Dunican, D. S., McWilliam, P., Tighe, O., Parle-McDermott, A., and Croke, D. T. (2002). Gene expression differences between the microsatellite instability (MIN) and chromosomal instability (CIN) phenotypes in colorectal cancer revealed by high-density cDNA array hybridization. Oncogene *21*, 3253-3257.

Dunker, A. K., Lawson, J. D., Brown, C. J., Williams, R. M., Romero, P., Oh, J. S., Oldfield, C. J., Campen, A. M., Ratliff, C. M., Hipps, K. W., *et al.* (2001). Intrinsically disordered protein. J Mol Graph Model *19*, 26-59.

Eirin-Lopez, J. M., Gonzalez-Romero, R., Dryhurst, D., Ishibashi, T., and Ausio, J. (2009). The evolutionary differentiation of two histone H2A.Z variants in chordates (H2A.Z-1 and H2A.Z-2) is mediated by a stepwise mutation process that affects three amino acid residues. BMC Evol Biol *9*, 31.

Eirin-Lopez, J. M., Ishibashi, T., and Ausio, J. (2008). H2A.Bbd: a quickly evolving hypervariable mammalian histone that destabilizes nucleosomes in an acetylation-independent way. Faseb J *22*, 316-326.

Faast, R., Thonglairoam, V., Schulz, T. C., Beall, J., Wells, J. R., Taylor, H., Matthaei, K., Rathjen, P. D., Tremethick, D. J., and Lyons, I. (2001). Histone variant H2A.Z is required for early mammalian development. Curr Biol *11*, 1183-1187.

Fan, J. Y., Gordon, F., Luger, K., Hansen, J. C., and Tremethick, D. J. (2002). The essential histone variant H2A.Z regulates the equilibrium between different chromatin conformational states. Nat Struct Biol *9*, 172-176.

Fan, J. Y., Rangasamy, D., Luger, K., and Tremethick, D. J. (2004). H2A.Z alters the nucleosome surface to promote HP1alpha-mediated chromatin fiber folding. Mol Cell *16*, 655-661.

Farris, S. D., Rubio, E. D., Moon, J. J., Gombert, W. M., Nelson, B. H., and Krumm, A. (2005). Transcription-induced chromatin remodeling at the c-myc gene involves the local exchange of histone H2A.Z. J Biol Chem *280*, 25298-25303.

Ferreira, H., Flaus, A., and Owen-Hughes, T. (2007). Histone modifications influence the action of Snf2 family remodelling enzymes by different mechanisms. J Mol Biol *374*, 563-579.

Fischle, W., Wang, Y., Jacobs, S. A., Kim, Y., Allis, C. D., and Khorasanizadeh, S. (2003). Molecular basis for the discrimination of repressive methyl-lysine marks in histone H3 by Polycomb and HP1 chromodomains. Genes Dev *17*, 1870-1881.

Flaus, A., Rencurel, C., Ferreira, H., Wiechens, N., and Owen-Hughes, T. (2004). Sin mutations alter inherent nucleosome mobility. Embo J *23*, 343-353.

Foltz, D. R., Jansen, L. E., Black, B. E., Bailey, A. O., Yates, J. R., 3rd, and Cleveland, D. W. (2006). The human CENP-A centromeric nucleosome-associated complex. Nat Cell Biol *8*, 458-469.

Fu, Y., Sinha, M., Peterson, C. L., and Weng, Z. (2008). The insulator binding protein CTCF positions 20 nucleosomes around its binding sites across the human genome. PLoS Genet *4*, e1000138.

Fuchs, M., Gerber, J., Drapkin, R., Sif, S., Ikura, T., Ogryzko, V., Lane, W. S., Nakatani, Y., and Livingston, D. M. (2001). The p400 complex is an essential E1A transformation target. Cell *106*, 297-307.

Garcia-Ramirez, M., Rocchini, C., and Ausio, J. (1995). Modulation of chromatin folding by histone acetylation. J Biol Chem *270*, 17923-17928.

Garcia, B. A., Mollah, S., Ueberheide, B. M., Busby, S. A., Muratore, T. L., Shabanowitz, J., and Hunt, D. F. (2007). Chemical derivatization of histones for facilitated analysis by mass spectrometry. Nat Protoc *2*, 933-938.

Gaszner, M., and Felsenfeld, G. (2006). Insulators: exploiting transcriptional and epigenetic mechanisms. Nat Rev Genet *7*, 703-713.

Gautier, T., Abbott, D. W., Molla, A., Verdel, A., Ausio, J., and Dimitrov, S. (2004). Histone variant H2ABbd confers lower stability to the nucleosome. EMBO Rep *5*, 715-720.

Gervais, A. L., and Gaudreau, L. (2009). Discriminating nucleosomes containing histone H2A.Z or H2A based on genetic and epigenetic information. BMC Mol Biol *10*, 18.

Gevry, N., Chan, H. M., Laflamme, L., Livingston, D. M., and Gaudreau, L. (2007). p21 transcription is regulated by differential localization of histone H2A.Z. Genes Dev *21*, 1869-1881.

Gevry, N., Hardy, S., Jacques, P. E., Laflamme, L., Svotelis, A., Robert, F., and Gaudreau, L. (2009). Histone H2A.Z is essential for estrogen receptor signaling. Genes Dev *23*, 1522-1533.

Ghosh, D. (2000). Object-oriented transcription factors database (ooTFD). Nucleic Acids Res *28*, 308-310.

Gleave, M., Tolcher, A., Miyake, H., Nelson, C., Brown, B., Beraldi, E., and Goldie, J. (1999). Progression to androgen independence is delayed by adjuvant treatment with antisense Bcl-2 oligodeoxynucleotides after castration in the LNCaP prostate tumor model. Clin Cancer Res *5*, 2891-2898.

Gorisch, S. M., Wachsmuth, M., Toth, K. F., Lichter, P., and Rippe, K. (2005). Histone acetylation increases chromatin accessibility. J Cell Sci *118*, 5825-5834.

Greaves, I. K., Rangasamy, D., Ridgway, P., and Tremethick, D. J. (2007). H2A.Z contributes to the unique 3D structure of the centromere. Proc Natl Acad Sci U S A *104*, 525-530.

Guenther, M. G., Levine, S. S., Boyer, L. A., Jaenisch, R., and Young, R. A. (2007). A chromatin landmark and transcription initiation at most promoters in human cells. Cell *130*, 77-88.

Guillemette, B., Bataille, A. R., Gevry, N., Adam, M., Blanchette, M., Robert, F., and Gaudreau, L. (2005). Variant histone H2A.Z is globally localized to the promoters of inactive yeast genes and regulates nucleosome positioning. PLoS Biol *3*, e384.

Hardy, S., Jacques, P. E., Gevry, N., Forest, A., Fortin, M. E., Laflamme, L., Gaudreau, L., and Robert, F. (2009). The Euchromatic and Heterochromatic Landscapes Are Shaped by Antagonizing Effects of Transcription on H2A.Z Deposition. PLoS Genet *5*, e1000687.

Hargreaves, D. C., Horng, T., and Medzhitov, R. (2009). Control of inducible gene expression by signal-dependent transcriptional elongation. Cell *138*, 129-145.

Hartley, P. D., and Madhani, H. D. (2009). Mechanisms that specify promoter nucleosome location and identity. Cell *137*, 445-458.

Hatch, C. L., and Bonner, W. M. (1990). The human histone H2A.Z gene. Sequence and regulation. J Biol Chem *265*, 15211-15218.

Hatch, C. L., and Bonner, W. M. (1995). Characterization of the proximal promoter of the human histone H2A.Z gene. DNA Cell Biol *14*, 257-266.

Heinlein, C. A., and Chang, C. (2002). Androgen receptor (AR) coregulators: an overview. Endocr Rev *23*, 175-200.

Henikoff, S., Henikoff, J. G., Sakai, A., Loeb, G. B., and Ahmad, K. (2009). Genome-wide profiling of salt fractions maps physical properties of chromatin. Genome Res *19*, 460-469.

Hoch, D. A., Stratton, J. J., and Gloss, L. M. (2007). Protein-protein Forster resonance energy transfer analysis of nucleosome core particles containing H2A and H2A.Z. J Mol Biol *371*, 971-988.

Hodges, C., Bintu, L., Lubkowska, L., Kashlev, M., and Bustamante, C. (2009). Nucleosomal fluctuations govern the transcription dynamics of RNA polymerase II. Science *325*, 626-628.

Hua, S., Kallen, C. B., Dhar, R., Baquero, M. T., Mason, C. E., Russell, B. A., Shah, P. K., Liu, J., Khramtsov, A., Tretiakova, M. S., *et al.* (2008). Genomic analysis of estrogen cascade reveals histone variant H2A.Z associated with breast cancer progression. Mol Syst Biol *4*, 188.

Huang, S. Y., Barnard, M. B., Xu, M., Matsui, S., Rose, S. M., and Garrard, W. T. (1986). The active immunoglobulin kappa chain gene is packaged by non-ubiquitin-conjugated nucleosomes. Proc Natl Acad Sci U S A *83*, 3738-3742.

Hublitz, P., Albert, M., and Peters, A. H. (2009). Mechanisms of transcriptional repression by histone lysine methylation. Int J Dev Biol *53*, 335-354.

Iouzalen, N., Moreau, J., and Mechali, M. (1996). H2A.ZI, a new variant histone expressed during Xenopus early development exhibits several distinct features from the core histone H2A. Nucleic Acids Res *24*, 3947-3952.

Ishibashi, T., Dryhurst, D., Rose, K. L., Shabanowitz, J., Hunt, D. F., and Ausio, J. (2009). Acetylation of Vertebrate H2A.Z and Its Effect on the Structure of the Nucleosome. Biochemistry.

Ishii, K., Arib, G., Lin, C., Van Houwe, G., and Laemmli, U. K. (2002). Chromatin boundaries in budding yeast: the nuclear pore connection. Cell *109*, 551-562.

Ivaldi, M. S., Karam, C. S., and Corces, V. G. (2007). Phosphorylation of histone H3 at Ser10 facilitates RNA polymerase II release from promoter-proximal pausing in Drosophila. Genes Dev *21*, 2818-2831.

Jackson, J. D., and Gorovsky, M. A. (2000). Histone H2A.Z has a conserved function that is distinct from that of the major H2A sequence variants. Nucleic Acids Res *28*, 3811-3816.

Jenuwein, T., and Allis, C. D. (2001). Translating the histone code. Science *293*, 1074-1080.

Jin, C., Zang, C., Wei, G., Cui, K., Peng, W., Zhao, K., and Felsenfeld, G. (2009). H3.3/H2A.Z double variant-containing nucleosomes mark 'nucleosome-free regions' of active promoters and other regulatory regions. Nat Genet *41*, 941-945.

John, S., Sabo, P. J., Johnson, T. A., Sung, M. H., Biddie, S. C., Lightman, S. L., Voss, T. C., Davis, S. R., Meltzer, P. S., Stamatoyannopoulos, J. A., and Hager, G. L. (2008). Interaction of the glucocorticoid receptor with the chromatin landscape. Mol Cell *29*, 611-624.

Kalocsay, M., Hiller, N. J., and Jentsch, S. (2009). Chromosome-wide Rad51 spreading and SUMO-H2A.Z-dependent chromosome fixation in response to a persistent DNA double-strand break. Mol Cell *33*, 335-343.

Kamakaka, R. T., and Thomas, J. O. (1990). Chromatin structure of transcriptionally competent and repressed genes. Embo J *9*, 3997-4006.

Keogh, M. C., Mennella, T. A., Sawa, C., Berthelet, S., Krogan, N. J., Wolek, A., Podolny, V., Carpenter, L. R., Greenblatt, J. F., Baetz, K., and Buratowski, S. (2006). The Saccharomyces cerevisiae histone H2A variant Htz1 is acetylated by NuA4. Genes Dev *20*, 660-665.

Kobor, M. S., and Lorincz, M. C. (2009). H2A.Z and DNA methylation: irreconcilable differences. Trends Biochem Sci *34*, 158-161.

Kobor, M. S., Venkatasubrahmanyam, S., Meneghini, M. D., Gin, J. W., Jennings, J. L., Link, A. J., Madhani, H. D., and Rine, J. (2004). A protein complex containing the conserved Swi2/Snf2-related ATPase Swr1p deposits histone variant H2A.Z into euchromatin. PLoS Biol *2*, E131.

Kouzarides, T. (2007). Chromatin modifications and their function. Cell *128*, 693-705.

Krogan, N. J., Baetz, K., Keogh, M. C., Datta, N., Sawa, C., Kwok, T. C., Thompson, N. J., Davey, M. G., Pootoolal, J., Hughes, T. R., *et al.* (2004). Regulation of chromosome stability by the histone H2A variant Htz1, the Swr1 chromatin remodeling complex, and the histone acetyltransferase NuA4. Proc Natl Acad Sci U S A *101*, 13513-13518.

Kumar-Sinha, C., Tomlins, S. A., and Chinnaiyan, A. M. (2008). Recurrent gene fusions in prostate cancer. Nat Rev Cancer *8*, 497-511.

Ladurner, A. G., Inouye, C., Jain, R., and Tjian, R. (2003). Bromodomains mediate an acetyl-histone encoded antisilencing function at heterochromatin boundaries. Mol Cell *11*, 365-376.

Laemmli, U. K. (1970). Cleavage of structural proteins during the assembly of the head of bacteriophage T4. Nature *227*, 680-685.

Larochelle, M., and Gaudreau, L. (2003). H2A.Z has a function reminiscent of an activator required for preferential binding to intergenic DNA. Embo J *22*, 4512-4522.

Li, A., Eirin-Lopez, J. M., and Ausio, J. (2005a). H2AX: tailoring histone H2A for chromatin-dependent genomic integrity. Biochem Cell Biol *83*, 505-515.

Li, B., Pattenden, S. G., Lee, D., Gutierrez, J., Chen, J., Seidel, C., Gerton, J., and Workman, J. L. (2005b). Preferential occupancy of histone variant H2AZ at inactive promoters influences local histone modifications and chromatin remodeling. Proc Natl Acad Sci U S A *102*, 18385-18390.

Liu, X., Li, B., and GorovskyMa (1996). Essential and nonessential histone H2A variants in Tetrahymena thermophila. Mol Cell Biol *16*, 4305-4311.

Liu, Y., Taverna, S. D., Muratore, T. L., Shabanowitz, J., Hunt, D. F., and Allis, C. D. (2007). RNAi-dependent H3K27 methylation is required for heterochromatin formation and DNA elimination in Tetrahymena. Genes Dev *21*, 1530-1545.

Loyola, A., and Almouzni, G. (2004). Histone chaperones, a supporting role in the limelight. Biochim Biophys Acta *1677*, 3-11.

Luger, K., Mader, A. W., Richmond, R. K., Sargent, D. F., and Richmond, T. J. (1997). Crystal structure of the nucleosome core particle at 2.8 A resolution. Nature *389*, 251-260.

Luk, E., Vu, N. D., Patteson, K., Mizuguchi, G., Wu, W. H., Ranjan, A., Backus, J., Sen, S., Lewis, M., Bai, Y., and Wu, C. (2007). Chz1, a nuclear chaperone for histone H2AZ. Mol Cell *25*, 357-368.

Lynch, M., and Conery, J. S. (2000). The evolutionary fate and consequences of duplicate genes. Science *290*, 1151-1155.

Malik, H. S., and Henikoff, S. (2003). Phylogenomics of the nucleosome. Nat Struct Biol *10*, 882-891.

Martin, C., and Zhang, Y. (2005). The diverse functions of histone lysine methylation. Nat Rev Mol Cell Biol *6*, 838-849.

Martin, S. E., Shabanowitz, J., Hunt, D. F., and Marto, J. A. (2000). Subfemtomole MS and MS/MS peptide sequence analysis using nano-HPLC micro-ESI fourier transform ion cyclotron resonance mass spectrometry. Anal Chem *72*, 4266-4274.

Martins, R. P., Ostermeier, G. C., and Krawetz, S. A. (2004). Nuclear matrix interactions at the human protamine domain: a working model of potentiation. J Biol Chem *279*, 51862-51868.

Marzluff, W. F., Wagner, E. J., and Duronio, R. J. (2008). Metabolism and regulation of canonical histone mRNAs: life without a poly(A) tail. Nat Rev Genet *9*, 843-854.

Meneghini, M. D., Wu, M., and Madhani, H. D. (2003). Conserved histone variant H2A.Z protects euchromatin from the ectopic spread of silent heterochromatin. Cell *112*, 725-736.

Meyer, A., and Van de Peer, Y. (2005). From 2R to 3R: evidence for a fish-specific genome duplication (FSGD). Bioessays *27*, 937-945.

Millar, C. B., and Grunstein, M. (2006). Genome-wide patterns of histone modifications in yeast. Nat Rev Mol Cell Biol *7*, 657-666.

Millar, C. B., Xu, F., Zhang, K., and Grunstein, M. (2006). Acetylation of H2AZ Lys 14 is associated with genome-wide gene activity in yeast. Genes Dev *20*, 711-722.

Mizuguchi, G., Shen, X., Landry, J., Wu, W. H., Sen, S., and Wu, C. (2004). ATP-driven exchange of histone H2AZ variant catalyzed by SWR1 chromatin remodeling complex. Science *303*, 343-348.

Mujtaba, S., Zeng, L., and Zhou, M. M. (2007). Structure and acetyl-lysine recognition of the bromodomain. Oncogene *26*, 5521-5527.

Mutskov, V., Gerber, D., Angelov, D., Ausio, J., Workman, J., and Dimitrov, S. (1998). Persistent interactions of core histone tails with nucleosomal DNA following acetylation and transcription factor binding. Mol Cell Biol *18*, 6293-6304.

Myers, F. A., Lefevre, P., Mantouvalou, E., Bruce, K., Lacroix, C., Bonifer, C., Thorne, A. W., and Crane-Robinson, C. (2006). Developmental activation of the lysozyme gene in chicken macrophage cells is linked to core histone acetylation at its enhancer elements. Nucleic Acids Res *34*, 4025-4035.

Oliva, R., Bazett-Jones, D. P., Locklear, L., and Dixon, G. H. (1990). Histone hyperacetylation can induce unfolding of the nucleosome core particle. Nucleic Acids Res *18*, 2739-2747.

Park, Y. J., Dyer, P. N., Tremethick, D. J., and Luger, K. (2004). A new fluorescence resonance energy transfer approach demonstrates that the histone variant H2AZ stabilizes the histone octamer within the nucleosome. J Biol Chem *279*, 24274-24282.

Pena, P. V., Davrazou, F., Shi, X., Walter, K. L., Verkhusha, V. V., Gozani, O., Zhao, R., and Kutateladze, T. G. (2006). Molecular mechanism of histone H3K4me3 recognition by plant homeodomain of ING2. Nature *442*, 100-103.

Pena, P. V., Hom, R. A., Hung, T., Lin, H., Kuo, A. J., Wong, R. P., Subach, O. M., Champagne, K. S., Zhao, R., Verkhusha, V. V., *et al.* (2008). Histone H3K4me3 binding is required for the DNA repair and apoptotic activities of ING1 tumor suppressor. J Mol Biol *380*, 303-312.

Perry, C. A., and Annunziato, A. T. (1991). Histone acetylation reduces H1-mediated nucleosome interactions during chromatin assembly. Exp Cell Res *196*, 337-345.

Placek, B. J., Harrison, L. N., Villers, B. M., and Gloss, L. M. (2005). The H2A.Z/H2B dimer is unstable compared to the dimer containing the major H2A isoform. Protein Sci *14*, 514-522.

Prigent, C., and Dimitrov, S. (2003). Phosphorylation of serine 10 in histone H3, what for? J Cell Sci *116*, 3677-3685.

Rada-Iglesias, A., Enroth, S., Ameur, A., Koch, C. M., Clelland, G. K., Respuela-Alonso, P., Wilcox, S., Dovey, O. M., Ellis, P. D., Langford, C. F., *et al.* (2007). Butyrate mediates decrease of histone acetylation centered on transcription start sites and down-regulation of associated genes. Genome Res *17*, 708-719.

Raisner, R. M., Hartley, P. D., Meneghini, M. D., Bao, M. Z., Liu, C. L., Schreiber, S. L., Rando, O. J., and Madhani, H. D. (2005). Histone variant H2A.Z marks the 5' ends of both active and inactive genes in euchromatin. Cell *123*, 233-248.

Rangasamy, D., Berven, L., Ridgway, P., and Tremethick, D. J. (2003). Pericentric heterochromatin becomes enriched with H2A.Z during early mammalian development. Embo J *22*, 1599-1607.

Rangasamy, D., Greaves, I., and Tremethick, D. J. (2004). RNA interference demonstrates a novel role for H2A.Z in chromosome segregation. Nat Struct Mol Biol *11*, 650-655.

Ren, Q., and Gorovsky, M. A. (2001). Histone H2A.Z acetylation modulates an essential charge patch. Mol Cell *7*, 1329-1335.

Ren, Q., and Gorovsky, M. A. (2003). The nonessential H2A N-terminal tail can function as an essential charge patch on the H2A.Z variant N-terminal tail. Mol Cell Biol *23*, 2778-2789.

Rhodes, D. R., Yu, J., Shanker, K., Deshpande, N., Varambally, R., Ghosh, D., Barrette, T., Pandey, A., and Chinnaiyan, A. M. (2004). Large-scale meta-analysis of cancer microarray data identifies common transcriptional profiles of neoplastic transformation and progression. Proc Natl Acad Sci U S A *101*, 9309-9314.

Ridgway, P., Brown, K. D., Rangasamy, D., Svensson, U., and Tremethick, D. J. (2004). Unique residues on the H2A.Z containing nucleosome surface are important for Xenopus laevis development. J Biol Chem *279*, 43815-43820.

Ridsdale, J. A., Hendzel, M. J., Delcuve, G. P., and Davie, J. R. (1990). Histone acetylation alters the capacity of the H1 histones to condense transcriptionally active/competent chromatin. J Biol Chem *265*, 5150-5156.

Rose, S. M., and Garrard, W. T. (1984). Differentiation-dependent chromatin alterations precede and accompany transcription of immunoglobulin light chain genes. J Biol Chem *259*, 8534-8544.

Ruhl, D. D., Jin, J., Cai, Y., Swanson, S., Florens, L., Washburn, M. P., Conaway, R. C., Conaway, J. W., and Chrivia, J. C. (2006). Purification of a human SRCAP complex that remodels chromatin by incorporating the histone variant H2A.Z into nucleosomes. Biochemistry *45*, 5671-5677.

Santisteban, M. S., Kalashnikova, T., and Smith, M. M. (2000). Histone H2A.Z regulats transcription and is partially redundant with nucleosome remodeling complexes. Cell *103*, 411-422.

Sapountzi, V., Logan, I. R., and Robson, C. N. (2006). Cellular functions of TIP60. Int J Biochem Cell Biol *38*, 1496-1509.

Sarcinella, E., Zuzarte, P. C., Lau, P. N., Draker, R., and Cheung, P. (2007). Monoubiquitylation of H2A.Z distinguishes its association with euchromatin or facultative heterochromatin. Mol Cell Biol *27*, 6457-6468.

Schones, D. E., Cui, K., Cuddapah, S., Roh, T. Y., Barski, A., Wang, Z., Wei, G., and Zhao, K. (2008). Dynamic regulation of nucleosome positioning in the human genome. Cell *132*, 887-898.

Schuettengruber, B., Chourrout, D., Vervoort, M., Leblanc, B., and Cavalli, G. (2007). Genome regulation by polycomb and trithorax proteins. Cell *128*, 735-745.

Schulz, W. A., and Hoffmann, M. J. (2009). Epigenetic mechanisms in the biology of prostate cancer. Semin Cancer Biol *19*, 172-180.

Shi, X., Hong, T., Walter, K. L., Ewalt, M., Michishita, E., Hung, T., Carney, D., Pena, P., Lan, F., Kaadige, M. R., *et al.* (2006). ING2 PHD domain links histone H3 lysine 4 methylation to active gene repression. Nature *442*, 96-99.

Shia, W. J., Li, B., and Workman, J. L. (2006). SAS-mediated acetylation of histone H4 Lys 16 is required for H2A.Z incorporation at subtelomeric regions in Saccharomyces cerevisiae. Genes Dev *20*, 2507-2512.

Shilatifard, A. (2008). Molecular implementation and physiological roles for histone H3 lysine 4 (H3K4) methylation. Curr Opin Cell Biol *20*, 341-348.

Shogren-Knaak, M., Ishii, H., Sun, J. M., Pazin, M. J., Davie, J. R., and Peterson, C. L. (2006). Histone H4-K16 acetylation controls chromatin structure and protein interactions. Science *311*, 844-847.

Siino, J. S., Yau, P. M., Imai, B. S., Gatewood, J. M., and Bradbury, E. M. (2003). Effect of DNA length and H4 acetylation on the thermal stability of reconstituted nucleosome particles. Biochem Biophys Res Commun *302*, 885-891.

Sims, R. J., 3rd, Millhouse, S., Chen, C. F., Lewis, B. A., Erdjument-Bromage, H., Tempst, P., Manley, J. L., and Reinberg, D. (2007). Recognition of trimethylated histone H3 lysine 4 facilitates the recruitment of transcription postinitiation factors and pre-mRNA splicing. Mol Cell *28*, 665-676.

Sims, R. J., 3rd, and Reinberg, D. (2006). Histone H3 Lys 4 methylation: caught in a bind? Genes Dev *20*, 2779-2786.

Sitnikova, T. (1996). Bootstrap method of interior-branch test for phylogenetic trees. Mol Biol Evol *13*, 605-611.

Snoek, R., Cheng, H., Margiotti, K., Wafa, L. A., Wong, C. A., Wong, E. C., Fazli, L., Nelson, C. C., Gleave, M. E., and Rennie, P. S. (2009). In vivo knockdown of the androgen receptor results in growth inhibition and regression of well-established, castration-resistant prostate tumors. Clin Cancer Res *15*, 39-47.

Strahl, B. D., and Allis, C. D. (2000). The language of covalent histone modifications. Nature *403*, 41-45.

Sun, Z. W., and Allis, C. D. (2002). Ubiquitination of histone H2B regulates H3 methylation and gene silencing in yeast. Nature *418*, 104-108.

Sutcliffe, E. L., Parish, I. A., He, Y. Q., Juelich, T., Tierney, M. L., Rangasamy, D., Milburn, P. J., Parish, C. R., Tremethick, D. J., and Rao, S. (2009). Dynamic histone variant exchange accompanies gene induction in T cells. Mol Cell Biol *29*, 1972-1986.

Suto, R. K., Clarkson, M. J., Tremethick, D. J., and Luger, K. (2000). Crystal structure of a nucleosome core particle containing the variant histone H2A.Z. Nat Struct Biol *7*, 1121-1124.

Syka, J. E., Coon, J. J., Schroeder, M. J., Shabanowitz, J., and Hunt, D. F. (2004). Peptide and protein sequence analysis by electron transfer dissociation mass spectrometry. Proc Natl Acad Sci U S A *101*, 9528-9533.

Thakar, A., Gupta, P., Ishibashi, T., Finn, R., Silva-Moreno, B., Uchiyama, S., Fukui, K., Tomschik, M., Ausio, J., and Zlatanova, J. (2009). H2A.Z and H3.3 Histone Variants Affect Nucleosome Structure: Biochemical and Biophysical Studies. Biochemistry.

Thalmann, G. N., Sikes, R. A., Wu, T. T., Degeorges, A., Chang, S. M., Ozen, M., Pathak, S., and Chung, L. W. (2000). LNCaP progression model of human prostate cancer: androgen-independence and osseous metastasis. Prostate *44*, 91-103 Jul 101;144(102).

Thambirajah, A. A., Dryhurst, D., Ishibashi, T., Li, A., Maffey, A. H., and Ausio, J. (2006). H2A.Z stabilizes chromatin in a way that is dependent on core histone acetylation. J Biol Chem *281*, 20036-20044.

Thambirajah, A. A., Li, A., Ishibashi, T., and Ausio, J. (2009). New developments in post-translational modifications and functions of histone H2A variants. Biochem Cell Biol *87*, 7-17.

Thompson, J. D., Gibson, T. J., Plewniak, F., Jeanmougin, F., and Higgins, D. G. (1997). The CLUSTAL_X windows interface: flexible strategies for multiple sequence alignment aided by quality analysis tools. Nucleic Acids Res *25*, 4876-4882.

Thomson, S., Clayton, A. L., and Mahadevan, L. C. (2001). Independent dynamic regulation of histone phosphorylation and acetylation during immediate-early gene induction. Mol Cell *8*, 1231-1241.

Tolstorukov, M. Y., Kharchenko, P. V., Goldman, J. A., Kingston, R. E., and Park, P. J. (2009). Comparative analysis of H2A.Z nucleosome organization in the human and yeast genomes. Genome Res *19*, 967-977.

Tomlins, S. A., Mehra, R., Rhodes, D. R., Cao, X., Wang, L., Dhanasekaran, S. M., Kalyana-Sundaram, S., Wei, J. T., Rubin, M. A., Pienta, K. J., *et al.* (2007). Integrative molecular concept modeling of prostate cancer progression. Nat Genet *39*, 41-51.

Turner, B. M. (2005). Reading signals on the nucleosome with a new nomenclature for modified histones. Nat Struct Mol Biol *12*, 110-112.

Valk-Lingbeek, M. E., Bruggeman, S. W., and van Lohuizen, M. (2004). Stem cells and cancer; the polycomb connection. Cell *118*, 409-418.

van Daal, A., and Elgin, S. C. (1992). A histone variant, H2AvD, is essential in Drosophila melanogaster. Mol Biol Cell *3*, 593-602.

Venkatasubrahmanyam, S., Hwang, W. W., Meneghini, M. D., Tong, A. H., and Madhani, H. D. (2007). Genome-wide, as opposed to local, antisilencing is mediated redundantly by the euchromatic factors Set1 and H2A.Z. Proc Natl Acad Sci U S A *104*, 16609-16614.

Vidali, G., Boffa, L. C., Bradbury, E. M., and Allfrey, V. G. (1978). Butyrate suppression of histone deacetylation leads to accumulation of multiacetylated forms of histones H3 and H4 and increased DNase I sensitivity of the associated DNA sequences. Proc Natl Acad Sci U S A *75*, 2239-2243.

Viens, A., Mechold, U., Brouillard, F., Gilbert, C., Leclerc, P., and Ogryzko, V. (2006). Analysis of human histone H2AZ deposition in vivo argues against its direct role in epigenetic templating mechanisms. Mol Cell Biol *26*, 5325-5335.

Vire, E., Brenner, C., Deplus, R., Blanchon, L., Fraga, M., Didelot, C., Morey, L., Van Eynde, A., Bernard, D., Vanderwinden, J. M., *et al.* (2006). The Polycomb group protein EZH2 directly controls DNA methylation. Nature *439*, 871-874.

Wang, Q., Li, W., Zhang, Y., Yuan, X., Xu, K., Yu, J., Chen, Z., Beroukhim, R., Wang, H., Lupien, M., *et al.* (2009a). Androgen receptor regulates a distinct transcription program in androgen-independent prostate cancer. Cell *138*, 245-256.

Wang, X., and Ausio, J. (2001). Histones are the major chromosomal protein components of the sperm of the nemerteans Cerebratulus californiensis and Cerebratulus lacteus. J Exp Zool *290*, 431-436.

Wang, X., He, C., Moore, S. C., and Ausio, J. (2001). Effects of histone acetylation on the solubility and folding of the chromatin fiber. J Biol Chem *276*, 12764-12768.

Wang, X., Moore, S. C., Laszckzak, M., and Ausio, J. (2000). Acetylation increases the alpha-helical content of the histone tails of the nucleosome. J Biol Chem *275*, 35013-35020.

Wang, Z., Zang, C., Cui, K., Schones, D. E., Barski, A., Peng, W., and Zhao, K. (2009b). Genome-wide mapping of HATs and HDACs reveals distinct functions in active and inactive genes. Cell *138*, 1019-1031.

Wang, Z., Zang, C., Rosenfeld, J. A., Schones, D. E., Barski, A., Cuddapah, S., Cui, K., Roh, T. Y., Peng, W., Zhang, M. Q., and Zhao, K. (2008). Combinatorial patterns of histone acetylations and methylations in the human genome. Nat Genet *40*, 897-903.

Wong, M. M., Cox, L. K., and Chrivia, J. C. (2007). The chromatin remodeling protein, SRCAP, is critical for deposition of the histone variant H2A.Z at promoters. J Biol Chem *282*, 26132-26139.

Wu, W. H., Alami, S., Luk, E., Wu, C. H., Sen, S., Mizuguchi, G., Wei, D., and Wu, C. (2005). Swc2 is a widely conserved H2AZ-binding module essential for ATP-dependent histone exchange. Nat Struct Mol Biol *12*, 1064-1071.

Wu, W. H., Wu, C. H., Ladurner, A., Mizuguchi, G., Wei, D., Xiao, H., Luk, E., Ranjan, A., and Wu, C. (2009). N terminus of Swr1 binds to histone H2AZ and provides a platform for subunit assembly in the chromatin remodeling complex. J Biol Chem *284*, 6200-6207.

Wysocka, J., Swigut, T., Xiao, H., Milne, T. A., Kwon, S. Y., Landry, J., Kauer, M., Tackett, A. J., Chait, B. T., Badenhorst, P., *et al.* (2006). A PHD finger of NURF couples histone H3 lysine 4 trimethylation with chromatin remodelling. Nature *442*, 86-90.

Zhang, H., Roberts, D. N., and Cairns, B. R. (2005). Genome-wide dynamics of Htz1, a histone H2A variant that poises repressed/basal promoters for activation through histone loss. Cell *123*, 219-231.

Zhang, K., Siino, J. S., Jones, P. R., Yau, P. M., and Bradbury, E. M. (2004). A mass spectrometric "Western blot" to evaluate the correlations between histone methylation and histone acetylation. Proteomics *4*, 3765-3775.

Zhou, Z., Feng, H., Hansen, D. F., Kato, H., Luk, E., Freedberg, D. I., Kay, L. E., Wu, C., and Bai, Y. (2008). NMR structure of chaperone Chz1 complexed with histones H2A.Z-H2B. Nat Struct Mol Biol *15*, 868-869.

Zilberman, D., Coleman-Derr, D., Ballinger, T., and Henikoff, S. (2008). Histone H2A.Z and DNA methylation are mutually antagonistic chromatin marks. Nature *456*, 125-129.

Zucchi, I., Mento, E., Kuznetsov, V. A., Scotti, M., Valsecchi, V., Simionati, B., Vicinanza, E., Valle, G., Pilotti, S., Reinbold, R., *et al.* (2004). Gene expression profiles of epithelial cells microscopically isolated from a breast-invasive ductal carcinoma and a nodal metastasis. Proc Natl Acad Sci U S A *101*, 18147-18152.

Appendix 1

GenBank Accession numbers for the histone variants H2A.Z-1 and H2A.Z-2 used in Figure 15. The ANNOTATION field denotes gene sequences newly isolated from draft genomes (In silico), gene sequences predicted as either H2A.Z-1 or H2A.Z-2 from databases and draft/complete genomes data (Pred), sequences defined either as H2A.Z-1 or H2A.Z-2 by the present analyses (a), sequences defined as H2A by the present analyses (b) and sequences whose annotation either as H2A.Z-1 or H2A.Z-2 has been corrected by the present work (c).

SPECIES	GENE	CHROMOSOME	ACCESSION NUMBER	ANNOTATION
Bos taurus (Cattle)	H2A.Z-1	4	NM_174809	
	H2A.Z-2	6	NM_001038197	
Canis familiaris (Dog)	H2A.Z-1 (1)	2	XM_535390	Pred
	H2A.Z-1 (2)	32	XM_535671	Pred (a)
	H2A.Z-1 (3)	32	XM_857355	Pred (a)
	H2A.Z-1 (4)	32	XM_857381	Pred (a)
	H2A.Z-2	16	XM_532724	Pred
Equus caballus (Horse)	H2A.Z-2	4	XM_001495899	Pred (a,b)
Homo sapiens (Human)	H2A.Z-1	4	NM_002106	
	H2A.Z-2 (1)	7	NM_012412	
	H2A.Z-2 (2)	7	NM_138635	
	H2A.Z-2 (3)	7	NM_201436	
Macaca mulatta (Rhesus Monkey)	H2A.Z-1 (1)	5	XM_001108067	Pred
	H2A.Z-1 (2)	5	XM_001108128	Pred
	H2A.Z-1 (3)	9	XP_001097247	Pred (c)
	H2A.Z-2	9	NC_007866	In silico (a,b)
Monodelphis domestica	H2A.Z-1	5	XM_001364009	Pred (a,b)
	H2A.Z-2	1	XM_001379779	Pred (a,b)
Mus musculus (Mouse)	H2A.Z-1	3	NM_016750	
	H2A.Z-2 (1)	11	XM_907680	Pred
	H2A.Z-2 (2)	11	XM_00147068	Pred
Pan troglodytes (Chimpanzee)	H2A.Z-1 (1)	8	XM_001163743	Pred (a,b)
	H2A.Z-1 (2)	8	XM_519801	Pred (a,b)
	H2A.Z-2	15	NW_001225258	In silico (a,b)
Rattus norvegicus (Rat)	H2A.Z-1	2	NM_022674	
	H2A.Z-2	14	NM_001106019	
Sus scrofa (Pig)	H2A.Z-1	8	NM001123122	